IOWA STATE UNIVERSITY
OF SCIENCE AND TECHNOLOGY

Center for Sustainable Environmental Technologies (CSET)
285 Metals Development Bldg.
Ames, Iowa 50011-3020
Phone: (515) 294-7934
Fax: (515) 294-3091

Project Title: **Development of a Biomass Fueled Stirling Engine for Combined Heat and Power Production**

Contract Number: **RD-110**

Report Date: **7/16/2007**

Principal Investigator: **Robert C. Brown** Contract Contact: **Matthew Bailey**

Phone **515-294-7934** Phone **515-294-5535**

Congressional District: (Corporate office) **Iowa 4**

Congressional District: (Project location) **Iowa 4**

FINAL REPORT

TABLE OF CONTENTS

LIST OF FIGURES

LIST OF TABLES

EXECUTIVE SUMMARY

Objective

The overall objective of this project was to demonstrate the integration of a biomass-fueled gasifier with a 55 kWe Stirling engine for the production of electricity. The original scope of the project involved integrating a custom-designed biomass gasifier with a commercially available Stirling engine.

Technical Progress

Early in the project, during efforts to procure an engine from our commercial partner, we learned that Stirling engines require some gas cleaning to remove particulate matter that would otherwise foul heat exchanger surfaces and that major problems in the manufacture of the engines would delay delivery of the 55 kW engine specified for our project. As a consequence, the early phases of the project focused on preparing a biomass gasifier with sufficient capacity (greater than 300 kW thermal input) and developing and testing a particulate removal system suitable for the gas cleaning requirements of a Stirling engine. Subsequently the Stirling engine manufacturer went out of business and no alternative manufacturer was found that could supply us with an engine large enough to integrate with our gasifier. Accordingly, we reduced the scope of our project and renegotiated our contract with the project sponsor. The reduced scope was limited to testing the biomass gasifier and demonstrating a gas cleaning systems suitable for Stirling engines.

Producer gas contains as much as 5 – 10 g/Nm^3 of particulate matter while the maximum acceptable particle loading for a Stirling engine is conservatively estimated to 0.05 g/Nm^3 of producer gas. Thus, 99% removal of particulate matter should be approached with gas cleaning systems.

Particulate filtration tests with a barrier filter constructed of FB700 high temperature fabric manufactured by 3M typically removed greater than 99% of particulate matter from the producer gas. This level of filtration meets the requirements of an internal combustion engine and should greatly exceed the requirements for more robust Stirling engines.

Project Benefits

The project demonstrated that it is possible to remove sufficient particulate matter from producer gas using filters fabricated from commercially available high temperature woven fabrics, thus supporting the technically feabsibility of integrating a biomass gasifier with a Stirling engine as part of a distributed biomass power system.

Project Lessons Learned

Despite many years of technology development, the Stirling engine industry is still struggling to achieve commercial viability. The Stirling engine supplier for this project, considered one of the most mature in the industry, was not able to supply an engine within the schedule of the project and eventually filed for bankruptcy. Thus, there may be better

choices than Stirling engines for developing distributed power systems, at least in the near-term.

Usefulness of Project Findings

Although the project had to be modified becauses of the inability of Stirling engine manufacturers to provide a viable engine of commercially significant size, the project demonstrated that commercially available particulate filtration technology can provide producer gas clean enough for distributed power applications using biomass as fuel. However, it revealed that the Stirling engine industry is not ready to fill this niche.

1. INTRODUCTION

The overall objective of this project was to demonstrate the integration of a biomass-fueled gasifier with a 55 kWe Stirling engine for the production of electricity. Although biomass gasifiers and Stirling engines are commercially available, the integration of these two technologies has yet to be demonstrated.

Biomass power offers an opportunity to displace fossil fuels and reduce net greenhouse gas emissions. Although direct combustion of biomass in utility boilers has been demonstrated, problems with ash fouling and relatively low heat rates have limited its commercial application. Gasification has advantages in these respects since lower operating temperatures reduces ash fouling and the resulting producer gas can be used in power systems with inherently higher thermal efficiencies (combined cycles and fuel cells). It also lends itself to distributed power systems, such as Stirling engines and microturbines.

The original scope of the project involved integrating a custom-designed biomass gasifier with a commercially available Stirling engine. The Stirling engine was selected over other prime movers because of its suitability for distributed power applications and its purported robustness to "dirty fuels." Early in the project, during efforts to procure an engine from our commercial partner, we learned that Stirling engines require some gas cleaning to remove particulate matter that would otherwise foul heat exchanger surfaces and that major problems in the manufacture of the engines would delay delivery of the 55 kW engine specified for our project. As a consequence, the early phases of the project focused on preparing a biomass gasifier with sufficient capacity (greater than 300 kW thermal input) and developing and testing a particulate removal system suitable for the gas cleaning requirements of a Stirling engine. Subsequently the Stirling engine manufacturer went out of business and no alternative manufacturer was found that could supply us with an engine large enough to integrate with our gasifier. Accordingly, we reduced the scope of our project and renegotiated our contract with the project sponsor. The reduced scope was limited to demonstrating a gas cleaning systems suitable for Stirling engines.

The maximum acceptable particle loading for producer gas to be burned in a Stirling engine is not well known. Internal combustion engines are generally limited to less than 0.05 g/Nm3 of producer gas. The fact that Stirling engines are external combustion devices greatly relaxes this requirement since the producer gas is isolated from the moving parts of the engine. However, particulate loadings need to be low enough to prevent rapid build-up of particulate on heat exchange surfaces, which makes necessary frequent scheduled maintenance of the engine. Producer gas contains as much as 5 – 10 g/Nm3 of particulate matter before cleaning. Thus, 99% removal of particulate matter would approach the gas cleaning standards of an internal combustion engine and represents a conservative target for Stirling engine applications.

2. BACKGROUND ON PARTICULATE FILTRATION

2.1 Types of Barrier Filters

There are four main types of barrier filters; fabric filters also known as baghouses, ceramic candle filters, sintered metal filters and cartridge filters. Ceramic candle and sintered metal filters are rigid devices made for high temperature applications, usually tubular in form; while fabric and cartridge filters can be produced for a variety of temperature ranges.

2.1.1 Ceramic Candle Filters

Ceramic candle filters are rigid and tubular in shape and are able to withstand temperatures above those seen in regular filtration devices [11]. The thicker they are the more susceptible they are to thermal stresses from temperature cycling [18]. There are two main types of ceramic filters, monolithic and composite. Monolithic candle filters will fail when the ceramic material begins to crack; they are made from clay-bonded silicon carbide / nitride or aluminum oxide particles which have a high elastic modulus' and coefficients of thermal expansion increasing there susceptibility to thermal stress [15]. The composite ceramic filters are made of ceramic fibers which help to hold the filter element together when cracks form, preventing complete failure.

Ceramic candle filters have been used in the filtering of fly ash at temperatures of 900°F (500°C) [11] and 1000°F (538°C) [1] without issues. There have also been tests preformed at 1600°F (870°C) [18], which is within the upper limit of suggested operation for ceramic filters. Some say the upper limit is 1400°F (760°C) [11] while others put is up around 2000°F (1100°C) [15]. Ceramic filters have also been found to be very resistive to degradation from chemicals although alkali compounds have been found to be unfriendly towards ceramics ([1], [11]).

2.1.2 Sintered Metal Filters

Sintered metal filters like ceramic candles are designed for high temperature applications [1]. They are constructed by sintering/melting together fine metal fibers or metal powder into a thin mat of material [11]. The type of material used depends on the temperature of the application, the environment in which the filtration takes place as well as the corrosiveness of the process stream; most materials used to make sintered metal filters are resistant to corrosive compounds such as solvents, acids and salts. Table 1, shows a table from the Mott Corporation's "Porous metal solutions" brochure that gives an idea of the temperature ranges for different materials in both oxidizing and reducing environments. These temperature ranges are similar to others found for materials without environmental information; 800°F (425°C) for stainless steel and 1200°F (650°C) for INCONEL (a registered trademark of International Nickel Company) [11].

Table 1 : Mott Corporation Sintered Metal Materials.

	Maximum Temperature	
Material	Oxidizing Atmosphere	Reducing Atmosphere
316L SS	750°F	900°F
Hastelloy® C-276	850°F	1000°F
Inconel® 600	1100°F	1500°F
Hastelloy® X	1450°F	1700°F

2.1.3 Cartridge Filters

Cartridge filters are made by wrapping a pleated material around a structural cage called a cartridge [11]. The design of the cartridge filter is the same as the air filters found in cars or the filters for Shop*Vac's. They are advantageous for their ability to provide a large surface area to volume ratio; which allows higher collection area per unit length of the filter [15]. This provides the advantage of smaller space requirements to get the same amount of filtration as normal fabric filters. The number of pleats around the circumference of the filter is recommended to be between 50 and 320 to avoid clogging the pleats with fine or sticky particulate [1].

2.1.4 Fabric Filters (Baghouses)

Fabric filters are the oldest and most widely used type of barrier filter. The first recorded use of a fabric filter was over 5000 years ago, when miners wore woven fabric sacks over their heads to protect them from lead oxide and dust [14]. Today there are over 200,000 fabric filters in use in industrial applications throughout the United States.

The fabric filters of today are somewhat of a recent technological advance as you look at the past of the fabric filter. Little work was done on increasing the efficiency or improving the technology of the fabric filter till Leonardo Da Vinci suggested in 1852 to wet cloth being placed over the facile region to increase filtration [14]. But the real advance in fabric technology came in the 1950's with the development of synthetic fabrics and coatings, which allowed fabric filters to be used in a much larger range of applications.

Today 80% of the fabric filtration units can be categorized as baghouses. The term baghouse was developed from the fabric filters being sewing into bag like structures and stored in large compartments called housings [15]. At the inlet an exit of the housing there are plenums which are used to decelerate the inlet gas and accelerate the cleaned gas. Within the compartment the gas passes through the fabric media which cleans the gas by removing particulate.

2.1.5 Design Break-down

Categorizing or designing an appropriate baghouse for a specific application can be a difficult and daunting task, with the number of variables that play a factor in the design; on top of the fact that the design is only part science, the rest is based on experience and results from previous designs [14]. Some variables that help to categorize a baghouse are the capacity of the unit, the required operating temperature and the type of operating conditions. The operating conditions can be broken into the type of cleaning method, the amount of service, the direction of flow and the type of fabric.

2.1.5.1 Unit Sizing

The capacity of a unit can be broken down into three categories: small volume (less than 10,000 acfm), medium volume (10-100,000 acfm) and large volume (more than 100,000 acfm).

2.1.5.2 Temperature Ranges

There are three main temperature ranges for fabric filters: low temperature (less than 200˚F), medium temperature (200˚F - 400˚F) and high temperature (greater than 400˚F). These temperature ranges have been the standard for many years; that is why the high temperature regime is somewhat misleading. There are many levels with in the regime, as there have been fabrics produced to reach temperatures of 2000˚F, such as the Nextel Ceramic Composite fabric that was manufactured by 3M.

2.1.5.3 Types of Fabric

There are hundreds of fabric manufactures within the United States, so there are groupings that many fabrics fall within. Each grouping of fabric may have many different grades of a particular fiber. Some common fiber groupings are: ceramic, cotton, Dacron, glass, Nomex, nylon, Microtain, Orlon, polypropylene, silica-glass, Teflon and wool. Cotton, nylon, polypropylene and wool are low temperature fibers. Dacron, Microtain and Orlon are medium temperature fibers. Glass, Nomex and Teflon fibers are lower high temperature fibers for the range of 400-500˚F. Silica-Glass fiber composites and coatings are mid high temperature fibers for the range of 750-900˚F, while Ceramic fiber composite fibers can reach the high end of the regime at 2000˚F.

The operating temperature is important for picking the fiber media but it is not the only parameter. Other issues to consider when picking a fiber media are chemical resistance to acids and alkali's, the abrasive resistance, the tensile strength of the material and whether it needs to be a non-combustible material. These parameters depend heavily on the type of contaminates in the process stream and the type of operation the filtration system follows. For instance filtration systems following boilers, furnaces or gasification units need fabric media that is non-combustible because the process stream may contain combustible products that could combust with sufficient oxygen and at the correct temperatures.

2.1.6 Cleaning

The fabric mediums used in baghouse applications achieve extremely high filtration efficiency for particulate down to the submicron size levels; the order of less than one micron. These filtration efficiencies are due to the formation of the dust cake on the filter medium during operation. Since the pressure drop across the filter element increases as the dust cake develops and all processes have some operational dependency on pressure drop. Whether it is to keep the system running or to decrease energy consumption, the fabric media must be occasionally cleaned. A few items of interest when considering how to clean a unit is the face velocity and whether online or off-line cleaning will be used.

2.1.6.1 Face Velocity

The face velocity, sometimes called the superficial velocity, is the volumetric flow rate divided by the surface area of the fabric. It is usually expressed in units of acfm/ft2 with ratios between 2:1 to 4:1 but sometimes as high at 12:1 [17]. The face velocity can affect the rate at which the pressure drop increases due to the formation of the dust cake as well as the installation expenses. Large face velocity decrease the amount of fabric needed, in turn decreasing the size of the filtration unit and the initial costs. Small face velocities decrease the initial pressure drop across the filter media, but increases the amount of fabric needed and hence increases initial costs. Using a lower face velocity allows for a thicker dust cake to develop before reaching the maximum pressure drop and increases the time between cleanings.

*2.1.6.2 Can Velocit*y

The effectiveness of online cleaning depends strongly on the can velocity. The can velocity is the volumetric flow rate divided by the difference between the housing cross-sectional area and the bags cross-sectional areas. The can velocity can vary depending on the size and density of particulate in the gas process stream; typical values for online cleaning are in the range of 2.5 to 3.5 ft/s [15]. The can velocity is important for online cleaning as it is directly correlated to the ability of particles released from the dust cake during cleaning to settle out and not become re-entrained in the gas flow. For that reason, lower can velocities are needed for gas streams with distributions of small particles as they take longer to settle.

In the case of off-line cleaning the can velocity is of less importance as the filtration system is split up into a number of compartments, which can be isolated from one another. The isolation of compartments allows for the dirty inlet stream to be shut-off while the bags in the compartment are cleaned. Therefore it drastically reduces the possibility of particles from the dust cake from being re-entrained in the flow and re-deposited on the filter media.

2.1.7 Cleaning Mechanisms

There are several variations of cleaning methods employed to clean fabric filters, but most fall with in two basic categories divided between low and high flow rates [6]. The low flow rate methods, which also require less energy, are either shaker, shake-deflate and reverse air type cleaning. All of the high flow rate cleaning methods can be categorized under pulse jets.

2.1.7.1 Shaker

The oldest and most reliable method of cleaning bags is by shaker cleaning [6]. The fabric bag is mechanically shaken to cause the dust cake to crack and release from the fabric. These units are usually designed with long tube bags, where the gas flow is from the inside of the tube to the outside [15]. The bottoms of the tubes are open and connected to a distributor plate in the bottom of the housing. The tops of the tubes are closed and connected to a mechanical shaking device. The dirty-gas enters towards the bottom of the housing flows up through the tubes and is discharged towards the top of the clean gas chamber, while the particulate and ash are discharged through the bottom of the housing. Figure 1, shows a schematic of baghouse with a shaker cleaning mechanism.

Units with shaker cleaning mechanisms are typically divided into smaller units or compartments allowing for one unit to be taken off-line and cleaned at a time. During cleaning the bags within a compartment are shaken in an oscillate motion to release the dust cake. For large units with several compartments that take compartments off-line for cleaning, the compartment is left off-line a short amount of time after the cleaning to allow the dust and particulate to settle. For smaller units which all the bags are cleaned at once, the blower or fan pulling air through the compartment is shut-off during cleaning.

The effectiveness of cleaning is dependant on the frequency and amplitude of the oscillation; the mode and duration of oscillation and the acceleration of the bag [10]. Bags are usually shaken in a harmonic or sinusoidal motion for, 30 seconds up to a few minutes [15], 15 to 100 seconds [6]. The frequency of shakes per cycle are typically in the range of 50 to 100 shakes/cycle ([6], [14]) and it has been found that there is no significant increase in dust removal for shaking more than 200-250 times per cycle [10]. Amplitudes of oscillation range from a fraction of an inch up to several inches depending on the length of the bag ([10], [15]). The peak acceleration, or how fast the bag is shaken, ranges from 1 to 10 times the force of gravity [15]. It has been found that peak accelerations above 8 times the force of gravity do not significantly increase the amount of the dust cake released from the fabric [10].

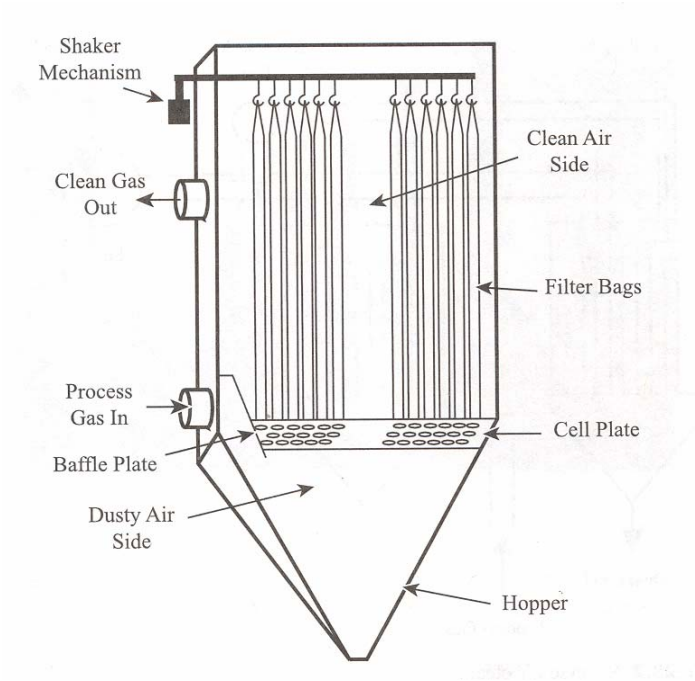

Figure 1: Baghouse schematic with shaker cleaning [15].

Shaker style filtration systems are less often used because they are implied to have shorter bag life due to fatigue failures from repeated high frequency cycling during cleaning. It is recommended to use face velocities in the range of 2 to 4 ft/min to obtain sufficient bag life ([6], [10], [14]).

2.1.7.2 Reverse-Air

Reverse-air cleaning mechanisms are low pressure high volume systems that use a low pressure reverse flow of gas through the system to help clean the bags. These units typically operate in the pressure range of 2 to 4 lb/in2 and use a centrifugal fan to create a reverse pressure flow of 6 to 15 lb/in2 [1]. Reverse-air filtration units are divided into several compartments, each having long tube like bags that are closed at one end and open at the other. Bags are on the order of 12 inches in diameter and 30 to 40 ft in length ([1], [15]). These bags are hung towards the top of the housing and the open end is connected to a distributor plate towards the bottom of the housing. Dirty gas is disbursed towards the bottom of the housing, flows up through the tubular bags which filter the particulate out and the clean gas leaves through the clean air compartment at the top of the housing. The gas flow is from the inside of the bag to the outside of the bag, as shown in Figure 2.

During cleaning a chamber is taken off-line by closing the dirty gas inlet and depressurizing the cabin as the clean gas outlet is closed. Once the compartment is off-line the clean gas from the other compartments is pumped through the exit of the compartment that is off-line using a fan for a range of 10 to 30 seconds [15]. The backwards pressure created causes the bags to collapse inward, cracking the dust cake and causing it to release from the fabric. Ribs are used every 3-4 ft down the length of the bags to stop the bags from completely collapsing [1]. Complete collapse of the bag would hamper the particulate from falling out

of the bag and into the hopper. Figure 3, gives a representation of the general cleaning process for reverse-air systems.

Cleaning can occur continuously by cleaning one compartment after another or the compartments can be cleaned once a specified pressure drop is reached. Typically face velocity ratios for reverse-air cleaning are less than 4:1 [14] or in the range of 2 to 6 ft/min ([1], [10]). Even though this is comparable to the face velocities seen in shaker cleaning, reverse-air cleaning is favored more often as it is gentler on the fabric. Reverse-air cleaning produces fewer vibrations on the fabric material per cycle of operation, decreasing fatigue and lengthening the life of the bag.

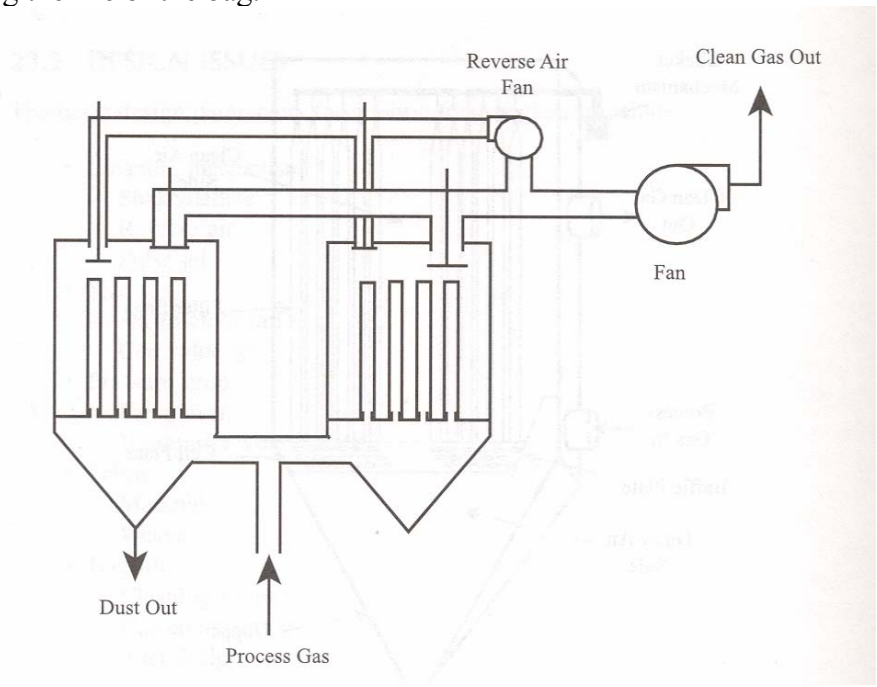

Figure 2 : Schematic of a reverse-air cleaning system [15]

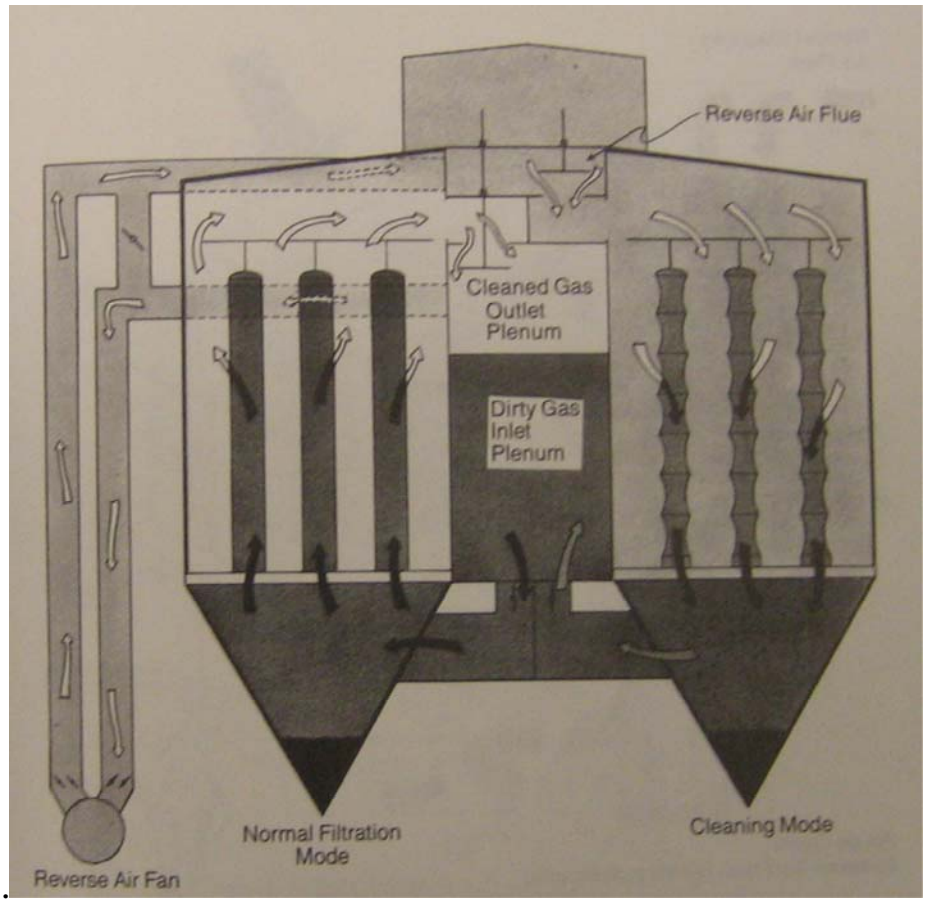

Figure 3 : Diagram of how reverse-air cleaning works [6].

2.1.7.3 Pulse Jets

Pulse jet cleaning mechanisms are the most effective at cracking and removing the dust cake built up on the fabric media [1]. These units were not introduced until the 1960's but have managed to take over half of the market share [14]. They operate using a pulse of compressed air to send a shockwave down the side of the bag to release the dust cake.

Units consist of a single housing, full of tubular bags hung on wire cages. Dirty gas enters the housing and flows through the filter media, which collects the particulate. The cleaned gas exits through the clean gas compartment at the top of the housing. The gas flows from the outside of the bag through the inside, as shown in the schematic in Figure 4.

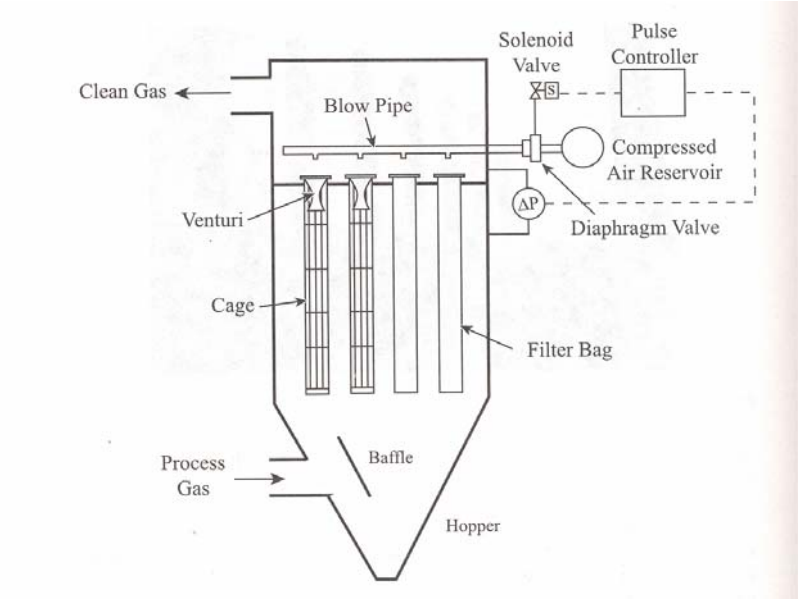

Figure 4 : Schematic of a pulse-jet cleaning system [15].

The housing is not divided into smaller compartments like other cleaning methods. Instead it is broken up into groups of bags; each group having its own compressed gas header. Nozzles off the gas header point down towards the exit of the bag.

Cleaning occurs while the unit is online. The unit can be cleaned as a whole when a desired pressure drop is achieved or continuously by cleaning one group of bags at a time. During cleaning a valve on the compressed gas header is opened for 50 to 100 msec ([1], [10]), allowing a pulse of pressurized gas to flow into the bag. The pulse creates a sudden increase in pressure within the bag, causing an acceleration of the fabric material and a reverse flow of gas through the bag resulting in the breakup and removal of the dust cake. This shockwave phenomenon is created by a pulse of compressed gas on the order of 60-120 lb/in2 [14], 70-100 lb/in2 [1] or 90-120 lb/in2 [10]. A detailed diagram of the cleaning process is shown in Figure 5.

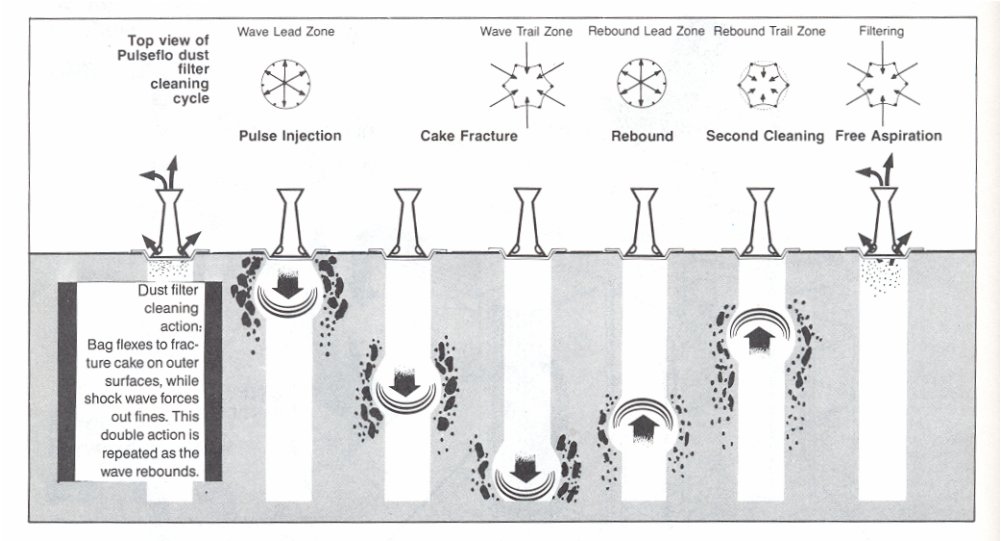

Figure 5 : Diagram of Pulse Jet Cleaning [6].

There exists a critical cleaning intensity above which the efficiency of cleaning only increases slightly. Cleaning intensity is the energy used in the removal of the dust cake, which is affect by the following parameters: tank size and pressure, pulse duration, particulate properties, blow tube diameter, type of venturi nozzle used, nozzle diameter and characteristics of the diaphragm valve [12]. Everything above the critical value is thought of as waste energy. The critical cleaning intensity is broken into three subcategories: peak pulse overpressure, pressure impulse within the bag and the acceleration of the fabric.

Pressure impulse is the integral of pressure versus time over the duration of a pulse. The overpressure is the pulse pressure minus the pressure drop across the bag. The critical overpressure is 600 Pa (.09 lb/in2) [12]. Above this critical value there is minimum improvement on the cleaning efficiency.

The necessary fabric acceleration varies between fabrics and is affected by the adhesive properties of the particulate. Typically for flexible fabrics the recommended acceleration appropriate for dislodging the dust cake is roughly 30g while non-flexible fabrics made need accelerations of 200-500g [12].

Pulse jets are advantages for lower temperature streams because they can be operated with larger face velocities on the order of 5-10 ft/min ([6], [10]). Applications that require maintaining the baghouse at high temperatures do not typically use pulse jet cleaning systems because pre-heating the pressurized gas before it is released into the bag is somewhat difficult. But in applications where pulse jet cleaning systems can be used, it is advantageous because smaller units can be used decreasing the overall cost. If venturi nozzles are used instead of regular nozzles, energy consumption during operation can be cut by up to 30% [12].

2.1.7.4 Shake-deflate

To improve the cleaning efficiency of shaker style systems, reverse-air and pulse jets have been added. The main combination is shakers and reverse-air sometimes called shake/deflate.

3. EXPERIMENTAL EQUIPMENT AND PROCEDURES

3.1 Multi-mode gasifier system

A multi-mode fluid bed reactor has been designed and installed at the Biomass Energy Conversion (BECON) Facility. With a thermal input of 150 – 1,500 kW, depending upon operating conditions, the reactor is suitable in scale for testing Stirling engines as large as 250 kW electric power. The new reactor is capable of operating as a bubbling fluid bed combustor, bubbling fluid bed gasifier, circulating fluid bed combustor, or circulating fluid bed gasifier.

The fluid bed reactor and associated feed vessels were built as ASME pressure vessels, enabling bubbling fluid bed operation to 75 psig. The modest pressure rating offers several benefits. Reactor throughput increases linearly with the ratio of absolute operating pressure to atmospheric pressure. Therefore operation at 65 psig (a value slightly lower than the pressure vessel rating) increases capacity approximately fivefold (80 psia / 16 psia). The nominal feed rates are shown in Table 2. Gasification at moderate pressures will alleviate one or more stages of pressurization if the resulting gas is used in a catalytic conversion process. Vessel construction using standard 150# fittings isn't significantly different than construction of an 'atmospheric' rated vessel. Biomass feed at moderate pressures should be more straightforward than biomass feed at high pressures (> 10 atmospheres).

Table 2: Biomass feed rates for various operating modes and at various operating pressures.

Operation Mode	Nominal biomass feed rate at atmospheric pressure[1]	Nominal biomass feed rate at elevated pressure[2]
Bubbling fluid bed combustion	10-30 lb/hr	35-125 lb/hr
Bubbling fluid bed gasification	40-130 lb/hr	200-650 lb/hr
Circulating fluid bed combustion	70-175 lb/hr	NA[3]
Circulating fluid bed gasification	350-900 lb/hr	NA[3]

[1] Atmospheric pressure is nominally 2 psig
[2] Atmospheric pressure is nominally 65 psig
[3] Circulating mode only possible at atmospheric pressure

Figure 6 is a drawing of the gasification system showing major components: fuel feeding system, reaction vessel, producer gas piping and cleaning. The inner diameter of the reaction vessel is 12-in from top-to-bottom. Three 6-ft long sections make up the body of the vessel for an overall fluid bed height of 18-ft. Two feed ports accommodate two biomass feed injection elevations. The lower feed elevation will typically be used for bubbling fluid bed operation but can also be used for circulating operation. The upper feed elevation is intended for use during circulating operation. It is hypothesized that carbon conversion can be increased during circulating gasification by creating an oxidation zone between the fluidization gas nozzles and the biomass injection nozzle. The recirculation of bed media

and biomass char near the bottom of this zone results in a one-second residence time for char/oxygen contact.

Pressurized bubbling operation is accomplished using a pressure modulation valve that will restrict gas flow exiting the reactor. This modulation valve will be removed and be replaced with a cyclone separator, a standpipe, and L-valve to separate elutriated bed media and char from the exiting gas and reinject the separated material into the bottom of the fluid bed above the distributor and below the biomass feed nozzle.

The biomass feed system consists of two pressure vessels in series. The 'metering bin' operates at process pressure at all times and has two different sized, speed controlled screw augers that meter biomass into a high speed injection auger. The 'cycling bin' cycles between atmospheric pressure and process pressure. At atmospheric pressure, the discharge of the cycling bin is isolated from the metering bin by a valve. Another valve at the inlet of the cycling bin opens and a fuel receiving hopper and bucket elevator deliver biomass to fill the cycling bin. When the cycling bin is full the inlet valve closes, the bin is brought to process pressure, the valve isolating the cycling bin from the metering bin opens, and biomass is transferred, filling the metering bin. A photograph of the assembled gasifier is shown in Figure 7.

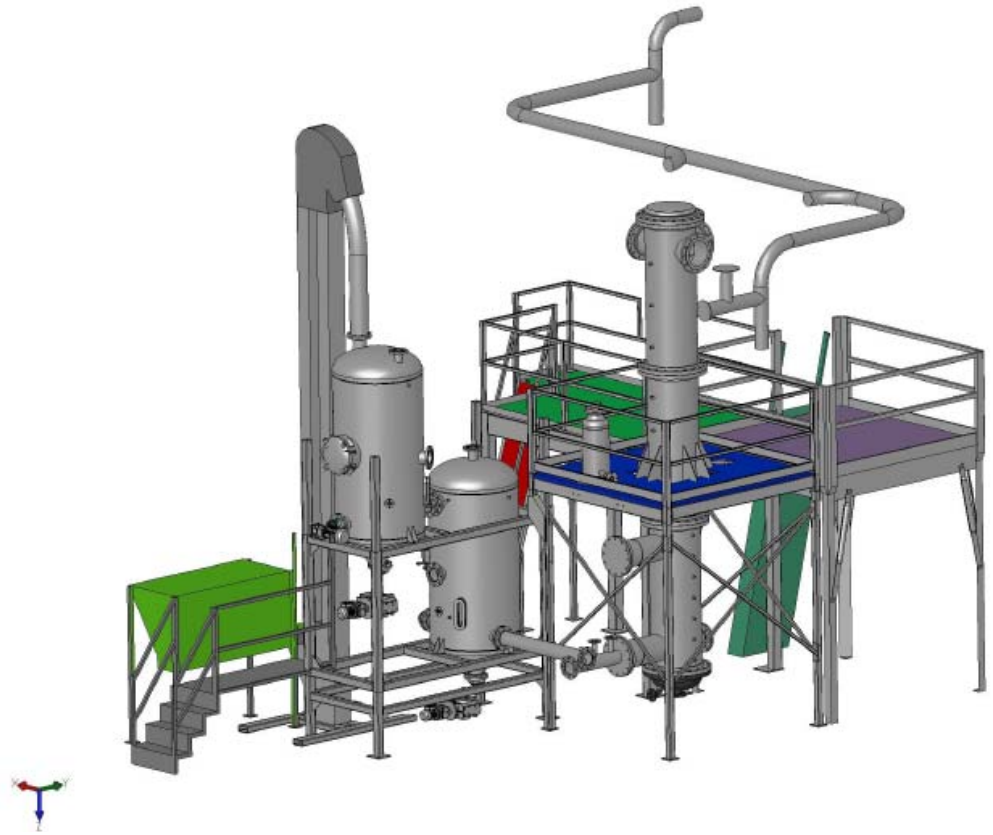

Figure 6: Drawing of the multi-mode gasifier

Figure 7: Gasification system shortly after installation (reaction vessel at center of photograph; pressurized fuel hopper at right).

3.2 Particulate filtration experiments

For the purpose of testing the ability to remove particulate from the hot produced gas created from corn gasification, a small scale baghouse was designed and tested on the lab scale gasification unit in 1056 Black Engineering Building at Iowa State University.

A baghouse was chosen over other types of barrier filters for the low cost involved in installation and operation during testing. As well as its resistance to fatigue from thermal stress involved with temperature cycling, like ceramic filters sometimes have.

3.2.1 Gasifier

The gasification unit located in 1056 Black Engineering is shown in Figure 8. Fuel is taken from the feed hopper by a metering auger and transported to the atmospheric gasifier via the high speed injection auger. Within the gasifier the fuel is transformed into producer gas and char using high temperatures. The gas and char are sent through a cyclone separator to remove the large particulate. From the cyclone the producer gas is piped to the combustor where it is burned and vented to the atmosphere. All piping between the gasifier and the combustor is wrapped with heater tapes and held to 450 °C to ensure none of the tar vapors leaving the gasifier condense before being burned in the combustor.

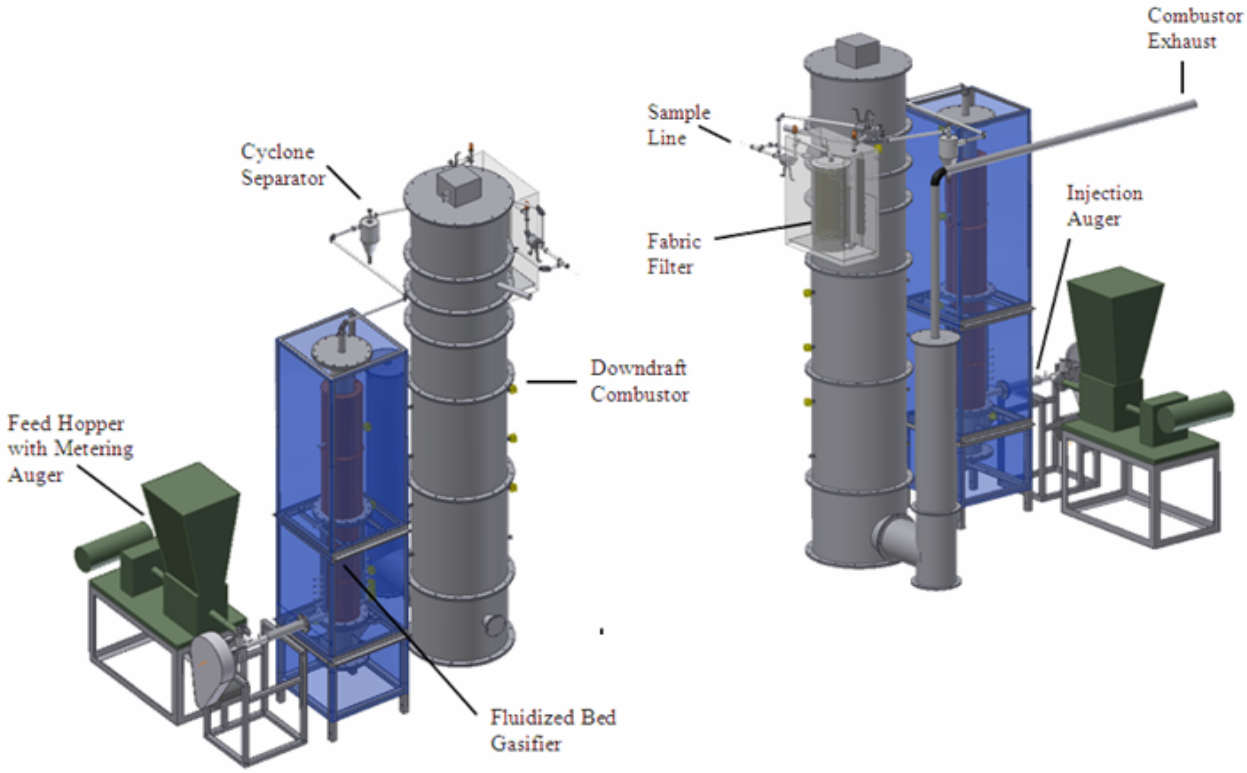

Figure 8 : Lab Scale Gasification unit in 1056 Black

3.2.2 Gasifier

The atmospheric fluidized bed gasifier contains a bed of sand and limestone which is fluidized with air to increase heat and mass transfer during the thermal decomposition of the fuel. The unit was constructed out of Inconel 625 to withstand the high temperatures needed to fuel the gasification reaction. Figure 9, shows a schematic of the gasification unit which can be broken down into 4 simple categories: the bed, plenum, freeboard and heaters.

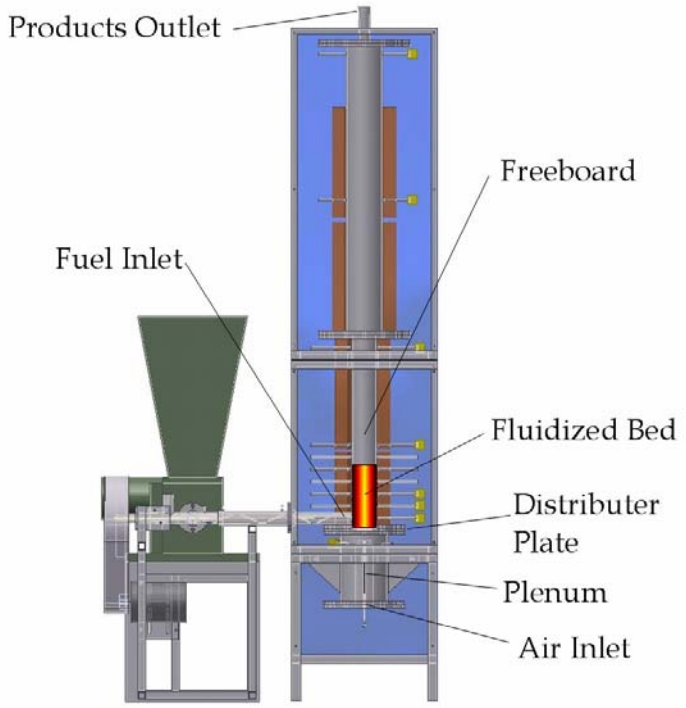

Figure 9: Diagram of the fluidized bed gasifier [7].

3.2.2.1 Fluidized Bed

The bed is comprised of a mixture of 70% sand on the order of 200-300 μm in diameter and 30% ground limestone weighing roughly 2200 g. The sand and limestone mixture rests on a distributor plate with 14, .36 cm (9/64 in) holes. The bed is 10.16 cm (4 in) in diameter and approximately 25.4 cm (10 in) deep. During operation air is used to fluidize the bed mixture and vigorously mix it with the incoming fuel. The vigorous mixing increases both heat and mass transfer during the chemical reaction.

Limestone is used as a bed material to react with the alkali compounds in the fuel to improve bed life. Alkali compounds which are sticky tend to build up in the bed overtime, without the limestone the alkali material will stick to sand and char forming clumps called agglomerates. As these agglomerates increase in size, fluidization decreases causing temperature fluctuations in the bed, decreasing the thermal decomposition of the fuel.

Fuel is injected into the bed slightly above the distributor plate through a two step process divided into a metering and injection segment. In the metering step an Acrison Model 105Z-E volumetric feeder is used to measure the amount of fuel released to the system. To insure

accurate fuel feed rates the variable speed motor used to control the feeder was manually calibrated. The fuel discharged from the Acrison feeder is injected into a high speed auger which injects it into the fluidized bed in the second step. A high speed auger was used to avoid any reactions from occurring before the fuel enters the fluidized bed. To further protect from decomposing the fuel before it is injected, a water cooling jacket is used on the portion of the injection auger leading up to the bed to keep fuel below the temperature at which combustion or gasification will occur.

3.2.2.2 Plenum

The plenum is the air inlet for the fluidized bed and is designed to have an appropriate pressure drop to obtain even air distribution through the distributor plate. The air coming into the plenum is cleaned of particulate and moisture with an air filter on the incoming compressed air line. An Alicat Laminar Mass Flow Controller, rated for the range of 0-150 slpm with an accuracy of +/- 1.5 slpm was used to control the incoming air. The incoming air was preheated to 260°C (500°F) by a Watlow (3000W) star wound heating element.

3.2.2.3 Freeboard

The freeboard is section of the gasifier directly above the fluidized bed to the exit of the gasifier. It starts off at the bed diameter of 10.16 cm (4 in) and then increases to 15.24 cm (6 in) in diameter at 81.28 cm (32 in) above the distributor plate. The increase in diameter is used to decrease the superficial velocity of producer gas leaving the bed. By decreasing the superficial velocity, the buoyancy force of the gas stream is decreased resulting in larger particulate dropping out. This provides for longer residence times for small portions of the fuel and slight increases in conversion rates.

3.2.2.4 Heaters

The gasifier walls are not lined with refractory material to decrease heat loss during the reaction process; instead Watlow radiant ceramic heaters are used to decrease heat loss during the gasification reaction. On portions of the gasifier not covered by the radiant heaters fiberglass insulation is used cut down on heat loss. The Watlow heaters are kept at temperatures slightly above the desired temperature of the bed, to maintain constant bed temperatures during the reaction process. As a result the bed temperature is not completely dependant on the fuel to air ratio and can be controlled slightly by the increasing or decreasing the temperature of the Watlow heaters. This eliminates the need for an initial combustion period to reach bed temperatures as the Watlow heaters provide sufficient enough energy to obtain minimum bed temperatures necessary for gasification to occur. Table 3 provides the specifications for all of the heaters on the gasifier, while Figure 10 shows the location of the heaters on the gasifier.

Table 3: Heater Specifications

	Max Power Output [W]	Diameter [cm]	Height [cm]
Heater 1	3000	7.6	15.2
Heater 2	2500	12.7	12
Heater 3	3500	12.7	18
Heater 4	4200	16.5	18
Heater 5	4200	16.5	18

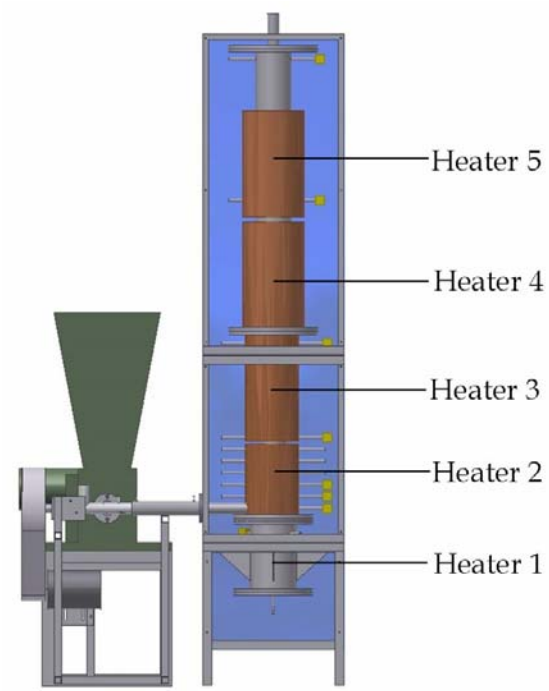

Figure 10: Diagram of gasifier heaters [7].

3.2.3 Fabric Filter

To remove fine particulate down stream of the cyclone separator a fabric filter was designed and installed. In the following sections the design of the fabric filter is discussed. Figure 11, shows a schematic of the fabric filter.

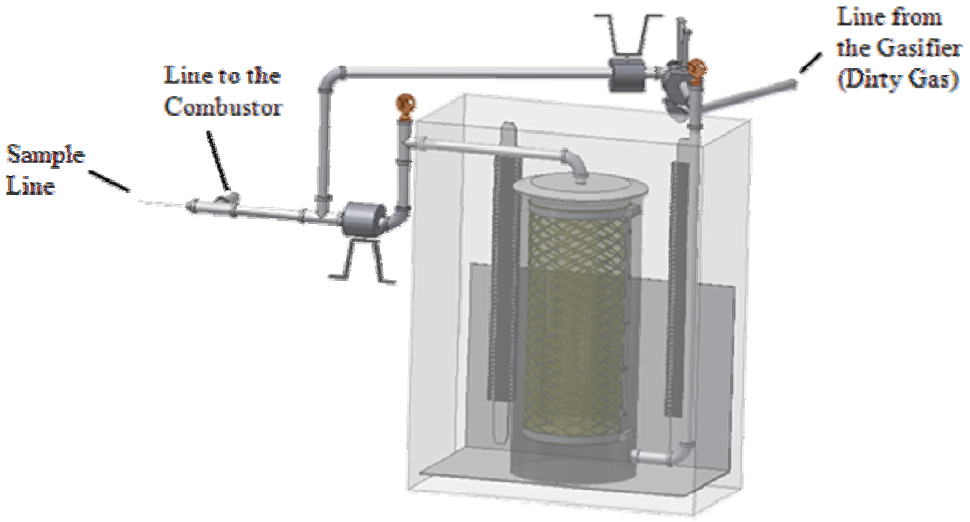

Figure 11 : Fabric Filter Schematic

3.2.3.1 Heated Enclosure

The fabric filter is encased in a stainless steel housing and held at 370 °C within a heated enclosure. The heated enclosure is a modified electrical enclosure with dimensions of 76.2 cm x 60.96 cm x 45.72 cm (30 in x 24 in x 18 in). Two layers of 2.54 cm (1 in) fiberglass insulation cover all interior walls of the enclosure. The back plate was bent, to create a shelf for the fabric filter housing and two Watlow 3000 watt fine heaters are used to maintain temperature within the enclosure.

3.2.3.2 Filter Element

The filter element is made from 3M's high temperature filtration fabric, FB-700, and supported by a stainless steel cage. The fabric is a coated fiberglass composite made for continuous operation at temperatures up to 371°C (700°F) with temperature excursions up to 427°C (800°F). The fabric was wrapped around the stainless steel cage and clamped at both ends with hose clamps while the seam down the side is compressed with a bar using 5 bolts. The cage is 20.32 cm (8 in) in diameter and 49.53 cm (19.5 in) tall. Detailed drawings of the wire cage can be found in APPENDIX A. The bottom of the cage is closed off with a welded stainless steal plate. The top of the cage also has a welded stainless steal plate; but the plate on the top has a 2.54 cm (1 in) pipe nipple welded in the center of the plate and a 2.54 cm (1 in) hole drilled through the plate for the clean gas exit. Shown in Figure 12 is a diagram of the filter cage and element; the left side is the stainless steel cage by itself and the right side depicts the fabric wrapped around the stainless steel cage and sealed.

Figure 12 : Filter cage

3.2.3.3 Filter Housing

The filter housing was designed to have the stainless steel cage thread into the housing via the 2.54cm (1 in) pipe nipple. The housing was fabricated at Ames Laboratory in the Metals Development Building at Iowa State University. Figure 13, demonstrates how the housing operates and a detailed drawing of the housing can be found in APPENDIX B. The flanges are made from 10" sanitary pipe fittings and connected with a sanitary pipe fitting shown in Figure 14. Instead of a gasket between the two flanges a high temperature gasket goop material was used. There is a 2.54 cm (1 in) x 1.27 cm (1/2 in) reducing pipe couple welded into the top of the housing. This coupling is the connection point for the stainless steel cage as well as the exit for the cleaned producer gas. A 1.27 cm (1/2 in) pipe couple welded into the side of the housing towards the bottom creates the inlet for the dirty gas. This was placed below the bottom of the cage as not to create uneven loading on the fabric and few inches above the bottom of the housing to create a small catch zone for char. Another use for the char catch zone is to keep the inlet flow of dirty gas unobstructed of blockage created from the build of char at the bottom of the housing.

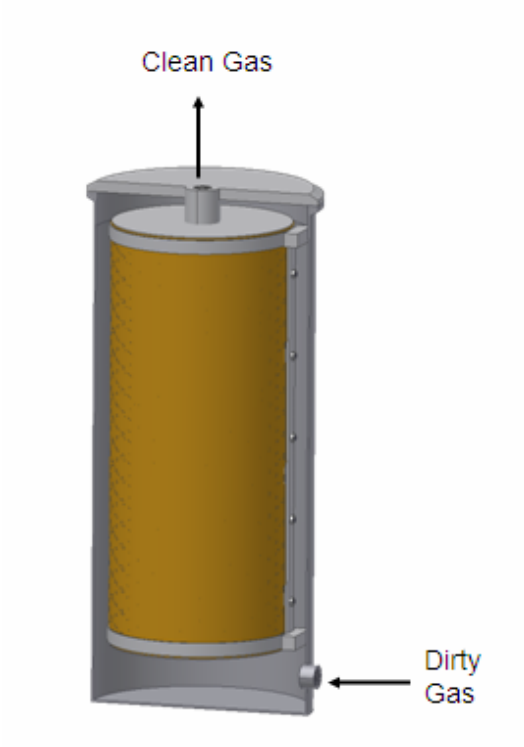

Figure 13 : Filter housing diagram

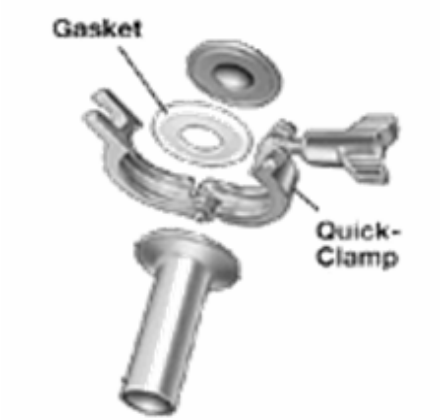

Figure 14 : Diagram of quick disconnect clamp

3.2.4 Isokinetic Sample Line

Downstream of the fabric filter is an isokinetic sample line. A schematic of the sample line is shown in Figure 15. The term isokinetic means that the velocity in the main duct is equal to the velocity in the sample line. EPA Method 1A regulations on isokinetic sampling taken from Vollaro (1977) were followed in the setup of the isokinetic sample line.

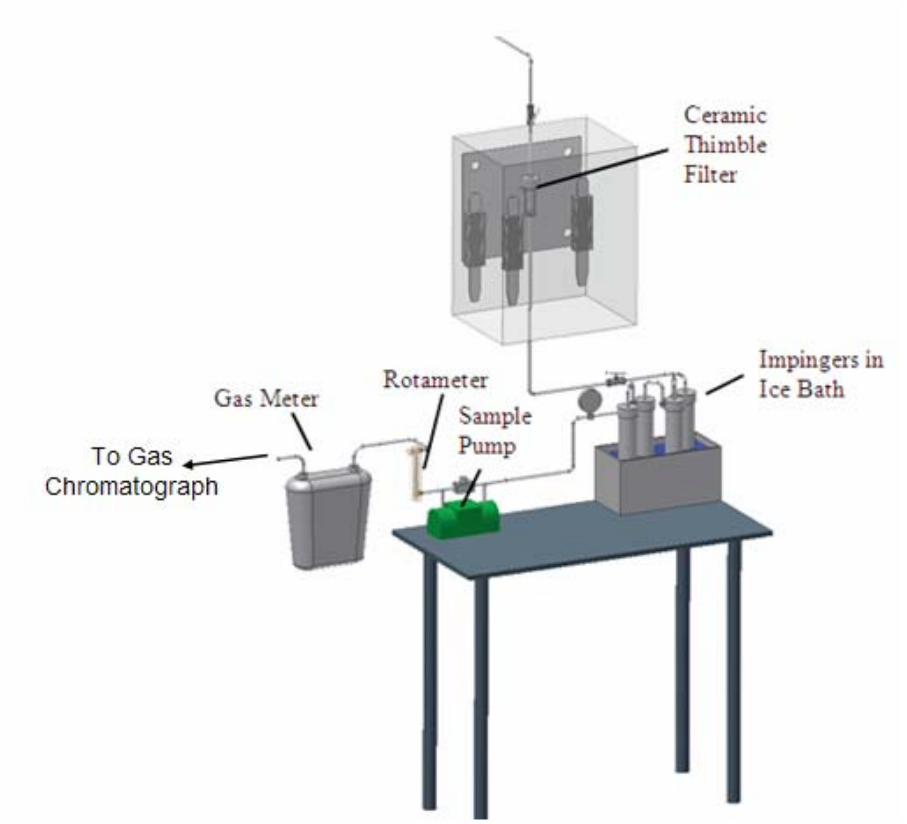

Figure 15 : Sample line schematic

The sampling probe was placed eight duct diameters downstream of any flow disturbances and two duct diameters upstream of any flow disturbances. The probe diameter was selected to achieve isokinetic conditions in velocity between the main duct and the sample probe. In addition to isokinetic conditions, the ratio of probe cross sectional area to actual duct cross sectional area was taken into account as not to disrupt flow patterns around the probe entrance. A vacuum pump and rotameter were used to maintain steady flow through the sample line. The high efficiency quartz filter was used to catch particulate and the impinger ice bath was used to condense water vapor and tar vapors. Last, the producer gas is sent through a gas meter to measure the flow in the sample line before being sent to a gas chromatograph for gas composition analysis.

The piping on the sample line up to the impinger ice bath is maintained at 450°C (842°F) with heater tapes. The quartz thimble filter is also maintained at 450°C (842°F) with in a heated enclosure held to temperature with three 500W Watlow fine heaters. There are also high temperature valves before and after the heated enclosure to shut-off the sample line during periods when it is not being used.

3.2.5 Instrumentation

Throughout the gasification system type K thermocouples are used to monitor temperatures on the system. Most of the thermal couples are connected to PID loops which control temperatures by controlling the current to heaters but some are just used for monitoring

purposes. In some locations pressure transducers are used to monitor pressure fluctuations in the system.

3.2.5.1 Gasifier Instrumentation

The gasifier itself has eight thermocouples placed at varying heights along the reactor to measure the temperature at the center of the reactor. The first thermal couple measures the temperature of the incoming plenum air. The next four thermocouples measure temperatures within the fluidized bed at heights of 5.08 cm (2 in), 10.16 cm (4 in), 15.24 cm (6 in), and 25.4 cm (10 in) above the distributor plate. The remaining three thermocouples measure the temperatures in the freeboard at height of 71.12 cm (28 in), 137.16 cm (54 in) and 198.12 cm (78 in) above the distributor plate. Four more thermal couples are used to monitor the temperature of the Watlow radiant ceramic heaters. These four thermal couples are connected to PID loops that control the temperature of the radiant heaters via the current sent to the heaters.

The pressure within the fluidized bed is monitored with pressure transducers, to diagnose uneven fluidization in the bed. This is accomplished with three pressure transducer. One transducer is used to measure the absolute pressure in the bed the other two transducers measure pressure differentials throughout the bed. The one measures the pressure differential from 10.16 cm (4 in) to 15.24 cm (6 in) above the distributor plate while the other one monitors the pressure differential from 10.16 cm (4 in) to 35.56 cm (14 in) above the distributor plate.

3.2.5.2 Piping Instrumentation

All piping in between the gasifier and downdraft combustor is insulated and heated. The temperatures within these gas lines are monitored with thermal couples place throughout the lines. The thermal couples are connected to PID loops which control the current to the heater tapes wrapped around the gas lines to maintain gas temperature at or above 450°C (842°F). It is important to maintain these temperatures to prevent tars vapors from condensing on pipe walls.

3.2.5.3 Fabric Filter Instrumentation

The temperature of the fabric filter is monitored in two ways. A thermal couple connected to a PID loop monitors the temperature within the heated enclosure, which is also used to control the temperature of the heated enclosure. The second thermal couple simply monitors the temperature of gas exiting the heated enclosure as a verification tool.

There are three high temperature ball valves used to create a bypass for the fabric filter during startup and shutdown of the reactor. The bypass may also be used if the pressure across the fabric filter reaches the maximum allowable to maintain steady operation of the atmospheric reactor. To monitor continuous pressure drop across the fabric filter a transducer connected to two pressure taps locations is used. These locations are at the entrance and exit of the heated enclosure.

3.2.5.4 Sample Line Instrumentation

The sample line piping up to the impinger ice bath is monitored and controlled with thermal couples connected to PID loops. The temperature of the heated enclosure for the high efficiency quartz thimble filter is monitored and controlled with a thermal couple connected to a PID loop. The quartz thimble filter is manufacture by Advantec MFS, Inc. The gas composition of the producer gas is analyzed for H_2, CO, N_2, O_2, CO_2, CH_4, C_2H_4, C_2H_6, and C_3H_8 with a Varian Micro Gas Chromatography (GC), Model CP-4900.

3.3 Testing Procedure

The experimental apparatus in the previous section was run to obtain data in order to analyze the fabric filters performance. During testing fuel was fed into the gasifier and converted to a flammable gas mixture of hydrogen (H_2), carbon monoxide (CO), nitrogen (N_2), oxygen (O_2), carbon dioxide (CO_2), methane (CH_4), acetylene (C_2H_2), ethylene (C_2H_4), ethane (C_2H_6), propane (C_3H_8) and char called producer gas. The producer gas was piped through a cyclone separator, which filtered out large particulate. From the cyclone the producer gas traveled through the fabric filter to filter out finer particulate. After the fabric filter the producer gas is sent to the downdraft combustor to be burned and exhausted to the atmosphere. All particulate caught by the cyclone separator and fabric filter is weighed to be used in calculating the mass concentration of particulate in the producer gas as well as the fabric filters efficiency.

Between the fabric filter and downdraft combustor an isokinetic sample line was used to measure the remaining concentration of particulate left in the producer gas and the gas composition.

3.3.1 Fabric Filter Procedure

The fabric filter was held off-line during startup and shutdown to maintain a constant mass loading on the filter during operation. Before and after each experiment the filter element was weighed to measure the amount of particulate collected during the experiment. An ACCULAB V1-10kg scale with an accuracy of 1 g was used to weigh the filter element as well as the char collected from the cyclone. The pressure drop across the filter during the course of the experiment and the time period that filter took place were also recorded.

3.3.2 Sample Line Procedure

The quartz thimble filter on the sample line measured the remaining particulate in the producer gas. Two samples were taken, one during the first portion of the experiment and one during the second portion of the experiment. This was done to show that as the filter cake develops the filter becomes more efficient at removing particulate. The pressure drop across the fabric filter was used as a deciding factor on when the thimble filters should be switched.

The ceramic filters were dried and weighed before and after each experiment to eliminate variations in humidity levels. Moisture was removed from the thimble filters by placing them in a toaster oven at 100°C (212°F) for no less than one hour. From the toaster oven the

filters were placed on an AE ADAM AAA/L Series high precision scale to be weighed. The scale has a repeatability of +/- 0.15 mg.

The particulate is not the only important information collected from the sample line. A gas meter is used to measure the total gas flow through the sample line and duration of sampling is recorded. The composition of the producer gas is also measured during the course of the experiment by the Gas Chromatograph (GC).

3.4 Analysis Procedure

The data collected during each experiment was used to develop elemental and mass balances to verify that all inlet and exit streams are accounted for. The data was also used in analyzing the effectiveness of the fabric filter. Sample calculations can be found in APPENDIX C.

3.4.1 Elemental Balances

Elemental balances of carbon, nitrogen, hydrogen and oxygen were preformed to verify what is put into the system leaves. The nitrogen balance is used to determine the flow rate of producer gas through the system. The carbon and oxygen balances are used to validate the gas composition read by the Gas Chromatograph (GC). And the hydrogen balance is used calculate the theoretical output of water from the gasification reaction. In each case the simple conservation equation shown in Equation 1 can be used.

Equation 1

$$moles_{in} = moles_{out}$$

3.4.1.1 Nitrogen Balance

The total molar flow rate of nitrogen in the producer gas can be calculated by balancing the inlet and outlet flows of nitrogen. There are two places nitrogen is put into the system and two places it is taken out. Nitrogen is put into the system with the air used to fluidize the bed and the fuel being converted. Nitrogen leaves the system as a fraction of the producer gas and char. Therefore, Equation 2 can be used to calculate the molar flow rate of nitrogen leaving the system.

Equation 2

$$\dot{n}_{Nitrogen\_producer\_gas} = \dot{n}_{Nitrogen\_air} + \dot{n}_{Nitrogen\_fuel} - \dot{n}_{Nitrogen\_char}$$

The molar flow rate ($\dot{n}$) of nitrogen in the air can be calculated knowing the volume percentage (x) of nitrogen in the air, the density (ρ) and molecular weight (M) of nitrogen and the volumetric feed rate ($\dot{V}$) of air into the system. Equation 3 demonstrates the calculation for the molar flow rate ($\dot{n}$) of nitrogen in the air.

Equation 3

$$\dot{n}_{Nitrogen\_air} = \frac{\dot{V}_{air\_in} \cdot x_{N2\_air} \cdot \rho_{N2}}{M_{N2}}$$

The molar flow rate ($\dot{n}$) of nitrogen in the fuel can be calculated from the mass flow rate ($\dot{m}$) of fuel, the volume percentage (x) of nitrogen in the fuel, and the molecular weight (M) of nitrogen. This is shown in Equation 4.

Equation 4

$$\dot{n}_{Nitrogen\_fuel} = \frac{\dot{m}_{fuel\_in} \cdot x_{N2\_fuel}}{M_{N2}}$$

The molar flow rate ($\dot{n}$) of nitrogen in the char can be calculated from the mass flow rate ($\dot{m}$) of char, the volume percentage (x) of nitrogen in the char, and the molecular weight (M) of nitrogen. The mass flow rate ($\dot{m}$) of char is just the mass collected divided by the duration of collection period. The molar flow rate ($\dot{n}$) of nitrogen in the char is shown in Equation 5.

Equation 5

$$\dot{n}_{Nitrogen\_char} = \frac{\dot{m}_{char} \cdot x_{N2\_char}}{M_{N2}}$$

With the balance of molar flow rates of nitrogen the volumetric flow rate of producer gas ($\dot{V}$) can be calculated. The volumetric flow rate of producer gas ($\dot{V}$) is calculated using the total molar flow rate ($\dot{n}$) of nitrogen in the producer gas, the density (ρ) and molecular weight (M) of nitrogen as well as the volume percentage (x) of nitrogen in the producer gas recorded by the GC. The volumetric flow rate of producer gas ($\dot{V}$) is calculated using Equation 6.

Equation 6

$$\dot{V}_{producer\_gas} = \frac{\dot{n}_{Nitrogen\_out} \cdot M_{Nitrogen}}{\rho_{Nitrogen} \cdot x_{Nitrogen\_in\_producer\_gas}}$$

3.4.1.2 Carbon Balance

The carbon balance has two important properties. It can be used to verify the flow rate of producer gas calculated from the nitrogen balance, since the volumetric flow rate of producer gas is used to determine the molar flow rates of the CO, CO_2, CH_4, C_2H_2, C_2H_4, C_2H_6 and C_3H_8. It can also be used to determine the carbon conversion efficiency.

The carbon balance has one input which is the carbon from the fuel. But it has many outputs, as there is carbon in the char, CO, CO_2, CH_4, C_2H_2, C_2H_4, C_2H_6 and C_3H_8. As long as the molar flow rates of carbon into the system balance the molar flow rates of carbon out, as in Equation 1 the volumetric flow rate of producer gas calculated is correct. The molar flow rates of CO, CO_2, CH_4, C_2H_2, C_2H_4, C_2H_6 and C_3H_8 are calculated using volumetric flow rate of producer gas ($\dot{V}$), the density (ρ) and molecular weights (M) of gas as well as their volume percentages (x) in the producer gas recorded by the GC. This is demonstrated in Equation 7 where the format is the same as Equation 3

Equation 7

$$\dot{n}_i = \frac{\dot{V}_{producer\_gas} \cdot x_i \cdot \rho_i}{M_i}$$

Where *i* stands for CO, CO_2, CH_4, C_2H_2, C_2H_4, C_2H_6 or C_3H_8. With the molar flow rates of CO, CO_2, CH_4, C_2H_2, C_2H_4, C_2H_6 and C_3H_8 the carbon balance can be written as shown in Equation 8.

Equation 8

$$\dot{n}_{Carbon\_fuel} = \dot{n}_{Carbon\_char} + \dot{n}_{Carbon\_CO} + \dot{n}_{Carbon\_CO2} + \dot{n}_{Carbon\_CH4} + \dot{n}_{Carbon\_C2H2} + \dot{n}_{Carbon\_C2H4} + \dot{n}_{Carbon\_C2H6} + \dot{n}_{Carbon\_C3H8}$$

The molar flow rate ($\dot{n}$) of carbon in the fuel can be calculated from the mass flow rate ($\dot{m}$) of fuel, the volume percentage (*x*) of carbon in the fuel, and the molecular weight (*M*) of carbon. This is shown in Equation 9.

Equation 9

$$\dot{n}_{Carbon\_fuel} = \frac{\dot{m}_{fuel\_in} \cdot x_{C\_fuel}}{M_C}$$

The molar flow rate ($\dot{n}$) of carbon in the char can be calculated from the mass flow rate ($\dot{m}$) of char, the volume percentage (*x*) of carbon in the char, and the molecular weight (*M*) of carbon. The mass flow rate ($\dot{m}$) of char is just the mass collected divided by the duration of collection period. The molar flow rate ($\dot{n}$) of carbon in the char is shown in Equation 10.

Equation 10

$$\dot{n}_{Carbon\_char} = \frac{\dot{m}_{char} \cdot x_{C\_char}}{M_C}$$

The carbon balance can also be used to calculate the carbon conversion efficiency (η). This is done by taking the ratio of carbon converted to gas to carbon put into the system. To simplify the calculation only the carbon in the fuel and char is used. This is demonstrated in Equation 11.

Equation 11

$$\eta_{Carbon\_conversion} = \frac{\dot{n}_{Carbon\_fuel} - \dot{n}_{Carbon\_char}}{\dot{n}_{Carbon\_fuel}}$$

3.4.1.3 Hydrogen Balance

The hydrogen balance is used to get a theoretical amount of water vapor on a volume basis produced from the gasification reaction. The amount of water vapor in the producer gas should be on the range of 8-12 % volume as see in experimental tests [R]. Using Equation 1, the hydrogen balance can be created on a molar basis. The system has two inputs of hydrogen which are the dry fuel and the water in the fuel. Again there are several outputs, as there is hydrogen in the char, CH_4, C_2H_2, C_2H_4, C_2H_6, C_3H_8 and water vapor produced from the gasification reaction. By rearranging the molar hydrogen balance the molar flow rate of water vapor ($H_2O_{(v)}$) produced can be solved for as seen in Equation 12.

Equation 12

$$\dot{n}_{Hydrogen\_fuel\_H2O} = \dot{n}_{Hydrogen\_fuel} + \dot{n}_{Hydrogen\_fuel\_water} - \dot{n}_{Hydrogen\_char} - \dot{n}_{Carbon\_CH4} - \dot{n}_{Carbon\_C2H2} - \dot{n}_{Carbon\_C2H4} - \dot{n}_{Carbon\_C2H6} - \dot{n}_{Carbon\_C3H8}$$

The molar flow rates of CH_4, C_2H_2, C_2H_4, C_2H_6 and C_3H_8 are calculated using volumetric flow rate of producer gas ($\dot{V}$), the density (ρ) and molecular weights (M) of gas as well as their volume percentages (x) in the producer gas recorded by the GC. This is demonstrated in Equation 13.

Equation 13

$$\dot{n}_i = \frac{\dot{V}_{producer\_gas} \cdot x_i \cdot \rho_i}{M_i}$$

Where i stands for CH_4, C_2H_2, C_2H_4, C_2H_6 or C_3H_8.

The molar flow rate ($\dot{n}$) of hydrogen in the fuel can be calculated from the mass flow rate ($\dot{m}$) of fuel, the volume percentage (x) of hydrogen in the fuel, and the molecular weight (M) of hydrogen as demonstrated in Equation 14.

Equation 14

$$\dot{n}_{Hydrogen\_fuel} = \frac{\dot{m}_{fuel\_in} \cdot x_{H2\_fuel}}{M_{H2}}$$

The molar flow rate ($\dot{n}$) of hydrogen in the char can be calculated from the mass flow rate ($\dot{m}$) of char, the volume percentage (x) of hydrogen in the char, and the molecular weight (M) of hydrogen. The mass flow rate ($\dot{m}$) of char is just the mass collected divided by the duration of collection period. Equation 15 illustrates how to calculate the molar flow rate ($\dot{n}$) of hydrogen.

Equation 15

$$\dot{n}_{Hydrogen\_char} = \frac{\dot{m}_{char} \cdot x_{H2\_char}}{M_{H2}}$$

3.4.1.4 Oxygen Balance

The oxygen balance is also used to verify the flow rate of producer gas calculated from the nitrogen balance for a second time, since the volumetric flow rate of producer gas is used to calculate the molar flow rates of the CO and CO_2. The oxygen balance has three inputs which is the oxygen in the air used to fluidize the bed, the oxygen in the fuel and the oxygen in the water from the fuel. The outputs are the oxygen in the char, CO, CO_2 and H_2O. Using Equation 1, the oxygen balance can be written as shown in Equation 16.

Equation 16

$$\dot{n}_{Oxygen\_fuel} + \dot{n}_{Oxygen\_fuel\_H2O} + \dot{n}_{Oxygen\_air} = \dot{n}_{Oxygen\_CO} + \dot{n}_{Oxygen\_CO2} + \dot{n}_{Oxygen\_H2O} + \dot{n}_{Oxygen\_char}$$

The molar flow rates of CO and CO_2 are calculated using volumetric flow rate of producer gas ($\dot{V}$), the density (ρ) and molecular weights (M) of gas as well as their volume percentages (x) in the producer gas recorded by the GC. As shown in Equation 17.

Equation 17

$$\dot{n}_i = \frac{\dot{V}_{producer\_gas} \cdot x_i \cdot \rho_i}{M_i}$$

Where *i* stands for CO and CO_2. The molar flow rate ($\dot{n}$) of oxygen in the air can be calculated knowing the volume percentage (x) of oxygen in the air, the density (ρ) and molecular weight (M) of oxygen and the volumetric feed rate ($\dot{V}$) of air into the system as seen in Equation 18.

Equation 18

$$\dot{n}_{Oxygen\_air} = \frac{\dot{V}_{air\_in} \cdot x_{O2\_air} \cdot \rho_{O2}}{M_{O2}}$$

The molar flow rate ($\dot{n}$) of oxygen in the fuel can be calculated from the mass flow rate ($\dot{m}$) of fuel, the volume percentage (x) of oxygen in the fuel, and the molecular weight (M) of oxygen as demonstrated in Equation 19.

Equation 19

$$\dot{n}_{Oxygen\_fuel} = \frac{\dot{m}_{fuel\_in} \cdot x_{O2\_fuel}}{M_{O2}}$$

The molar flow rate of oxygen in the water from the fuel is solved by dividing the molar flow rate of hydrogen from the fuel water in half. The molar flow rate of hydrogen in the water from the fuel can be taken from Equation 12.

The molar flow rate ($\dot{n}$) of oxygen in the char can be calculated from the mass flow rate ($\dot{m}$) of char, the volume percentage (x) of oxygen in the char, and the molecular weight (M) of oxygen. The mass flow rate ($\dot{m}$) of char is just the mass collected divided by the duration of collection period. Equation 20 illustrates how to calculate the molar flow rate ($\dot{n}$) of oxygen.

Equation 20

$$\dot{n}_{Oxygen\_char} = \frac{\dot{m}_{char} \cdot x_{O2\_char}}{M_{O2}}$$

3.4.2 Mass Balance

From Newton's 2nd Law mass is neither created nor destroyed [ ]. Therefore a mass balance was conducted on the gasification system. The input sources of mass are the air used to fluidize the bed, the fuel converted to producer gas and the water in the fuel. The outputs are the producer gas, water vapor and the char created during the gasification reaction. The tar vapors are ignored as they are assumed to be of negligible weight compared to the rest of the components. The mass balance can be written in terms of mass flow rates ($\dot{m}$) as shown in Equation 21.

Equation 21

$$\dot{m}_{air} + \dot{m}_{dry\_fuel} + \dot{m}_{H2O\_fuel} = \dot{m}_{producer\_gas} + \dot{m}_{char} + \dot{m}_{H2Ov}$$

The mass flow rate of air is the volumetric flow rate of air multiplied by the density of air. The mass flow rate of fuel is set by the metering auger. This value is divided into a dry fuel and water using the moisture content of the fuel. The mass flow rate of producer gas is the

volumetric flow rate of producer gas multiplied by the density of the producer gas. The density of the producer gas can be solved using the ideal gas law, shown in Equation 22.

Equation 22

$$\rho_{producer\_gas} = \frac{P}{\frac{\vec{R}}{M_{producer\_gas}}T}$$

Where P is the pressure of the gas, T is the temperature of the gas, $\vec{R}$ is the ideal gas constant and $M_{producer\_ga}$ is the molecular weight of the producer gas. The molecular weight of the producer gas is solved by summing the molecular weights of each gas multiplied by its volume fraction in the producer gas as shown in Equation 23.

Equation 23

$$M_{producer\_gas} = \sum_i M_i \cdot x_i$$

Where i stands for CO, CO_2, CH_4, C_2H_2, C_2H_4, C_2H_6 and C_3H_8.

The mass flow rate of char is the weight of char collected during the experiment divided by the duration of the experiment. The mass flow rate of water vapor is the molar flow rate of water vapor multiplied by the molecular weight of water vapor. The molar flow rate of water vapor is solved with Equation 12.

3.4.3 Fabric Filter Efficiency

The purpose of the research was to test the filtration efficiency the high temperature fabric filter. This was accomplished using the mass concentration (c) of particulate upstream and downstream of the fabric filter. The equation for the efficiency of the fabric filter is shown in Equation 24.

Equation 24

$$\eta_{fabric} = \frac{c_{upstream} - c_{downstream}}{c_{upstream}}$$

The downstream mass concentration is calculated using the isokinetic sample line downstream of the fabric filter. This was accomplished by taking the mass caught in the quartz thimble filter divided by the volume of gas sampled. The upstream mass concentration was back calculated from the downstream mass concentration. This was done by adding the mass collection rate for the fabric filter to the downstream mass concentration. The mass collection rate for the fabric filter is the mass collected on the fabric filter divided by the time period the fabric filter was open.

4. RESULTS

4.1 Mass balances on the particulate filter

Mass and elemental balances were constructed to calculate and verify the results obtained for the efficiency of the fabric filter. Detailed results of these experiments can be found in Appendix D. The uncertainty in the results was determined by doing an uncertainty analysis. The approach for the uncertainty analysis is shown in Appendix E and sample calculations can be found in Appendix C.

Mass, carbon, and oxygen balances were used to verify the results obtained from the nitrogen and hydrogen balances for the gas flow rate in the system and percentage of water vapor in the products. Since these were the only two unknowns needed to complete all the molar and mass balances for the system. As the inlet molar and mass flow rates of air and fuel for the gasification system were controlled by an air mass flow controller and metering fuel auger; and the outlet mass flows of char could be measured by weighing the char caught in the particulate removal devices: cyclone, fabric filter, and quartz thimble filter.

4.1.1 Nitrogen Balances

A nitrogen balance was constructed for each experiment to determine the gas flow rate in the system because there was only one unknown needed to complete balance, which was the outlet molar flow rate of nitrogen from the system. Therefore, the nitrogen balance was balanced to 100 %v to determine the outlet molar flow rate of nitrogen. With all the components of the nitrogen balance, an uncertainty analysis was performed.

The average uncertainty of all the nitrogen balances was 7.1412 %v with a standard deviation of 0.1263 %v. A graph of the nitrogen balances for the 12 experiments performed is shown in Figure 16.

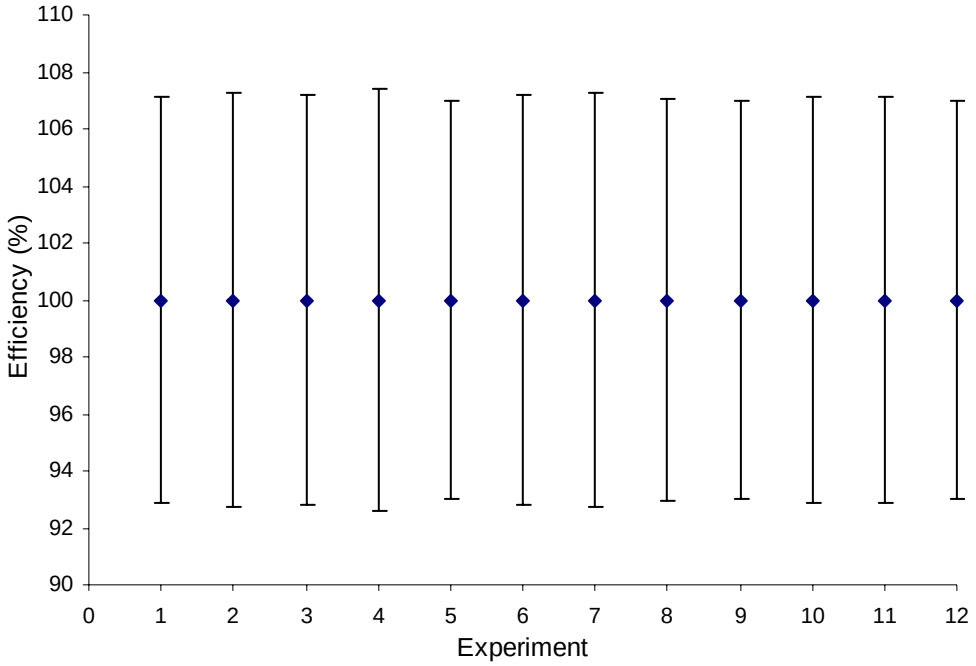

Figure 16 : Nitrogen balances

With the outlet molar flow rate of nitrogen and the volume percentage of nitrogen in the producer gas, from the Gas Chromatograph (GC), the flow rate of producer gas in the system was calculated. Figure 17, shows a plot of the producer gas flow rates and their calculated uncertainties. The flow rates ranged from 88.941 to 100.075 slpm with an average uncertainty of 4.722 +/- 0.2306 slpm.

The variations in flow rate are due to changes in reactions rates in the bed between experiments. The exact cause for reaction rate changes between experiments is unknown. But it is assumed to be a function of the differences in operating conditions between experiments, consisting of variations in reactor temperature and pressure, fuel and air feed rates, as well as the age of the sand and limestone bed within the reactor.

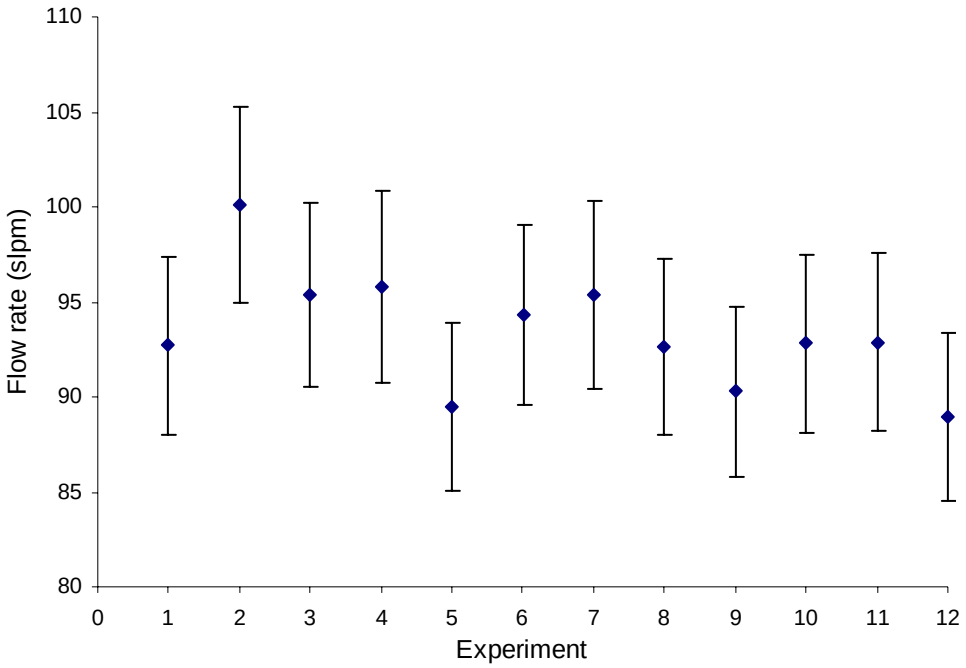

Figure 17 : Gas flow rates through the gasification system

4.1.2 Hydrogen Balances

A hydrogen balance was constructed to obtain the percentage of water in the products created during the gasification reaction. As it was difficult to quantify the amount of water vapor in the products, since it was condensed out with the tar vapors by a train of impingers emerged in an ice bath.

Since all input molar flow rates of hydrogen were known and the outlet molar flow rates of hydrogen from the producer gas could be calculated with the flow rate of producer gas and the gas composition, from the GC analysis. The hydrogen balance was balanced to 100 %v to calculate the molar flow rate of hydrogen in the water vapor. The hydrogen balances from the 12 experiments are shown in Figure 18, with an average uncertainty of 10.2352 +/- 0.1104 %v.

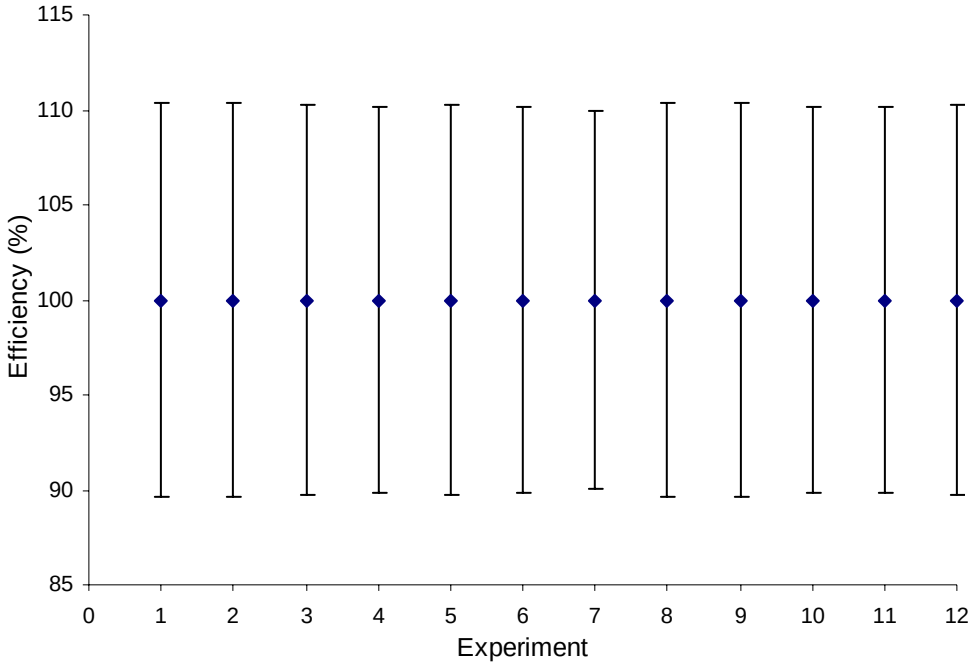

Figure 18 : Hydrogen balances

With the molar flow rate of hydrogen in the water, the molar flow rate of water vapor was calculated. The molar flow rate of water vapor in conjunction with the molar flow rates of components in the producer gas were used to calculate the percentage of water vapor in the products created from the gasification reaction during each experiment. The percentage of water vapor produced ranged from 2.738 to 10.443 %v with an average uncertainty of 2.583 +\- .1236 %v (seen in Figure 19). The wide variation in results is due to changes in the reactors operating temperature between experiments. The temperature in the reactor during early experiments was allowed to increase during the experiment, reaching temperatures of 718-732°C (1325-1350°F); while the temperature in later experiments was held around 700°C (1300°F). The trend of the percentage of water in the products increasing as the temperature during the reaction was lowered follows results discovered by Ming Xu (et al. 2005).

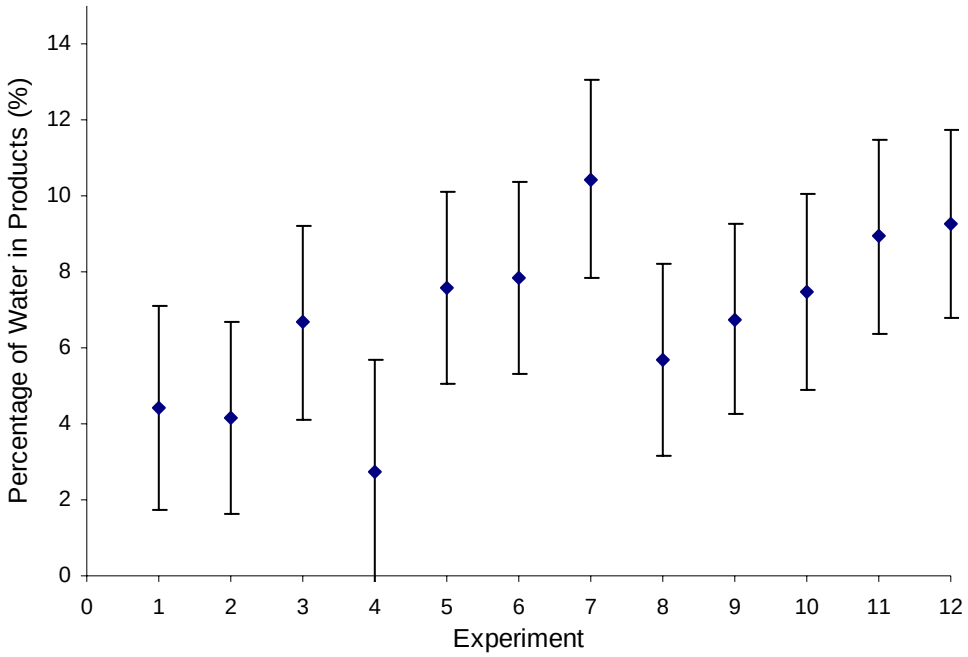

Figure 19 : Percentage of water produced during gasification reactions

4.1.3 Mass Balances

The mass balance was used to verify the calculated values of the producer gas flow rate and the percentage of water vapor in the products for each experiment. As the producer gas flow rate was used to calculate the mass flow rates of producer gas constituents and the percentage of water vapor was used to calculate the mass flow rate of water vapor produced from the gasification reaction. All other aspects of the mass balances were measured from inputs or outputs to the system. The results from the mass balances are shown in Figure 20. The balances average to 103.6544 +/- 1.2507 %v with an average uncertainty of 4.514 +/-.059437 %v. As, all the mass balances except two encase 100% within the uncertainty bounds the method for calculating the producer gas flow rates and percentage of water vapor in the products was verified.

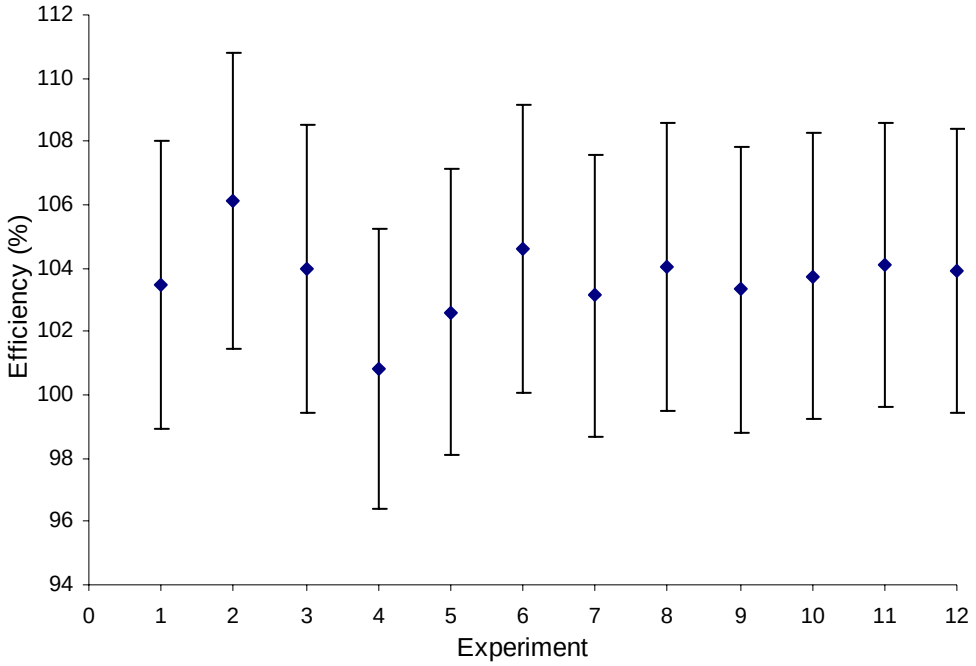

Figure 20 : Mass balances

4.1.4 Carbon Balances

The carbon balance was used to verify the calculated values of the producer gas flow rate for each experiment. As the producer gas flow rate was used to calculate the molar flow rates of producer gas constituents from the gasification reaction. All other aspects of the carbon balances were measured from inputs or outputs to the system. The results from the carbon balances are shown in Figure 21, they average to 109.2806 +/- 3.9697 %v with an average uncertainty of 7.7568 +/- .2476 %v. Since all the uncertainty bounds of the carbon balances are with in 10% of balancing the method for calculating the producer gas flow rates was verified.

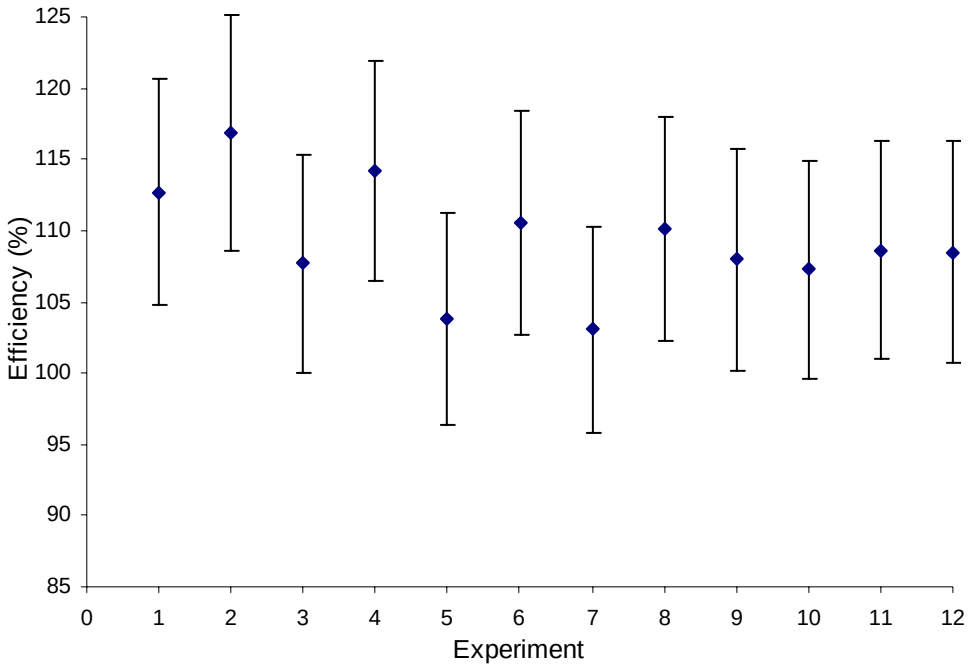

Figure 21 : Carbon balances

4.1.5 Oxygen Balances

The oxygen balance was used to verify the calculated values of the producer gas flow rate and the percentage of water vapor in the products for each experiment. As the producer gas flow rate was used to calculate the molar flow rates of producer gas constituents and the percentage of water vapor was used to calculate the molar flow rate of water vapor produced from the gasification reactions. All other aspects of the oxygen balance were measured from inputs or outputs to the system. The results from the oxygen balances are shown in Figure 22. The balances average to 107.1177 +/- 4.0735 %v with an average uncertainty of 7.9206 +/-.1298 %v. Since all the oxygen balances near 100% within the uncertainty bounds and most balances are within 10% of balancing, the method for calculating the producer gas flow rates and percentage of water vapor in the products was verified.

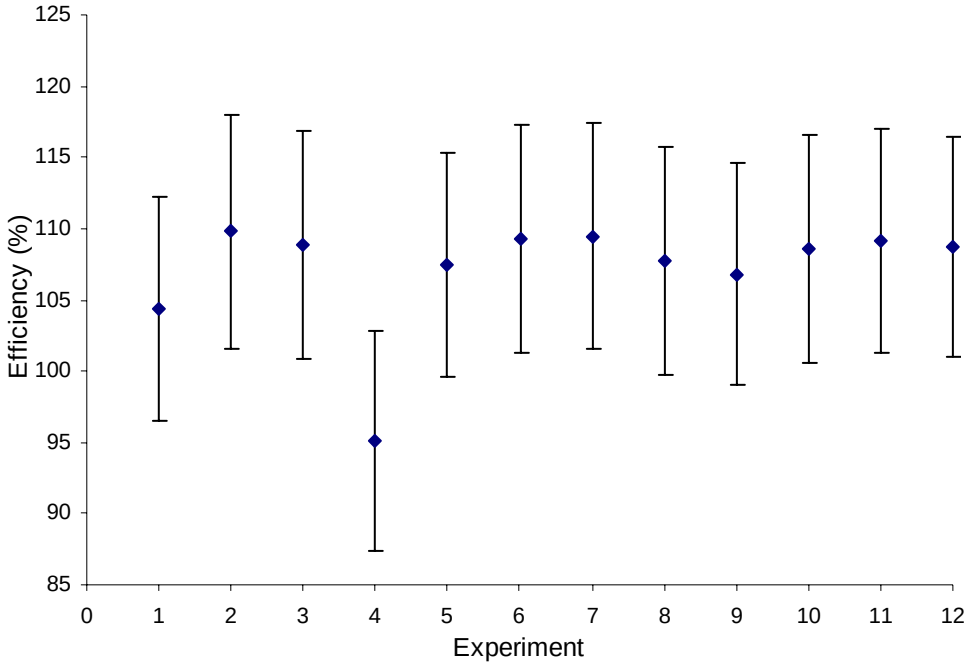

Figure 22 : Oxygen balances

4.2 Filtration Performance

The performance of the fabric filter was the most important aspect of the project. Twelve experiments were performed to verify that the FB700, 3M's high temperature fabric, would filter greater than 99.9% of the char out of the producer gas. To determine the filtration efficiency during each experiment the mass concentration of particulate downstream and upstream of the fabric filter were used. The downstream concentration was calculated using the quartz thimble filter in the sample line and the upstream concentration was back calculated off the mass caught by the fabric filter.

Between each experiment the fabric was cleaned by vacuuming off the dust cake. This was done to reduce the pressure differential over the fabric to avoid damaging the system. As it would be difficult for the system to handle large pressure differentials because the reactor was operated at atmospheric pressure.

The efficiencies for each experiment are shown in Figure 23.

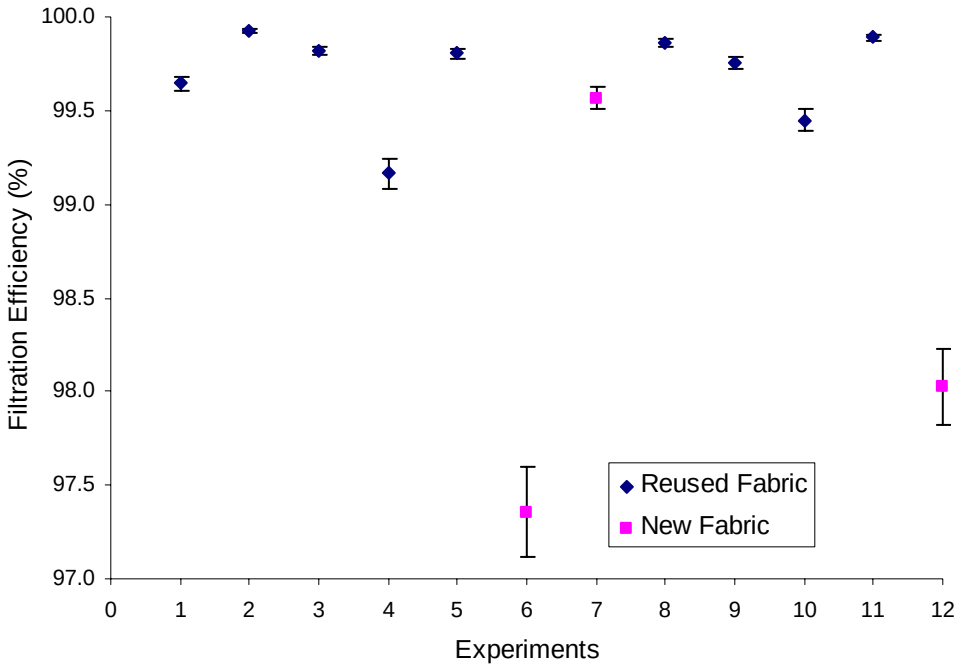

Figure 23: Filtration efficiency vs. experiments

The trend with the uncertainties decreasing as the filtration efficiency approaches 100%, is a result of the mass concentration calculated downstream of the fabric filter. The equation for the uncertainty (σ) in the filtration efficiency is Equation 25; where con_{UP} is the mass concentration upstream of the fabric filter, con_{DS} is the mass concentration downstream of the fabric filter, σ_{UP} is the uncertainty in the upstream mass concentration, and σ_{DS} is the uncertainty in the downstream mass concentration.

Equation 25

$$\sigma_{Filtration\_EFF} = \sqrt{\left(\frac{1}{con_{UP}}\right)^2 \sigma_{DS}{}^2 + \left(\frac{-con_{DS}}{con_{UP}{}^2}\right)^2 \sigma_{UP}{}^2}$$

As it turns out the second term in the square root, $\left(\frac{-con_{DS}}{con_{UP}{}^2}\right)^2 \sigma_{UP}{}^2$, is a factor of 10 or greater than the first term in the square root, $\left(\frac{1}{con_{UP}}\right)^2 \sigma_{DS}{}^2$. Since the value of the second term is dependant on the concentration downstream of the fabric filter. The dependence on the downstream concentration leads to a fairly consistent relationship between uncertainty in the fabric filtration efficiency and the square of the mass concentration downstream of the fabric, as seen in Figure 24.

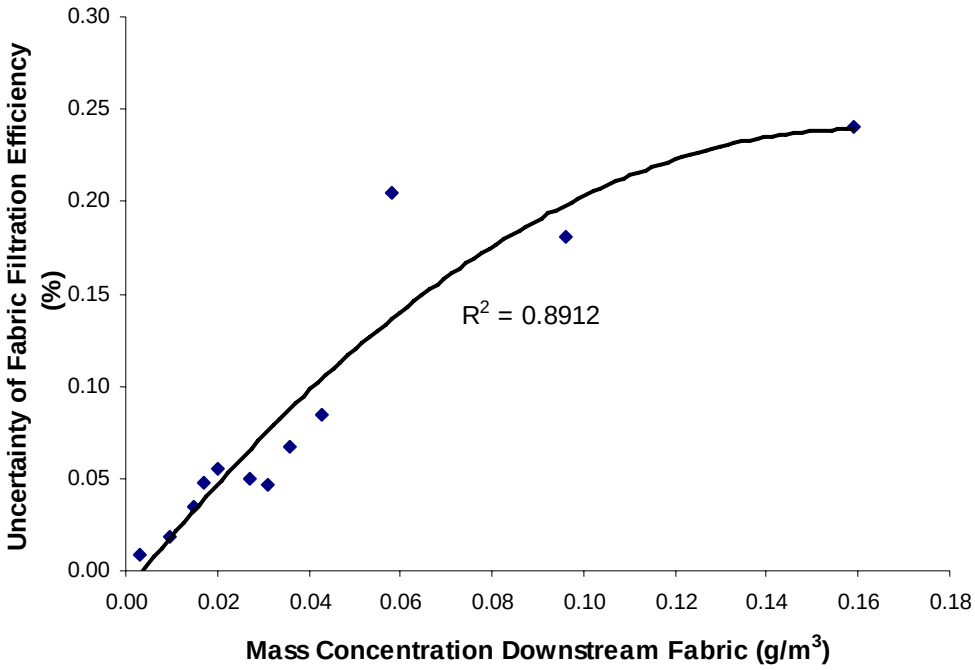

Figure 24: Effect of fabric filtration efficiency due to mass concentration downstream of the fabric

Going back to Figure 23, the times when the fabric was replaced were lumped into a separate category, labeled "New Fabric", as the fabric is in a transitional phase during the first time it is used. The transitional phase is a period during which the fabric becomes saturated with fine particulate that acts to increase the filtration efficiency of the fabric. The fine particulate stays entrained in the fibers of the fabric during cleaning which is proven by a Scanning Electron Microscope (SEM) shown in Figure 25. This is why the reused fabric experiments see filtration efficiencies above 99%.

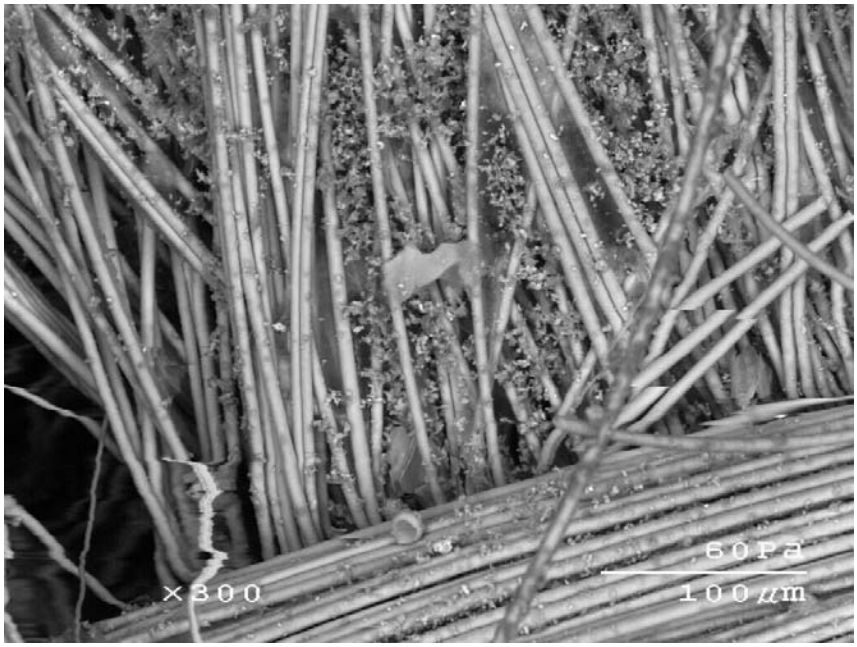

Figure 25 : SEM of used fabric after cleaning

Since filtration efficiencies of 99.9+% were not seen further analysis was performed on the fabric filter. In later tests the ability of the dust cake to increase filtration efficiency was studied. As the efficiency of the fabric filter should increase as the dust cake develops because the pores in the cake become smaller [14].

During each experiment the filtration efficiency of the fabric was determined during the development of the dust cake and after a dust cake had developed. The first filtration efficiency was calculated during the first 4-5 hours of the development of the dust cake. While the second filtration efficiency was calculated over a 1-4 hour time period, roughly 2 hours after the first filtration period was ended. The 2 hour segment in between filtration periods was used to change the quartz thimble filter, which was used to calculate the mass concentration downstream of the fabric filter. The results from these experiments are shown in Figure 26.

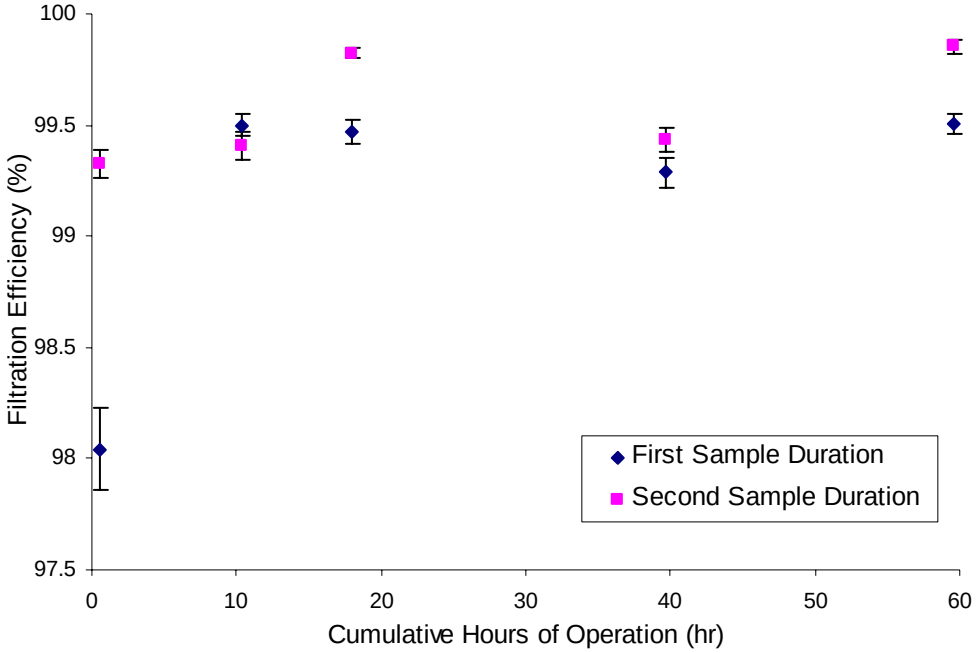

Figure 26 : Effect of dust cake and fabric usage on filtration efficiency

From the figure it is seen that the filtration efficiency increases as the dust cake develops, as expected. Another interesting result shown by Figure 26 is the saturation phenomenon discussed previously. Since all the experiments done to create Figure 26 were completed using the same piece of fabric, it seen that there is a lower filtration efficiency during the first time the fabric was used due to the saturation phenomenon.

Although filtration efficiencies of 99.9+% were not seen in these tests either, the fabric filtration is assumed to be greater than 99.9% from SEM analyses performed on the quartz thimble filters used to calculate the downstream mass concentration. Figure 27, Shows SEM analyses from two tests that prove the filtration efficiency becomes very efficient after the dust cake has developed.

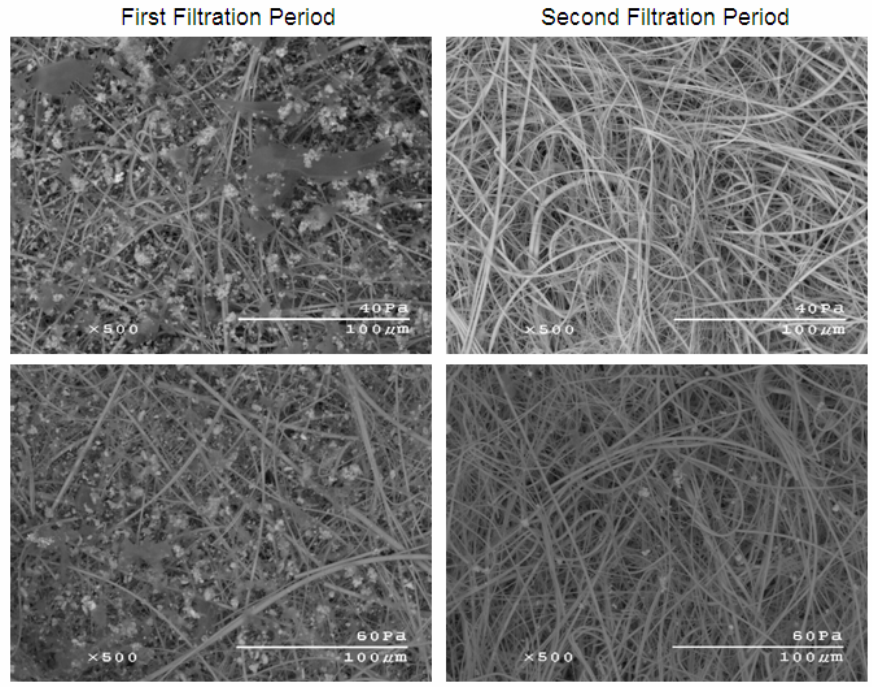

Figure 27 : SEM analyses of the quartz thimble filters during the first and second filtration periods

On the left side are the thimble filters used in determining the filtration efficiency during the development of the dust cake and on the right side are the thimble filters used in determining the filtration efficiency after a dust cake had developed. The first test shows nothing in the second thimble filter suggesting > 99.9% filtration. The second test shows small amounts of particulate caught in the filter, which were linked to alkali materials (Phosphorus, Potassium, and Calcium) by an X-ray map of the sample. Also suggesting > 99.9% filtration, since alkali solids are condensed vapors from the gasification reaction.

Although the SEM analyses in Figure 27 are only for two points on the graph in Figure 26, it assumed that the slightly low filtration efficiencies in all tests are due to condensation of either tar vapors or alkali compounds. This hypothesis is proven by two other SEM pictures and X-ray maps, shown in Figure 28 and Figure 29, performed on two other second half thimble filters from the graph in Figure 26.

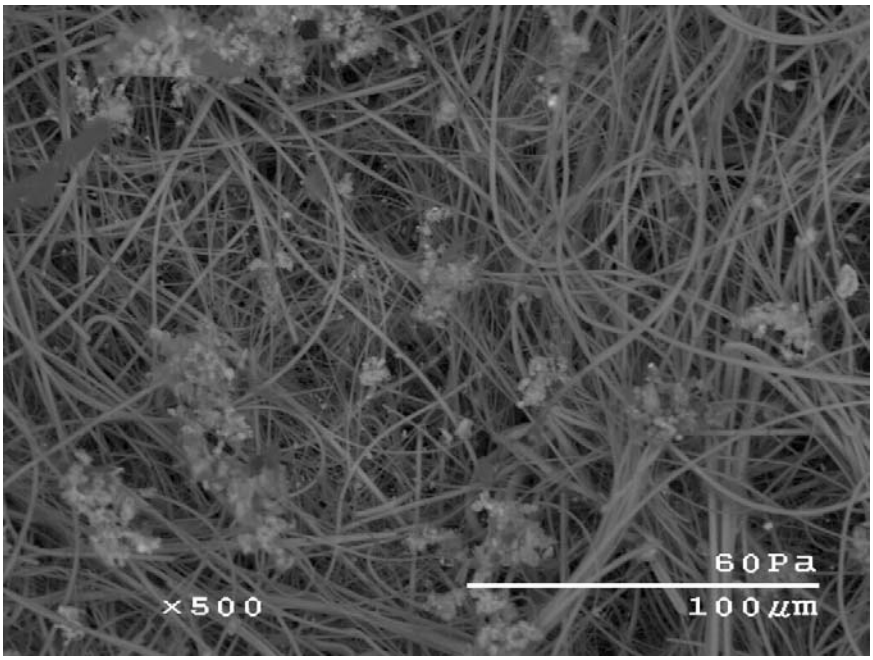

a) SEM of quartz thimble filter

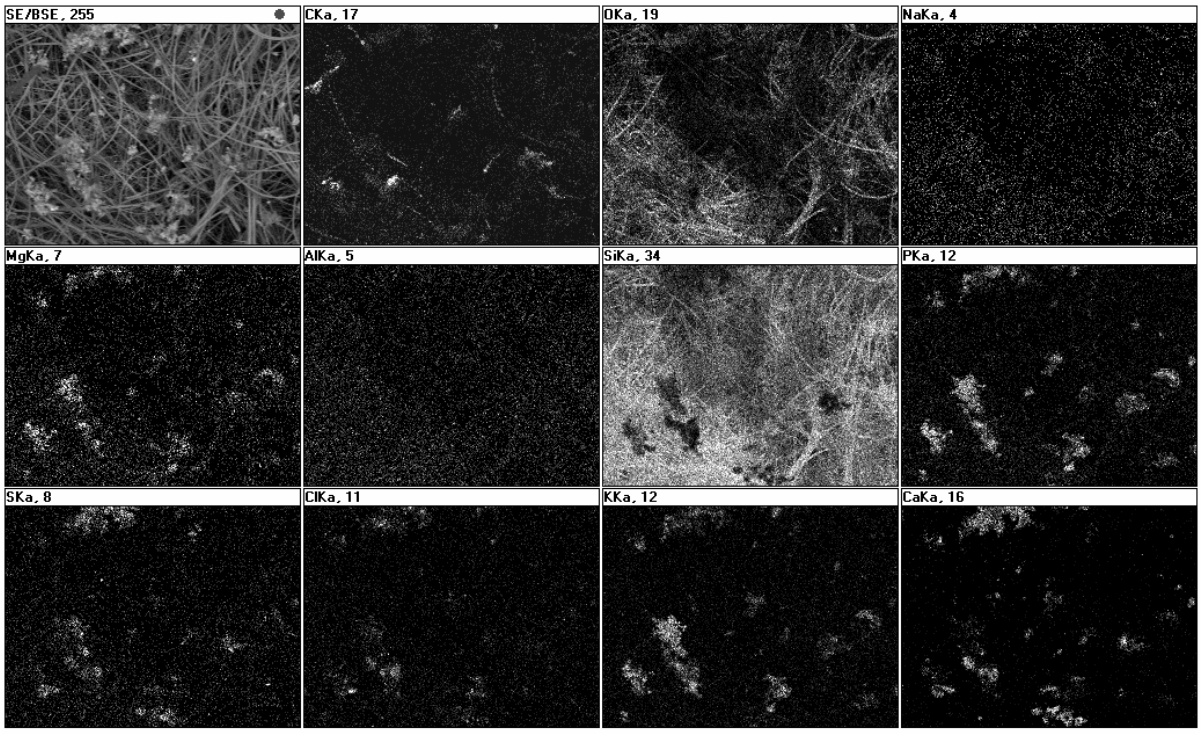

b) X-ray map of SEM sample

Figure 28 : X-ray map and SEM of quartz thimble filter during second filtration period

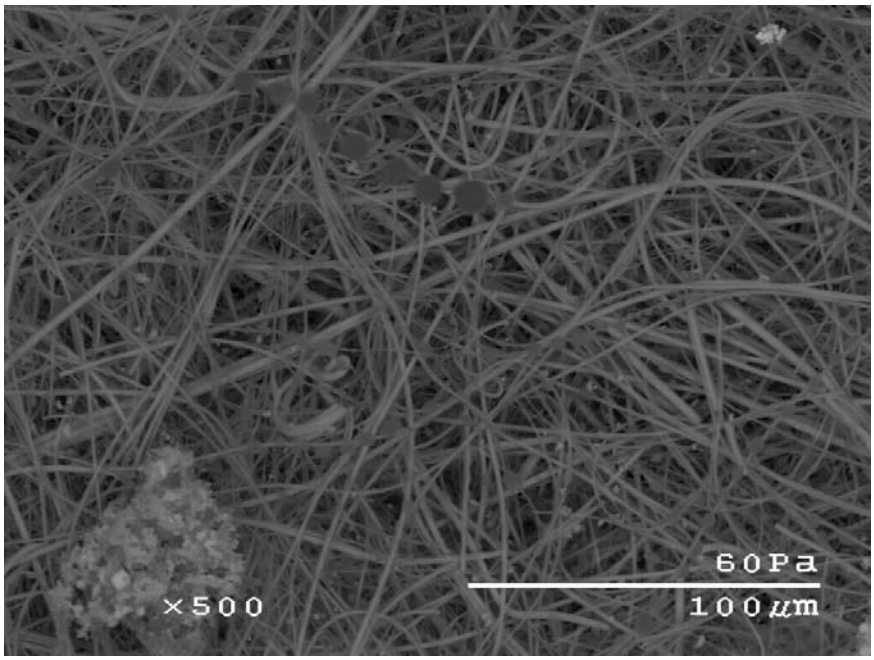

a) SEM of quartz thimble filter

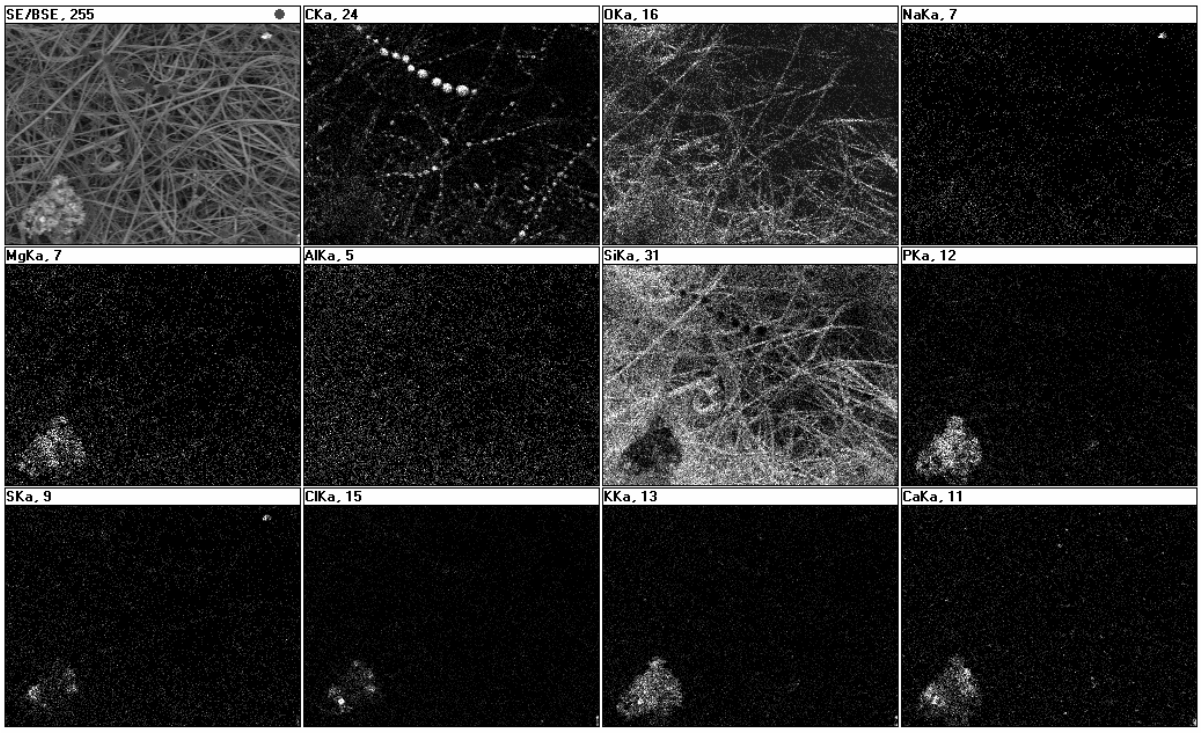

b) X-ray map of SEM sample

Figure 29 : X-ray map and SEM of quartz thimble filter during second filtration period

These X-ray maps show that tars vapors condensed on the fibers of the thimble filter and that particulate trapped by the thimble filter is composed of phosphorus, potassium, calcium,

sulfur, chlorine, and magnesium not carbon as would be expected if the particulate was char. Since char is composed of 40-60% carbon.

4.2.1 Items Affecting Filtration Performance

With ability of the fabric to achieve high filtration efficiencies and the dust cake's ability to increase the filtration efficiency during cake development known, the effect of pressure drop across the filter element, filtration time, and mass loading on filtration efficiency was studied. Since the differential pressure across a fabric filter is suppose to increase as the dust cake develops [15] and the dust cake development has been linked to improvements in filtration efficiencies. It was assumed that the filtration efficiency would increase with an increasing pressure differential because the cake development was linked to increases in filtration efficiency. This was not discovered, as seen in Figure 30.

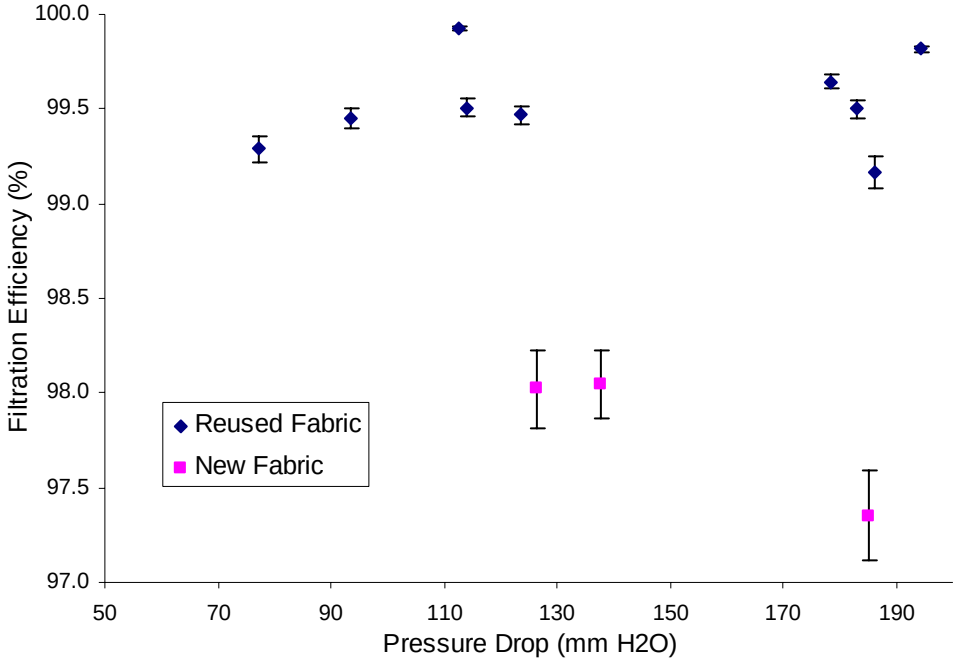

Figure 30 : Effect of pressure drop on filtration efficiency

Since the pressure drop across the fabric filter was not linked to the filtration efficiency, the filtration time was examined for a correlation between the time of filtration and the filtration efficiency. As with the pressure drop there were no similarities discovered between the filtration time and filtration efficiency, seen in Figure 31.

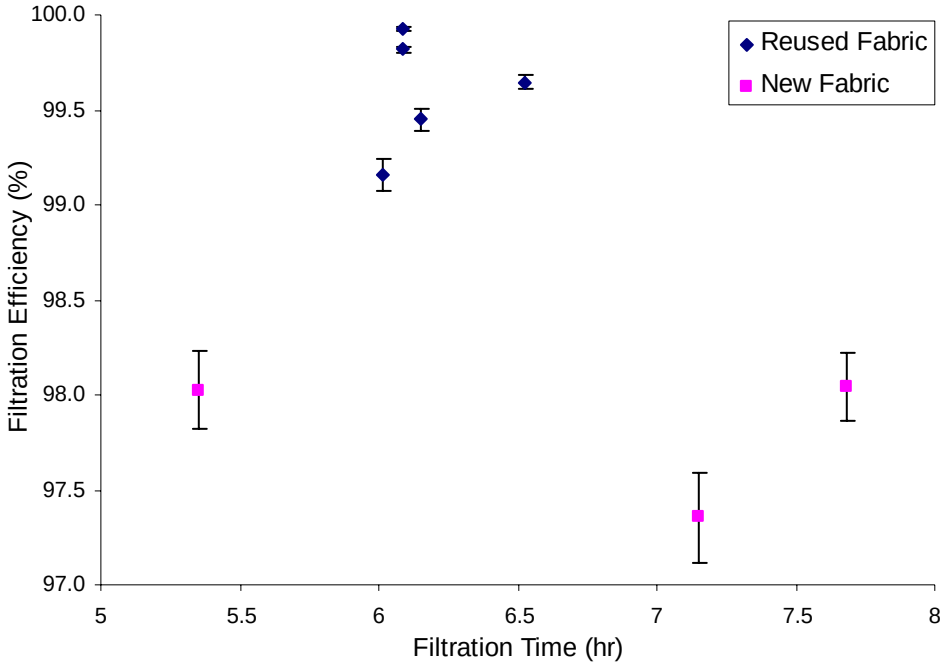

Figure 31 : Effect of filtration time on filtration efficiency

With no linkages between either pressure drop or filtration time and efficiency the mass concentration (mass loading) at the inlet to the fabric filter was studied with respect to the filtration time and differential pressure across the filter. There was no relationship discovered between the mass loading, filtration time and filtration efficiency. There was also no relationship discovered between the mass loading pressure drop across the filter and the filtration efficiency. Data from the twelve experiments is compiled into Table 4. Experiment numbers 5, 6, and 12 are experiments where new pieces of fabric were used.

Table 4 : Compiled data from 12 experiments

	Mass Conc. Inlet		Fabric Filter Eff.		Filtration	Press Drop	Rate Press Drop Inc.
Experiment	g/m^3	stdev	%	stdev	Time (hrs)	mm h2o	mm h2o
1	4.244	0.273	99.645	0.035	6.528	178.406	27.330
2	4.100	0.269	99.928	0.008	6.083	112.643	18.517
3	5.309	0.324	99.818	0.018	6.086	194.337	31.930
4	5.119	0.337	99.162	0.085	6.014	186.204	30.963
5	5.999	0.331	97.353	0.240	7.683	185.010	24.079
6	4.915	0.275	98.044	0.181	5.350	137.874	29.916
7	6.179	0.348	99.500	0.047	4.717	183.001	38.666
8	5.012	0.281	99.469	0.050	4.667	123.749	26.030
9	5.030	0.277	99.289	0.067	4.500	77.084	14.347
10	3.585	0.236	99.449	0.055	6.150	93.637	15.392
11	3.477	0.207	99.504	0.048	4.617	113.980	25.892
12	2.922	0.180	98.023	0.205	7.153	126.495	17.685

The difference in the experimental results and the expected for the effects of pressure drop, filtration time, and the mass concentration on filtration efficiency is perhaps due to changes

in char composition between experiments. Figure 32, shows SEM analysis of the dust cake from four different experiments. From these SEM analyses it is seen that the char is not a constant shape or size, which may have an effect on the formation of the dust cake. But according to Mckenna, J.D. and Haley, L.H. Jr. (1986) there may not be enough data collected to make a claim about the relationships between pressure drop, filtration time, and mass concentration vs. filtration efficiency for the FB700©, high temperature filtration fabric.

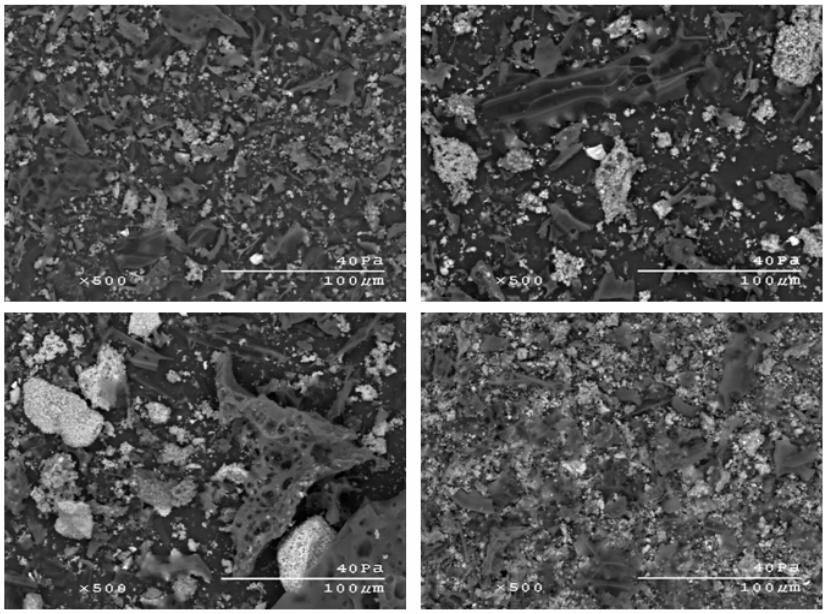

Figure 32 : SEM of 4 dust cake samples from 4 experiments

4.3 Theoretical Efficiencies

The operating conditions for the fabric filter where used to obtain a theoretical efficiency range for the fabric filter. These calculations were based on three modes of particle capture: interception, inertial impaction, and diffusion. For all three methods the size of particulate being capture is important. Therefore, to start the average particle size for each experiment was calculated from the mass caught on the filter through equations taken form Ergudenlar, Ali (et al., 1996). Since the cake thickness, t, was not measure it was calculated with Equation 26; where m_{cake} is the mass of the cake, R_i is the radius of the filter fabric filter, L is the length of the filter, and ρ_B is the bulk density of the char on the filter cake.

Equation 26

$$t = \sqrt{\left(\frac{\frac{m_{cake}}{\rho_B L} + \pi R_i}{\pi}\right)} - R_i$$

With the thickness of the cake the average particle size, d_v, was calculated using Equation 27; where C is the Carman-Kozeny constant, μ is the dynamic viscosity of the gas, U is the face

velocity, ΔP_{cake} is the pressure drop across the filter, ε is the packing density of the cake or voidage factor, and ϕ is the sphericity of the particles.

Equation 27

$$d_v = \sqrt{\frac{tC\mu(1-\varepsilon)^2 U}{\Delta P_{cake}\phi^2\varepsilon^3}}$$

The dynamic viscosity, μ, of the producer gas was calculated using Equation 28 where values of m and μ_o taken from Golubev, I.F. (1970), where T_o is zero degrees Celsius, μ_o is the viscosity of the gas at zero degrees Celsius, m is a constant dependant on the type of gas, and x is the fraction of the gas in the producer gas. The fractions of gases in the producer gas were solved by using the gas composition taken from the Gas Chromatograph (GC) and adjusting the fractions accordingly so all fractions summed to one.

Equation 28

$$\mu = \sum_i \mu_{o_i} \left(\frac{T}{T_o}\right)^{m_i} x_i$$

In Equation 28, i represents nitrogen (N_2), hydrogen (H_2), methane (CH_4), carbon dioxide (CO_2), carbon monoxide (CO), ethane (C_2H_6) and propane (C_3H_8). Acetylene (C_2H_2) and Ethylene (C_2H_4) were ignored for the viscosity calculation because values for Equation 28 were not found and the fractions of C_2H_2 and C_2H_4 in the producer gas are small.

The theoretical efficiencies were calculated using the following equations from Hinds, W.C. (1999), where E is the total efficiency, E_R is the single fiber efficiency for interception, E_l is the single fiber efficiency for inertial impaction, E_D is the single fiber efficiency for diffusion, E_{DR} is the enhanced diffusion efficiency due to interception of diffusing particles:

$$E = 1-(1-E_R)(1-E_l)(1-E_D)(1-E_{DR})$$ **Equation 29**

$$E_R = \frac{(1-\alpha)R^2}{Ku(1-R)}$$ **Equation 30**

In Equation 30, α is the solidity, Ku is the Kuwabara hydrodynamic factor which is a function of the solidity shown in Equation 31, and R is the ration of the particle diameter to the fiber diameter.

Equation 31

$$Ku = -\frac{\ln\alpha}{2} - \frac{3}{4} + \alpha - \frac{\alpha^2}{4}$$

The single fiber efficiency for inertial impaction shown in Equation 32 is a function of the Stokes number (Stk) the Kuwabara hydrodynamic factor (Ku) and a function, J. Since all values of R were greater than 0.4, J was simplified to equal 2.

Equation 32

$$E_l = \frac{(Stk)J}{2(Ku)^2}$$

The Stokes number is a function of the particle density (ρ_p), particle diameter (d_p), face velocity (U), gas viscosity (μ), and the diameter of the fiber (d_f) shown in Equation 33.

Equation 33

$$Stk = \frac{\rho_p d_p^{\,2} U}{18 \mu d_f}$$

The single fiber efficiency for diffusion shown in Equation 34 is a function of the Peclet number, Pe.

Equation 34

$$E_D = 2Pe^{-2/3}$$

The enhanced diffusion filtration efficiency due to interception of diffusing particles is a function of the Peclet number (Pe), the Kuwabara hydrodynamic factor (Ku) and the ratio of particle diameter to fiber diameter.

Equation 35

$$E_{DR} = \frac{1.24R^{2/3}}{(Ku \cdot Pe)^{1/2}}$$

The Peclet number, Pe, in Equation 34 and Equation 35 is a function of the fiber diameter (d_f), the face velocity and the diffusion coefficient for the particle (D) as shown in Equation 36.

Equation 36

$$Pe = \frac{d_f U}{D}$$

Table 5, has results from the theoretical efficiency calculations performed. The efficiencies are dependant on the average particle size calculated from Equation 27. The average particle size varied from 4.509 to 7.849 µm. These are reasonable values as the cyclone upstream of the fabric filter is efficient in removing particles down to 10 µm.

Table 5 : Theoretical efficiency results

dv	Stokes	Er	El	Ed	Edr	Eff
4.853	0.0527	65.26	21.18	0.90	2.65	73.59
6.017	0.0809	90.60	32.52	0.78	2.75	93.88
5.164	0.0595	71.84	23.91	0.86	2.68	79.32
5.000	0.0558	68.35	22.43	0.88	2.66	76.31
6.037	0.0812	91.06	32.63	0.78	2.74	94.19
4.992	0.0557	68.18	22.39	0.88	2.66	76.18
4.906	0.0535	66.36	21.51	0.89	2.65	74.52
5.458	0.0662	78.18	26.61	0.83	2.69	84.55
7.849	0.1241	133.79	49.86	0.61	2.73	116.38
6.142	0.0833	93.43	33.48	0.76	2.74	95.78
4.509	0.0445	58.17	17.89	0.93	2.59	66.85
5.158	0.0587	71.70	23.58	0.86	2.66	79.13

The efficiencies calculated for the average particle diameters ranged from 66.85 to 100 %. Again the efficiencies are dependant on the particle size, so as the particle diameter increases

so does the efficiency. These efficiencies only account for the interactions of one fiber so it is not surprising that most of the efficiencies are below those found experimentally because the fabric filter is complex mat of woven fibers which increases interactions between particles and fibers. It is also not surprising that the most dominate particle capture mechanisms are interception and inertial impact as diffusion is only relevant for particle diameters in the submicron range, as seen by Figure 33.

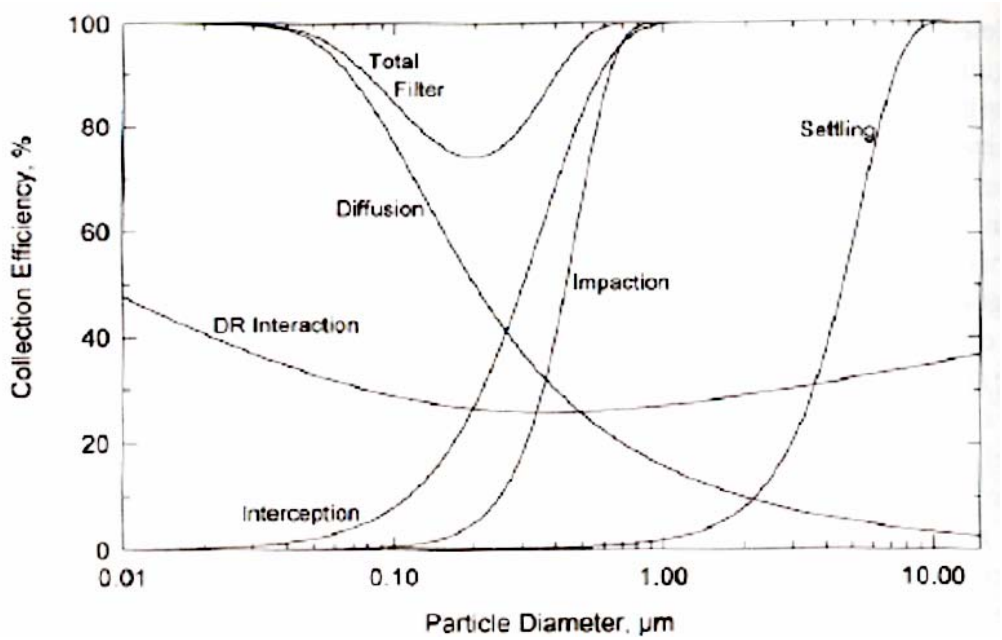

Figure 33 : Comparison of particle capture mechanisms with particle diameters vs. filtration efficiency [9]

5. CONCLUSIONS

Particulate filtration tests with a barrier filter constructed of FB700 high temperature fabric manufactured by 3M typically removed greater than 99% of particulate matter from the producer gas. This level of filtration meets the requirements of an internal combustion engine and should greatly exceed the requirements for more robust Stirling engines.

Thus, it appears technically feasible to integrate a biomass gasifier with a Stirling engine as part of a distributed biomass power system. Unfortunately, the company that was to supply us a Stirling engine suspended manufacture of engines soon after we placed our order with them. The project was cancelled when it became clear that no other Stirling engine companies would supply us with an engine of the size required for the planned demonstration.

REFERENCES

[1] Croom, M.L. (1995). *Filter Dust Collectors: Design and Application.* United States: McGraw-Hill, Inc.

[2] Cushing, K.M., Meritt, R.L. & Chang, R.L. (1990). Operating History and Current Status of Fabric Filters in the Utility Industry. Air & Waste Management Association, 40(7):1051-1058.

[3] Deffeyes, K.S. (2005). *Beyond Oil The view from Hubbert's Peak.* New York, Hill and Wang.

[4] Demirbas, A. and Meydan, F. (2004). Utilization of Biomass as Alternative Fuel for External Combustion Engines. Energy Sources 26:1219-1226.

[5] Duncan, R.C. and Youngquist, W. The World Petroleum Life-Cycle. Oct. 1998

[6] Donovan, R.P. (1985). *Fabric Filtration for Combustion Sources: Fundamentals and Basic Technology.* New York, NY: Marcel Dekker, Inc.

[7] Emsick, Nathan (2004). Switchgrass derived producer gas as a reburn fuel.

[8] Giampaolo, Tony. (2003). *The Gas Turbine Handbook: Principles and Practices.* Lilburn, GA, Fairmont Press, Inc.

[9] Hinds, W.C. (1999) *Aerosol Technology: properties, behavior and measurement of airborne particles.* New York, Wiley, Inc.

[10] Hesketh, Howard E. (1991). *Air Pollution Control Traditional and Hazardous Pollutants.* Lancaster, Pennsylvania, Technomic Publishing Company, Inc.

[11] Heumann, William L. (1997). *Industrial Air Pollution Control Systems.* McGraw Hill

[12] Lu, Hsin-Chung & Tsai, Chuen-Jinn (1998). A Pilot-Scale Study of the Design and Operation Parameters of a Pulse-Jet Baghouse. Aerosol Science and Technology, 29:510-524.

[13] Muller-Steinhagen, H. (2000). *Heat Exchanger Fouling – Mitigation and Cleaning Technologies.* Germany, PUBLICO Publications

[14] Mycock, J.C., McKenna, J.D. & Theodore, L. (1995). *Handbook of Air Pollution Control Engineering and Technology.* Boca Raton, FL: CRC Press, Inc.

[15] Schnelle, K.B. Jr. & Brown, C.A. (2002). *Air Pollution Control Technology Handbook.* Boca Raton, FL: CRC Press LLC.

[16] Vollaro, Robert F. (1977). Recommended Procedure for Sampling Traverses in Ducts Smaller Than 12 Inches in Diameter. U.S. Environmental Protection Agency, Emissions Measurement Branch, Research Triangle Park, North Carolina.

[17] Wark, K., Warner, C.F., Davis, W.T. (1998). *Air Pollution Its Origin and Control,* Addison Wesley Longman, Inc.

[18] White, Lloyd R. (1991). Ceramic Filters for use at High Temperature. The American Society of Mechanical Engineers, 91-GT-188

LEGAL NOTICE

APPENDIX A

Cage Drawings

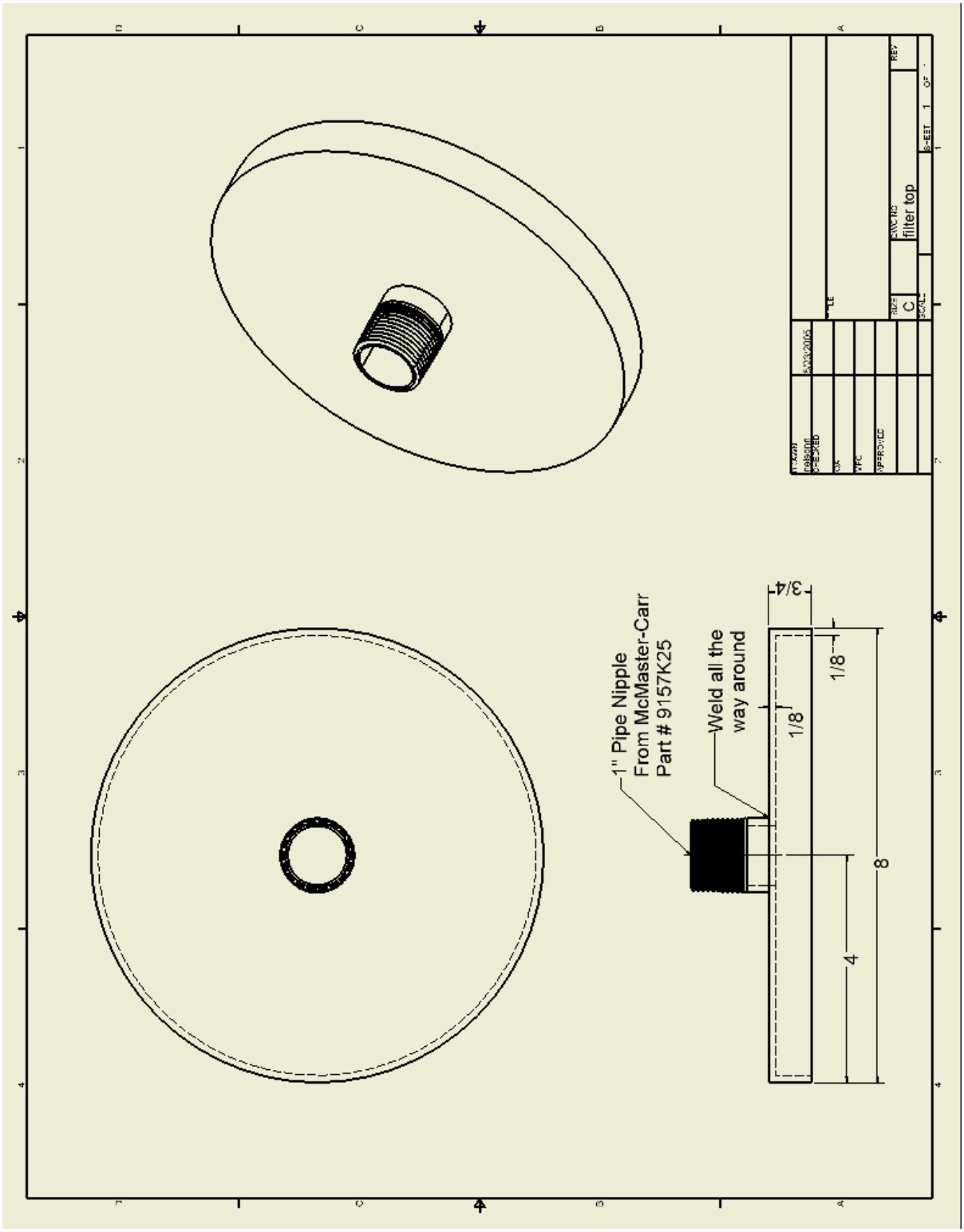
filter top
C
1" Pipe Nipple
From McMaster-Carr
Part # 9157K25
Weld all the
way around
3/4
1/8
1/8
8
4

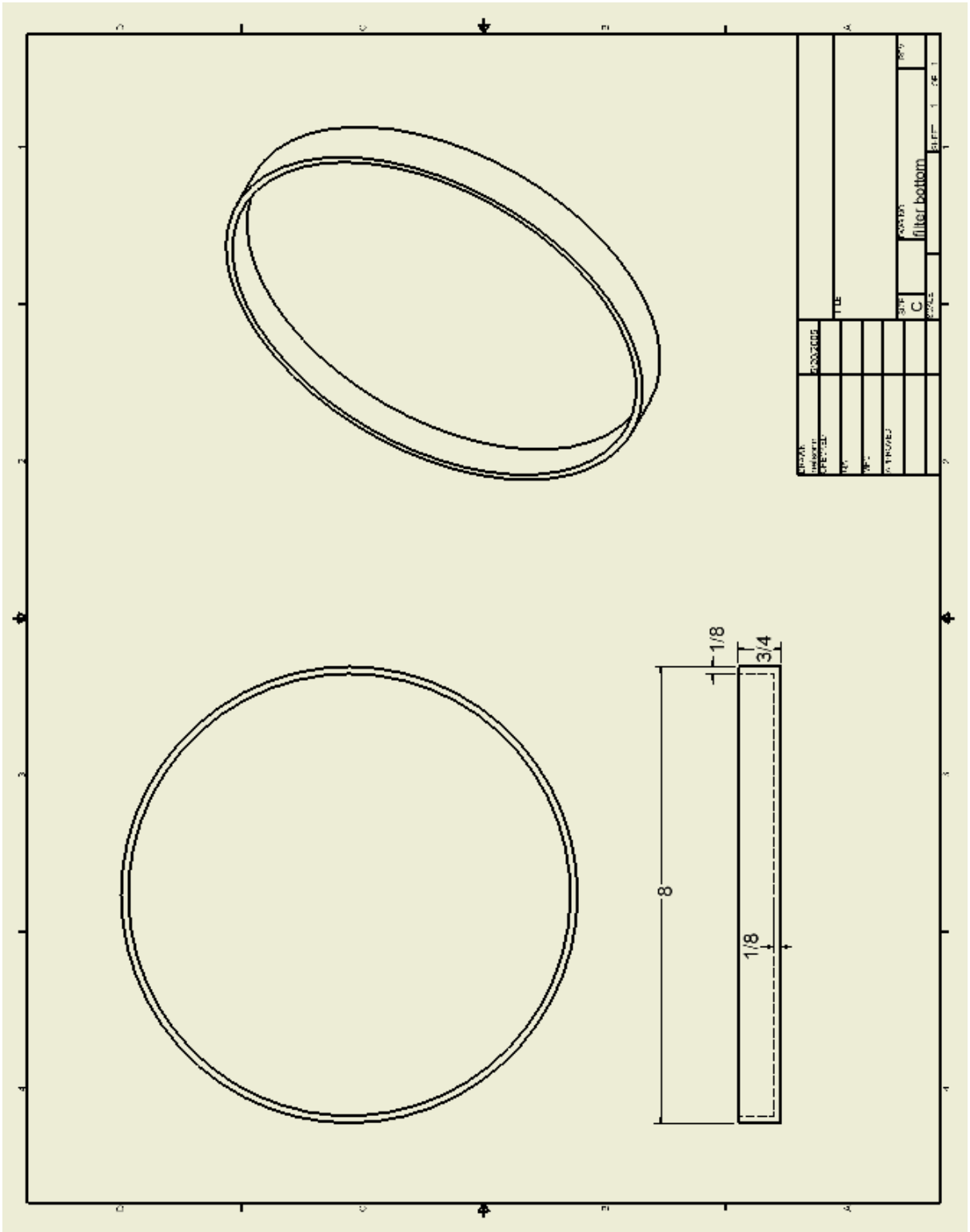
filter bottom
1/8
3/4
8
1/8

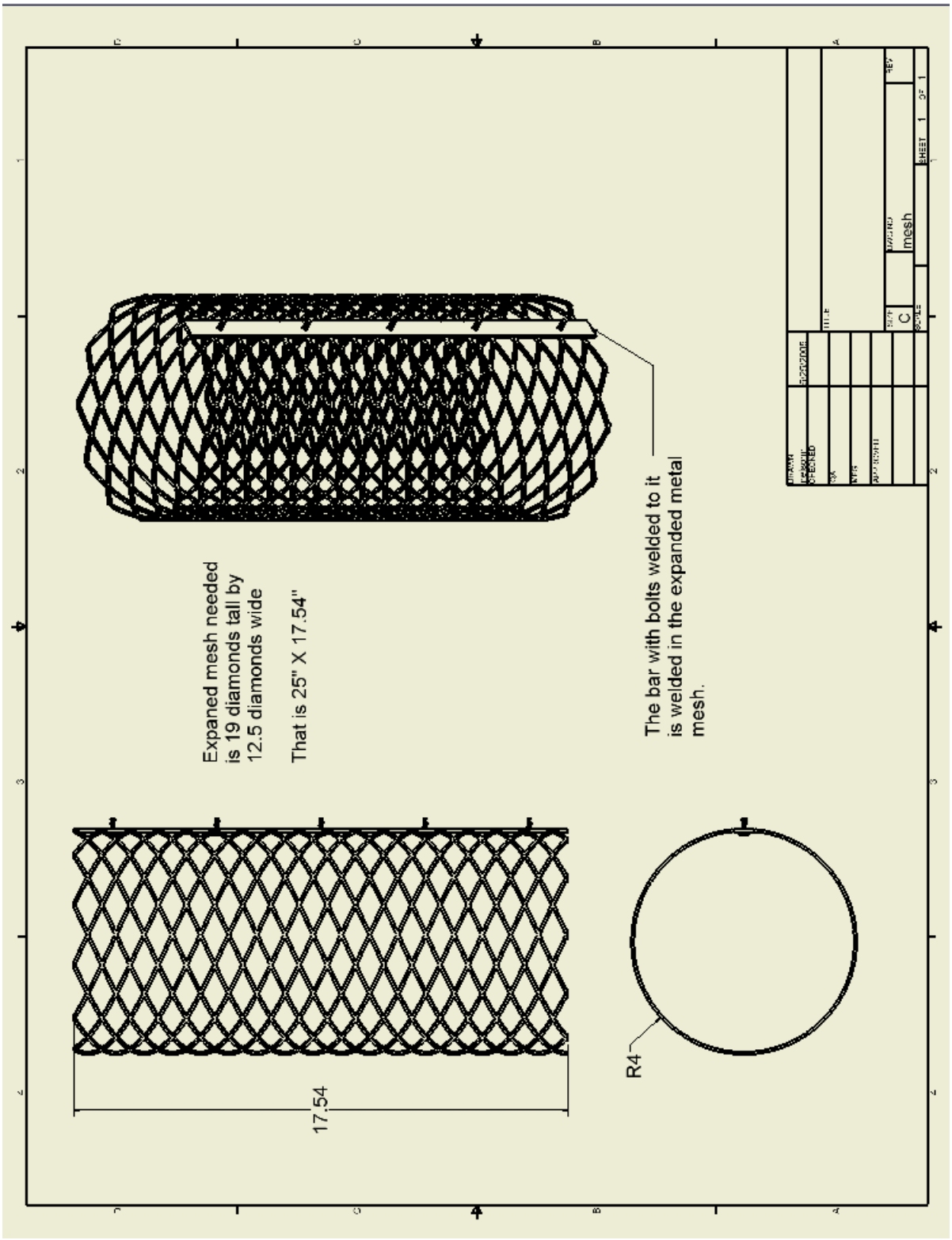
Expaned mesh needed
is 19 diamonds tall by
12.5 diamonds wide
That is 25" X 17.54"
The bar with bolts welded to it
is welded in the expanded metal
mesh.
17.54
R4
mesh

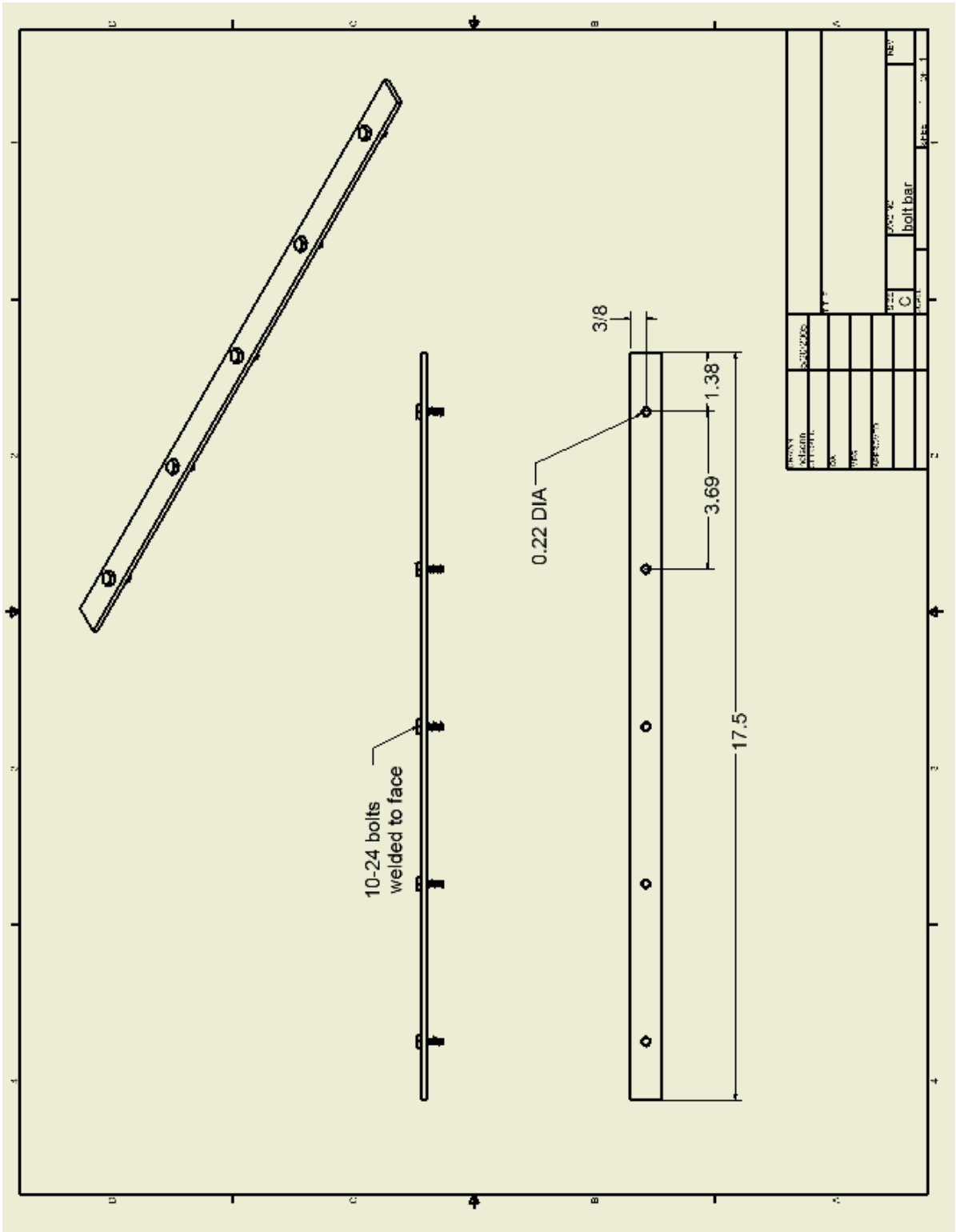
3/8
1.38
3.69
17.5
0.22 DIA
10-24 bolts
welded to face
bolt bar

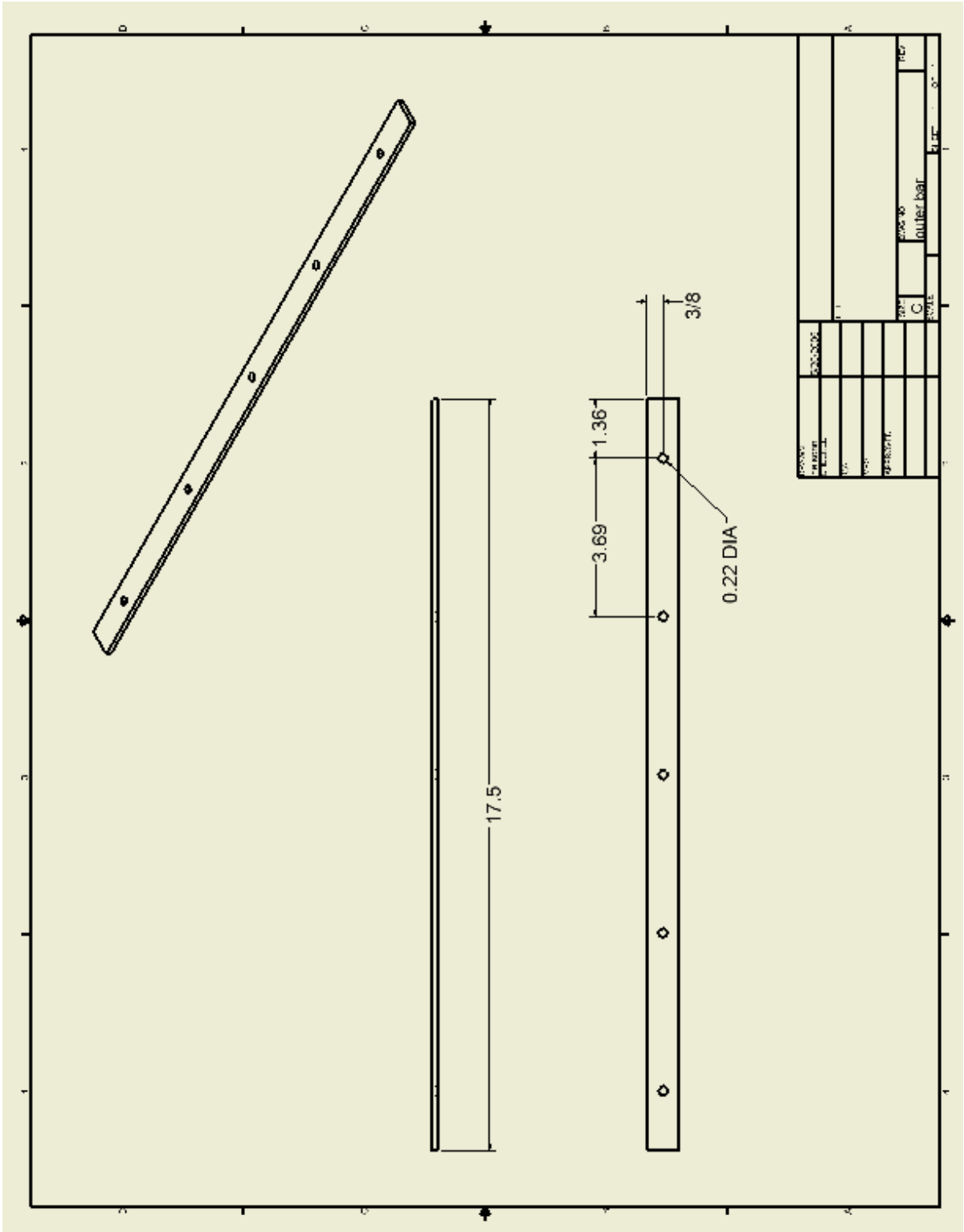
3/8
1.36
3.69
0.22 DIA
17.5
outter bar

APPENDIX B

Housing Drawings

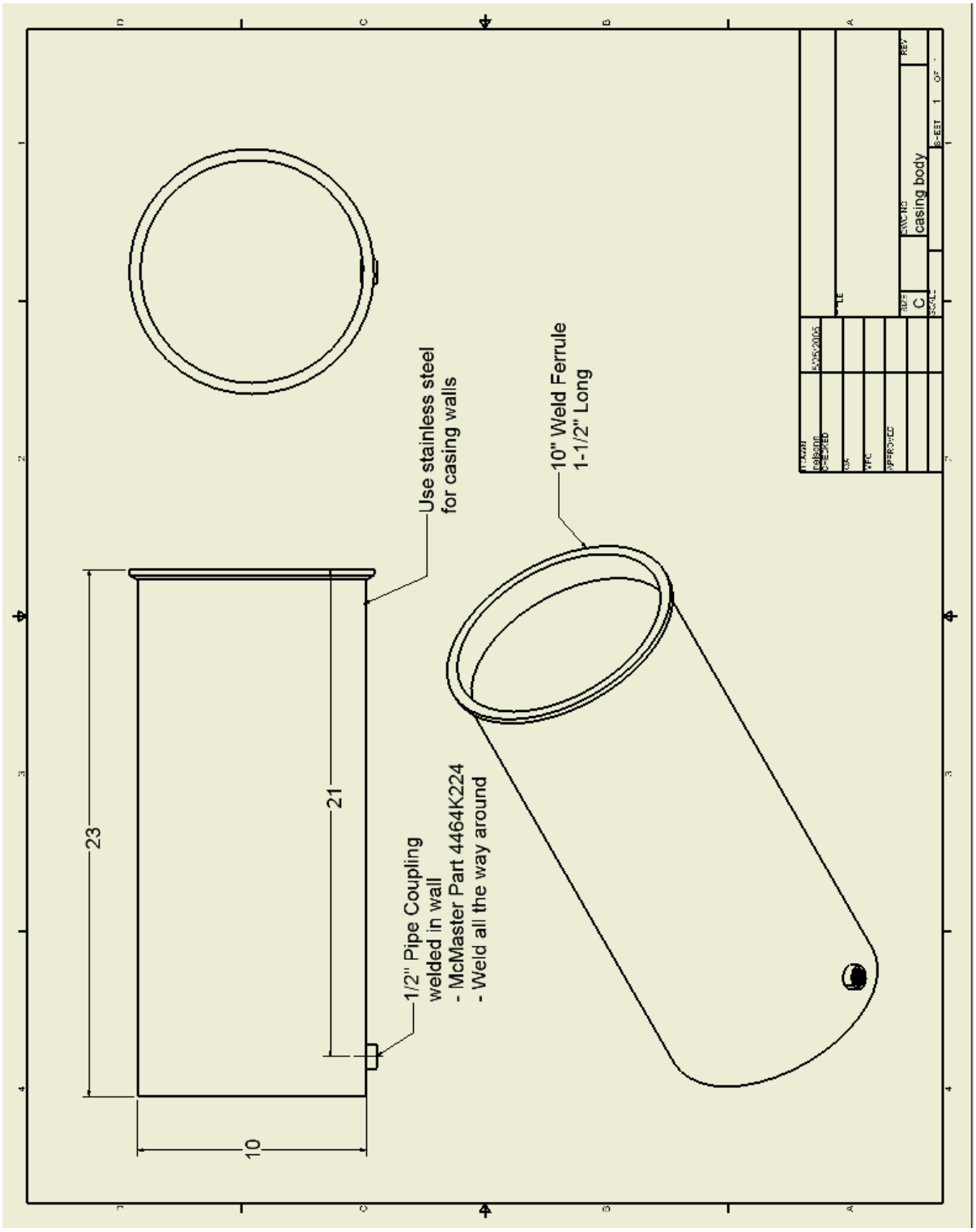
Use stainless steel
for casing walls
10" Weld Ferrule
1-1/2" Long
23
21
10
1/2" Pipe Coupling
welded in wall
- McMaster Part 4464K224
- Weld all the way around
casing body
C

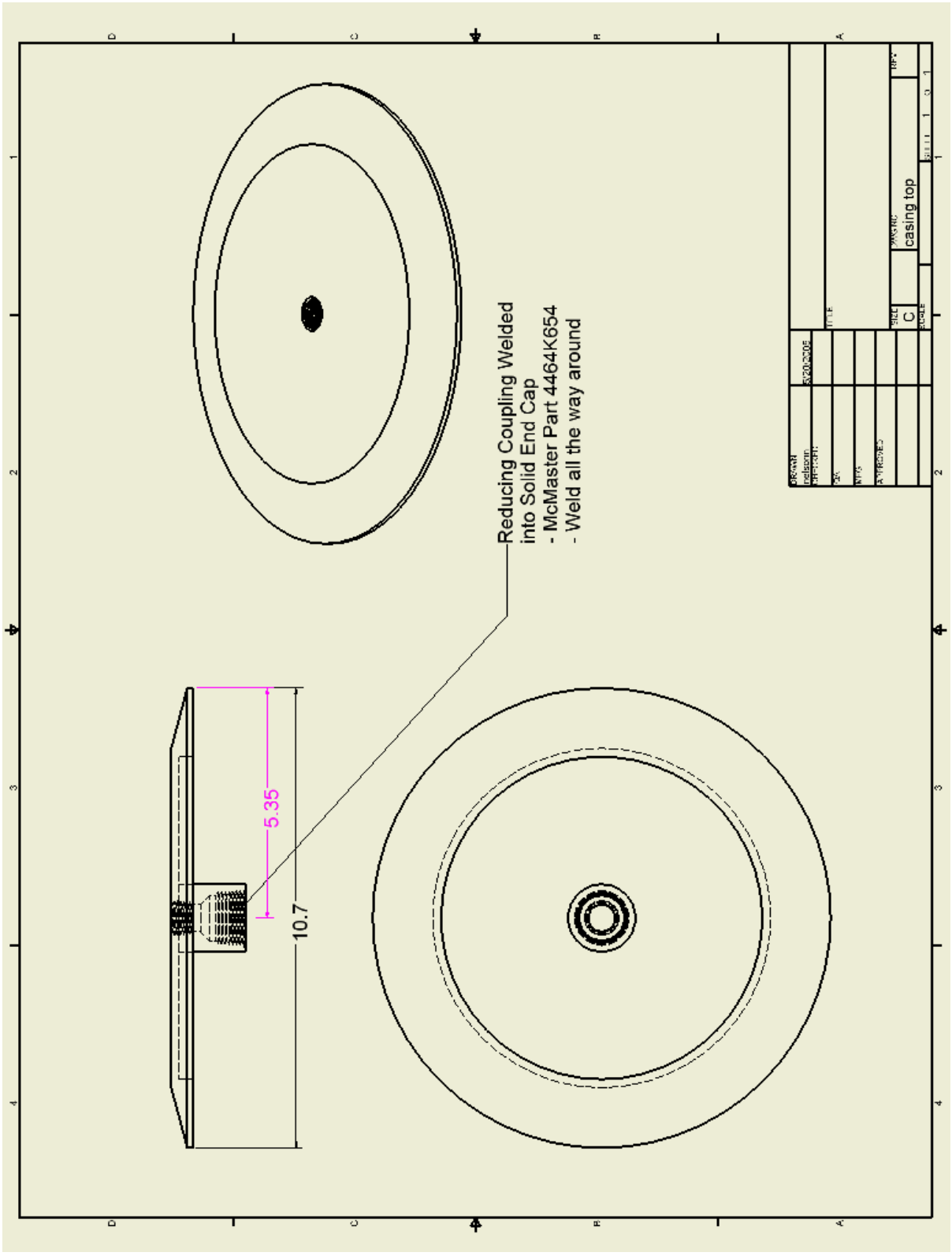
Reducing Coupling Welded
into Solid End Cap
- McMaster Part 4464K654
- Weld all the way around
5.35
10.7
casing top
C

APPENDIX C

MathCAD Sample Calculations

INPUTS

Fuel Feed Rate

$mdot_{fuel} := 6 \cdot \frac{lb}{hr}$

Air Flow Rate

$mdot_{air} := 50 \cdot \frac{L}{min}$

Cyclone Catch

$mass_{cy} := 439 \cdot gm$

Filter Catch

$mass_{fltr} := 168 \cdot gm$

Temperature Filter

$T_{fltr} := (345 + 273.15) \cdot K$

Time of Experiment

$t_{exp} := 8hr + 15min$

Temperature of Cyclone

$T_{cy} := (450 + 273.15) \cdot K$

Temperature of atmosphere

$T_{in} := (27 + 273.15) \cdot K$

Percent Volumes of Producer Gas

$x_{CO} := .205832$ $x_{C2H4} := 0.025397$ $x_{H2} := .086228$ $x_{O2} := 0$ $x_{C2H6} := .004177$ $x_{N2} := .443738$

$x_{CO2} := .150593$ $x_{C2H2} := .000958$ $x_{CH4} := .05726$ $x_{H2O} := 0$ $x_{C3H8} := .000199$

$x_T := x_{CO} + x_{CO2} + x_{H2} + x_{CH4} + x_{C2H4} + x_{C2H2} + x_{N2} + x_{C2H6} + x_{C3H8}$

$x_T = 0.974$

Percent Compound of Fuel

$x_{N\_fuel} := .0131$ $x_{H\_fuel} := .0608$ $x_{ash} := .0121$

$x_{O\_fuel} := .4254$ $x_{C\_fuel} := .4874$ $x_{S\_fuel} := .0012$ $moisture_{fuel} := .0522$

Sensitivity Values

$\sigma_V := .01ft^3$ $\sigma_{fab} := 5gm$ $\sigma_{fuel} := .2 \cdot \frac{lb}{hr}$

$\sigma_t := 5min$ $\sigma_{cy} := 2gm$ $\sigma_{water} := .02$

$\sigma_w := .0005gm$ $\sigma_{air} := 1.5 \cdot \frac{liter}{min}$

$\sigma_{CO} := .002788$ $\sigma_{C2H2} := .000015$

$\sigma_{CO2} := .000552$ $\sigma_{C2H4} := .000339$

$\sigma_{CH4} := .001131$ $\sigma_{C2H6} := .000093$

$\sigma_{H2} := .001536$ $\sigma_{O2} := 0$

$\sigma_{N2} := .004893$ $\sigma_{C3H8} := .000005$

$\sigma_{N\_fuel} := .05 \cdot x_{N\_fuel}$

$\sigma_{H\_fuel} := .05 \cdot x_{H\_fuel}$

$\sigma_{C\_fuel} := .05 \cdot x_{C\_fuel}$

Thimble Filter

$t_{filt1\_start} := 1.6226gm$ $t_{filt2\_start} := 1.6427gm$

$t_{filt1\_fin} := 1.6324gm$ $t_{filt2\_fin} := 1.6435gm$

$vol_{meter1\_start} := 1895.34ft^3$ $vol_{meter2\_start} := 1915.42ft^3$

$vol_{meter1\_fin} := 1915.42ft^3$ $vol_{meter2\_fin} := 1921.02ft^3$

$t_1 := (4 \cdot 60 + 37)min$ $t_2 := (1 \cdot 60 + 18)min$

$flow_{sample1} := \frac{vol_{meter1\_fin} - vol_{meter1\_start}}{t_1}$ $flow_{sample1} = 2.053 \cdot \frac{liter}{min}$

$flow_{sample2} := \frac{vol_{meter2\_fin} - vol_{meter2\_start}}{t_2}$ $flow_{sample2} = 2.033 \cdot \frac{liter}{min}$

Constants

$R_{bar} := 8.134 \cdot \frac{J}{mol \cdot K}$ $P_{atm} := 14.5 \cdot psi$

$P_{atm} = 9.997 \times 10^4 \cdot \frac{mass}{length\ time^2}$

Molecular Weights

$M_{CO} := 28 \cdot \frac{gm}{mol}$ $M_{CO2} := 44 \cdot \frac{gm}{mol}$ $M_{O2} := 32 \cdot \frac{gm}{mol}$ $M_{H2} := 2 \cdot \frac{gm}{mol}$ $M_{C2H4} := 28 \cdot \frac{gm}{mol}$ $M_{O} := 16 \cdot \frac{gm}{mol}$ $M_{H} := 1 \cdot \frac{gm}{mol}$

$M_{N2} := 28 \cdot \frac{gm}{mol}$ $M_{CH4} := 16 \cdot \frac{gm}{mol}$ $M_{C2H2} := 26 \cdot \frac{gm}{mol}$ $M_{H2O} := 18 \cdot \frac{gm}{mol}$ $M_{C} := 12 \frac{gm}{mol}$ $M_{N} := 14 \frac{gm}{mol}$ $M_{C2H6} := 30 \frac{gm}{mol}$

$M_{air} := .21 \cdot M_{O2} + .79 \cdot M_{N2}$ $M_{air} = \blacksquare \frac{gm}{mol}$

Density of Gases

$\rho_{CO} := \frac{P_{atm}}{\left(\frac{R_{bar}}{M_{CO}}\right) \cdot T_{in}}$ $\rho_{CO} = \blacksquare \frac{kg}{m^3}$

$\rho_{CO2} := \frac{P_{atm}}{\left(\frac{R_{bar}}{M_{CO2}}\right) \cdot T_{in}}$ $\rho_{CO2} = \blacksquare \frac{kg}{m^3}$

$\rho_{O2} := \frac{P_{atm}}{\left(\frac{R_{bar}}{M_{O2}}\right) \cdot T_{in}}$ $\rho_{O2} = \blacksquare \frac{kg}{m^3}$

$\rho_{C2H4} := \frac{P_{atm}}{\left(\frac{R_{bar}}{M_{C2H4}}\right) \cdot T_{in}}$ $\rho_{C2H4} = \blacksquare \frac{kg}{m^3}$

$\rho_{N2} := \frac{P_{atm}}{\left(\frac{R_{bar}}{M_{N2}}\right) \cdot T_{in}}$ $\rho_{N2} = \blacksquare \frac{kg}{m^3}$

$\rho_{CH4} := \frac{P_{atm}}{\left(\frac{R_{bar}}{M_{CH4}}\right) \cdot T_{in}}$ $\rho_{CH4} = \blacksquare \frac{kg}{m^3}$

$\rho_{C2H2} := \frac{P_{atm}}{\left(\frac{R_{bar}}{M_{C2H2}}\right) \cdot T_{in}}$ $\rho_{C2H2} = \blacksquare \frac{kg}{m^3}$

$\rho_{O} := \frac{P_{atm}}{\left(\frac{R_{bar}}{M_{O}}\right) \cdot T_{in}}$ $\rho_{O} = \blacksquare \frac{kg}{m^3}$

$\rho_{H2} := \frac{P_{atm}}{\left(\frac{R_{bar}}{M_{H2}}\right) \cdot T_{in}}$ $\rho_{H2} = \blacksquare \frac{kg}{m^3}$

$\rho_{C2H6} := \frac{P_{atm}}{\left(\frac{R_{bar}}{M_{C2H6}}\right) \cdot T_{in}}$ $\rho_{C2H6} = \blacksquare \frac{kg}{m^3}$

$\rho_{air} := \frac{P_{atm}}{\left(\frac{R_{bar}}{M_{air}}\right) \cdot T_{in}}$ $\rho_{air} = \blacksquare \frac{kg}{m^3}$

$\rho_{H2O} := \frac{P_{atm}}{\left(\frac{R_{bar}}{M_{H2O}}\right) \cdot T_{in}}$ $\rho_{H2O} = \blacksquare \frac{kg}{m^3}$

MASS BALANCE

MASS IN

$mass_{air} := mdot_{air} \cdot \rho_{air}$ $mass_{air} = \blacksquare \frac{lb}{hr}$

$mass_{fuel} := mdot_{fuel}$ $mass_{fuel} = \blacksquare \frac{lb}{hr}$

$mass_{in} := mass_{fuel} + mass_{air}$

$mass_{in} = \blacksquare \frac{lb}{hr}$

Mass of Air

$$\sigma_{mair} := \sqrt{(\rho_{air})^2 \cdot \sigma_{air}^2}$$

$$\sigma_{mair} = \blacksquare \frac{lb}{hr}$$

Mass of Fuel

$$\sigma_{mfuel} := \sqrt{\left[(1)^2 \cdot \sigma_{fuel}^2\right]}$$

$$\sigma_{mfuel} = \blacksquare \frac{lb}{hr}$$

Mass In

$$\sigma_{massin} := \sqrt{\left[(1)^2 \cdot \sigma_{mfuel}^2 + (1)^2 \cdot \sigma_{mair}^2\right]}$$

$$\sigma_{massin} = \blacksquare \frac{lb}{hr}$$

MASS OUT

water from fuel

$$water_{fuel} := \frac{moisture_{fuel} \cdot mass_{fuel}}{\rho_{H2O}}$$

$$water_{fuel} = \blacksquare \frac{liter}{min}$$

dry fuel

$$dry_{fuel} := mass_{fuel} - moisture_{fuel} \cdot mass_{fuel}$$

$$dry_{fuel} = \blacksquare \frac{lb}{hr}$$

Mass of Fuel

$$\sigma_{wfuel} := \sqrt{\left[\left(\frac{moisture_{fuel}}{\rho_{H2O}}\right)^2 \cdot \sigma_{fuel}^2 + \left(\frac{mass_{fuel}}{\rho_{H2O}}\right)^2 \cdot \sigma_{water}^2\right]}$$

$$\sigma_{wfuel} = \blacksquare \frac{liter}{min}$$

Dry fuel error

$$\sigma_{dfuel} := \sqrt{\left[\left(1 - moisture_{fuel}\right)^2 \cdot \sigma_{fuel}^2 + \left(-mass_{fuel}\right)^2 \cdot \sigma_{water}^2\right]}$$

$$\sigma_{dfuel} = \blacksquare \frac{lb}{hr}$$

Char Collection Rates

$$m_{cy} := \frac{mass_{cy}}{t_{exp}}$$

$$m_{cy} = \blacksquare \frac{lb}{hr}$$

$$m_{filter} := \frac{mass_{fltr}}{t_{exp}}$$

$$m_{filter} = \blacksquare \frac{lb}{hr}$$

$$char_{pro} := mdot_{fuel} \cdot x_{ash}$$

$$char_{pro} = \blacksquare \frac{gm}{hr}$$

$$mass_{char} := m_{cy} + m_{filter}$$

$$mass_{char} = \blacksquare \frac{lb}{hr}$$

$$mass_{char} = \blacksquare \frac{gm}{hr}$$

Mass of Fuel

$$\sigma_{wfuel} := \sqrt{\left[\left(\frac{moisture_{fuel}}{\rho_{H2O}}\right)^2 \cdot \sigma_{fuel}^{\ 2} + \left(\frac{mass_{fuel}}{\rho_{H2O}}\right)^2 \cdot \sigma_{water}^{\ 2}\right]}$$

$$\sigma_{wfuel} = \blacksquare \frac{liter}{min}$$

Dry fuel error

$$\sigma_{dfuel} := \sqrt{\left[\left(1 - moisture_{fuel}\right)^2 \cdot \sigma_{fuel}^{\ 2} + \left(-mass_{fuel}\right)^2 \cdot \sigma_{water}^{\ 2}\right]}$$

$$\sigma_{dfuel} = \blacksquare \frac{lb}{hr}$$

Char Collection Rates

$$m_{cy} := \frac{mass_{cy}}{t_{exp}} \qquad m_{filter} := \frac{mass_{fltr}}{t_{exp}}$$

$$m_{cy} = \blacksquare \frac{lb}{hr} \qquad m_{filter} = \blacksquare \frac{lb}{hr}$$

$$mass_{char} := m_{cy} + m_{filter}$$

$$mass_{char} = \blacksquare \frac{lb}{hr} \qquad mass_{char} = \blacksquare \frac{gm}{hr}$$

$$char_{pro} := mdot_{fuel} \cdot x_{ash}$$

$$char_{pro} = \blacksquare \frac{gm}{hr}$$

Weight of Char on Filter

$$mf := \frac{mass_{fltr}}{t_{exp}}$$

$$\sigma_{mf} := \sqrt{\left[\left(\frac{1}{t_{exp}}\right)^2 \cdot \sigma_{fab}^{\ 2} + \left(\frac{-mass_{fltr}}{t_{exp}^{\ 2}}\right)^2 \cdot \sigma_t^{\ 2}\right]}$$

$$\sigma_{mf} = \blacksquare \frac{gm}{hr}$$

Weight of Char from Cyclone

$$mcy := \frac{mass_{cy}}{t_{exp}}$$

$$\sigma_{mcy} := \sqrt{\left[\left(\frac{1}{t_{exp}}\right)^2 \cdot \sigma_{cy}^{\ 2} + \left(\frac{-mass_{cy}}{t_{exp}^{\ 2}}\right)^2 \cdot \sigma_t^{\ 2}\right]}$$

$$\sigma_{mcy} = \blacksquare \frac{gm}{hr}$$

Cyclone and Fabric Filter

$$\sigma_{mchar} := \sqrt{\left(1^2 \cdot \sigma_{mf}^{\ 2} + 1^2 \cdot \sigma_{mcy}^{\ 2}\right)}$$

$$\sigma_{mchar} = \blacksquare \frac{gm}{hr}$$

Nitrogen Balance

Nitrogen In

Nitrogen from air

$$mol_{N2\_air} := .7808 \cdot mdot_{air} \cdot \frac{\rho_{air}}{M_{air}}$$

$$mol_{N2\_air} = \blacksquare \frac{mol}{hr}$$

Nitrogen from dry fuel

$$mol_{N2\_fueldry} := \frac{dry_{fuel} \cdot x_{N\_fuel}}{2M_N}$$

$$mol_{N2\_fueldry} = \blacksquare \frac{mol}{hr}$$

$$mole_{N2\_IN} := mol_{N2\_fueldry} + mol_{N2\_air}$$

$$mole_{N2\_IN} = \blacksquare \frac{mol}{hr}$$

Nitrogen Out

Nitrogen from char

$$mol_{N2\_char} := \frac{.0305 \cdot mass_{char}}{2M_N}$$

$$mol_{N2\_char} = \blacksquare \frac{mol}{hr}$$

Nitrogen

$$mol_{N2} := mol_{N2\_air} + mol_{N2\_fueldry} - mol_{N2\_char}$$

$$mol_{N2} = \blacksquare \frac{mol}{hr}$$

Mole N2 in Air

$$\sigma_{N2air} := \sqrt{\left[\left(.7808\cdot\frac{\rho_{air}}{M_{air}}\right)^2\cdot\sigma_{air}^{\,2}\right]}$$

$$\sigma_{N2air} = 2.878\,\frac{mol}{hr}$$

Mole N2 in dry fuel

$$\sigma_{N2dfuel} := \sqrt{\left[\left(\frac{x_{N\_fuel}}{2\cdot M_N}\right)^2\cdot\sigma_{fuel}^{\,2} + \left(\frac{dry_{fuel}}{2\cdot M_N}\right)^2\cdot\sigma_{N\_fuel}\right]}$$

$$\sigma_{N2dfuel} = 2.358\,\frac{mol}{hr}$$

Mole N2 in Char

$$\sigma_{N2char} := \sqrt{\left[\left(\frac{.0305}{2\cdot M_N}\right)^2\cdot\sigma_{mchar}^{\,2}\right]}$$

$$\sigma_{N2char} = 9.479\times 10^{-4}\,\frac{mol}{hr}$$

Nitrogen Balance

$$\sigma_{N2b} := \sqrt{\left(\sigma_{N2air}^{\,2} + \sigma_{N2dfuel}^{\,2} + \sigma_{N2char}^{\,2}\right)}$$

$$\sigma_{N2b} = 3.72\,\frac{mol}{hr}$$

Calculations for dry flow

$$mass_{N2} := mol_{N2}\cdot M_{N2}$$

$$mass_{N2} = 5.991\,\frac{lb}{hr}$$

$$flow_{dry} := \frac{mass_{N2}}{\rho_{N2}\cdot x_{N2}}$$

$$flow_{dry} = 89.013\,\frac{liter}{min}$$

$$flow1_{dry} := 90\,\frac{liter}{min}$$

$$\sigma_{flow} := \sqrt{\left[\left(\frac{M_{N2}}{\rho_{N2}\cdot x_{N2}}\right)^2\cdot\sigma_{N2b}^{\,2} + \left(\frac{-mol_{N2}\cdot M_{N2}}{\rho_{N2}\cdot x_{N2}^{\,2}}\right)^2\cdot\sigma_{N2}^{\,2}\right]}$$

$$\sigma_{flow} = 3.551\,\frac{liter}{min}$$

Mass of Producer Gas Products

$$mass_{CO} := \rho_{CO}\cdot x_{CO}\cdot flow_{dry}$$

$$mass_{CO} = 2.779\,\frac{lb}{hr}$$

$$mass_{CO2} := \rho_{CO2}\cdot x_{CO2}\cdot flow_{dry}$$

$$mass_{CO2} = 3.195\,\frac{lb}{hr}$$

$$mass_{H2} := \rho_{H2}\cdot x_{H2}\cdot flow_{dry}$$

$$mass_{H2} = 0.083\,\frac{lb}{hr}$$

$$mass_{N2} := \rho_{N2}\cdot x_{N2}\cdot flow_{dry}$$

$$mass_{N2} = 5.991\,\frac{lb}{hr}$$

$$mass_{O2} := \rho_{O2}\cdot x_{O2}\cdot flow_{dry}$$

$$mass_{O2} = 0\,\frac{lb}{hr}$$

$$mass_{CH4} := \rho_{CH4}\cdot x_{CH4}\cdot flow_{dry}$$

$$mass_{CH4} = 0.442\,\frac{lb}{hr}$$

$$mass_{C2H2} := \rho_{C2H2}\cdot x_{C2H2}\cdot flow_{dry}$$

$$mass_{C2H2} = 0.012\,\frac{lb}{hr}$$

$$mass_{C2H4} := \rho_{C2H4}\cdot x_{C2H4}\cdot flow_{dry}$$

$$mass_{C2H4} = 0.343\,\frac{lb}{hr}$$

$$mass_{H2O} := \rho_{H2O}\cdot x_{H2O}\cdot flow_{dry}$$

$$mass_{H2O} = 0\,\frac{lb}{hr}$$

$$mass_{C2H6} := \rho_{C2H6}\cdot x_{C2H6}\cdot flow_{dry}$$

$$mass_{C2H6} = 0.06\,\frac{lb}{hr}$$

$$mass_{producer} := mass_{CO} + mass_{CO2} + mass_{H2} + mass_{N2} + mass_{O2} + mass_{CH4} + mass_{C2H2} + mass_{C2H4} + mass_{H2O} + mass_{C2H6}$$

$$mass_{producer} = 12.904\,\frac{lb}{hr}$$

ERROR IN MASS OF GASES

$$\sigma_{COmass} := \sqrt{\left[\left(\rho_{CO}\cdot flow_{dry}\right)^2\cdot\sigma_{CO}^{\ 2} + \left(\rho_{CO}\cdot x_{CO}\right)^2\cdot\sigma_{flow}^{\ 2}\right]}$$

$$\sigma_{COmass} = 0.117\,\frac{lb}{hr}$$

$$\sigma_{H2mass} := \sqrt{\left[\left(\rho_{H2}\cdot flow_{dry}\right)^2\cdot\sigma_{H2}^{\ 2} + \left(\rho_{H2}\cdot x_{H2}\right)^2\cdot\sigma_{flow}^{\ 2}\right]}$$

$$\sigma_{H2mass} = 3.633\times10^{-3}\,\frac{lb}{hr}$$

$$\sigma_{CO2mass} := \sqrt{\left[\left(\rho_{CO2}\cdot flow_{dry}\right)^2\cdot\sigma_{CO2}^{\ 2} + \left(\rho_{CO2}\cdot x_{CO2}\right)^2\cdot\sigma_{flow}^{\ 2}\right]}$$

$$\sigma_{CO2mass} = 0.128\,\frac{lb}{hr}$$

$$\sigma_{CH4mass} := \sqrt{\left[\left(\rho_{CH4}\cdot flow_{dry}\right)^2\cdot\sigma_{CH4}^{\ 2} + \left(\rho_{CH4}\cdot x_{CH4}\right)^2\cdot\sigma_{flow}^{\ 2}\right]}$$

$$\sigma_{CH4mass} = 0.02\,\frac{lb}{hr}$$

$$\sigma_{C2H2mass} := \sqrt{\left[\left(\rho_{C2H2}\cdot flow_{dry}\right)^2\cdot\sigma_{C2H2}^{\ 2} + \left(\rho_{C2H2}\cdot x_{C2H2}\right)^2\cdot\sigma_{flow}^{\ 2}\right]}$$

$$\sigma_{C2H2mass} = 5.146\times10^{-4}\,\frac{lb}{hr}$$

$$\sigma_{C2H6mass} := \sqrt{\left[\left(\rho_{C2H6}\cdot flow_{dry}\right)^2\cdot\sigma_{C2H6}^{\ 2} + \left(\rho_{C2H6}\cdot x_{C2H6}\right)^2\cdot\sigma_{flow}^{\ 2}\right]}$$

$$\sigma_{C2H6mass} = 2.76\times10^{-3}\,\frac{lb}{hr}$$

$$\sigma_{C2H4mass} := \sqrt{\left[\left(\rho_{C2H4}\cdot flow_{dry}\right)^2\cdot\sigma_{C2H4}^{\ 2} + \left(\rho_{C2H4}\cdot x_{C2H4}\right)^2\cdot\sigma_{flow}^{\ 2}\right]}$$

$$\sigma_{C2H4mass} = 0.014\,\frac{lb}{hr}$$

$$\sigma_{N2mass} := \sqrt{\left[\left(\rho_{N2}\cdot flow_{dry}\right)^2\cdot\sigma_{N2}^{\ 2} + \left(\rho_{N2}\cdot x_{N2}\right)^2\cdot\sigma_{flow}^{\ 2}\right]}$$

$$\sigma_{N2mass} = 0.248\,\frac{lb}{hr}$$

ERROR IN MASS OF GAS

$$\sigma_{mpro} := \sqrt{\left(\sigma_{N2mass}^{\ 2} + \sigma_{H2mass}^{\ 2} + \sigma_{COmass}^{\ 2} + \sigma_{CO2mass}^{\ 2} + \sigma_{CH4mass}^{\ 2} + \sigma_{C2H2mass}^{\ 2} + \sigma_{C2H4mass}^{\ 2} + \sigma_{C2H6mass}^{\ 2}\right)}$$

$$\sigma_{mpro} = 0.304\,\frac{lb}{hr}$$

Hydrogen Balance (Moles)

Hydrogen In

Hydrogen from water in fuel

$$mol_{h\_fuelwater} := \frac{water_{fuel}\cdot\rho_{H2O}}{M_{H2O}}$$

$$mol_{h\_fuelwater} = 7.893\,\frac{mol}{hr}$$

Hydrogen from dry fuel

$$mol_{h\_fueldry} := \frac{dry_{fuel}\cdot x_{H\_fuel}}{2M_H}$$

$$mol_{h\_fueldry} = 78.416\,\frac{mol}{hr}$$

$$mole_{H2\_IN} := mol_{h\_fuelwater} + mol_{h\_fueldry}$$

$$mole_{H2\_IN} = 86.309\,\frac{mol}{hr}$$

Hydrogen from water in fuel

$$\sigma_{hwfuel} := \sqrt{\left[\left(\frac{\rho_{H2O}}{M_{H2O}}\right)^2\cdot\sigma_{wfuel}^{\ 2}\right]}$$

$$\sigma_{hwfuel} = 3.035\,\frac{mol}{hr}$$

Hydrogen from dry fuel

$$\sigma_{hdfuel} := \sqrt{\left[\left(\frac{x_{H\_fuel}}{2\cdot M_H}\right)^2\cdot\sigma_{dfuel}^{\ 2} + \left(\frac{dry_{fuel}}{2\cdot M_H}\right)^2\cdot\sigma_{H\_fuel}^{\ 2}\right]}$$

$$\sigma_{hdfuel} = 4.994\,\frac{mol}{hr}$$

Hydrogen In

$$\sigma_{hin} := \sqrt{\left[(1)^2\cdot\sigma_{hwfuel}^{\ 2} + (1)^2\cdot\sigma_{hdfuel}^{\ 2}\right]}$$

$$\sigma_{hin} = 5.844\,\frac{mol}{hr}$$

Hydrogen Out

Hydrogen

$$mol_{h\_H2} := \frac{mass_{H2}}{M_{H2}}$$

$$mol_{h\_H2} = 18.858 \frac{mol}{hr}$$

Hydrogen in CH4

$$mol_{h\_CH4} := \frac{2mass_{CH4}}{M_{CH4}}$$

$$mol_{h\_CH4} = 25.046 \frac{mol}{hr}$$

Hydrogen in C2H2

$$mol_{h\_C2H2} := \frac{mass_{C2H2}}{M_{C2H2}}$$

$$mol_{h\_C2H2} = 0.21 \frac{mol}{hr}$$

Hydrogen in C2H4

$$mol_{h\_C2H4} := \frac{2mass_{C2H4}}{M_{C2H4}}$$

$$mol_{h\_C2H4} = 11.109 \frac{mol}{hr}$$

Hydrogen from Char

$$mol_{h\_char} := \frac{.01mass_{char}}{2M_H}$$

$$mol_{h\_char} = 0.368 \frac{mol}{hr}$$

Hydrogen in C2H6

$$mol_{h\_C2H6} := \frac{3mass_{C2H6}}{M_{C2H6}}$$

$$mol_{h\_C2H6} = 2.741 \frac{mol}{hr}$$

Hydrogen in producer gas

$$\sigma_{hpg} := \sqrt{\left[\left(\frac{1}{M_{H2}}\right)^2 \cdot \sigma_{H2mass}{}^2\right]}$$

$$\sigma_{hpg} = 0.824 \frac{mol}{hr}$$

Hydrogen in CH4

$$\sigma_{hCH4} := \sqrt{\left[\left(\frac{2}{M_{CH4}}\right)^2 \cdot \sigma_{CH4mass}{}^2\right]}$$

$$\sigma_{hCH4} = 1.115 \frac{mol}{hr}$$

Hydrogen in C2H2

$$\sigma_{hC2H2} := \sqrt{\left[\left(\frac{1}{M_{C2H2}}\right)^2 \cdot \sigma_{C2H2mass}{}^2\right]}$$

$$\sigma_{hC2H2} = 8.978 \times 10^{-3} \frac{mol}{hr}$$

Hydrogen in Char

$$\sigma_{hchar} := \sqrt{\left[\left(\frac{.01}{2 \cdot M_H}\right)^2 \cdot \sigma_{mchar}{}^2 + \left(\frac{mass_{char}}{2 \cdot M_H}\right)^2 \cdot (.05 \cdot .01)^2\right]}$$

$$\sigma_{hchar} = 0.019 \frac{mol}{hr}$$

Hydrogen in C2H6

$$\sigma_{hC2H6} := \sqrt{\left[\left(\frac{3}{M_{C2H6}}\right)^2 \cdot \sigma_{C2H6mass}{}^2\right]}$$

$$\sigma_{hC2H6} = 0.125 \frac{mol}{hr}$$

Hydrogen in C2H4

$$\sigma_{hC2H4} := \sqrt{\left[\left(\frac{2}{M_{C2H4}}\right)^2 \cdot \sigma_{C2H4mass}{}^2\right]}$$

$$\sigma_{hC2H4} = 0.467 \frac{mol}{hr}$$

Hydrogen out

$$\sigma_{hout} := \sqrt{\left(1^2 \cdot \sigma_{hpg}{}^2 + 1^2 \cdot \sigma_{hCH4}{}^2 + 1^2 \cdot \sigma_{hC2H2}{}^2 + 1^2 \cdot \sigma_{hC2H4}{}^2 + 1^2 \cdot \sigma_{hC2H6}{}^2 + 1^2 \cdot \sigma_{hchar}{}^2\right)}$$

$$\sigma_{hout} = 1.468 \frac{mol}{hr}$$

$$mole_{H2\_OUT} := mol_{h\_H2} + mol_{h\_CH4} + mol_{h\_C2H2} + mol_{h\_C2H4} + mol_{h\_char} + mol_{h\_C2H6}$$

$$mole_{H2\_OUT} = 58.33 \frac{mol}{hr}$$

$$mol_{water} := mole_{H2\_IN} - mole_{H2\_OUT}$$

Error in water

$$\sigma_{H2O} := \sqrt{\left(1^2 \cdot \sigma_{hin}{}^2 + 1^2 \cdot \sigma_{hout}{}^2\right)}$$

$$\sigma_{H2O} = 6.026 \frac{mol}{hr}$$

$$mol_{water} = 27.979 \frac{mol}{hr}$$

$$mass_{water} := mol_{water} \cdot M_{H2O}$$

$$flow_{water} := mol_{water} \cdot \frac{M_{H2O}}{\rho_{H2O}}$$

$$mass_{water} = 1.11 \frac{lb}{hr}$$

$$flow_{water} = 11.388 \frac{liter}{min}$$

$$flow_{wet} := flow_{dry} + flow_{water}$$

Error in mass water

$$\sigma_{massH2O} := \sqrt{\left(M_{H2O}^{2} \cdot \sigma_{H2O}^{2}\right)}$$

$$\sigma_{massH2O} = 0.239 \frac{lb}{hr}$$

Error in flow wet

$$\sigma_{flowwet} := \sqrt{\left[1^{2} \cdot \sigma_{flow}^{2} + \left(\frac{M_{H2O}}{\rho_{H2O}}\right)^{2} \cdot \sigma_{H2O}^{2}\right]}$$

$$\sigma_{flowwet} = 4.316 \frac{liter}{min}$$

Error flow water

$$\sigma_{flowwater} := \sqrt{\left(\frac{M_{H2O}}{\rho_{H2O}}\right)^{2} \cdot \sigma_{H2O}^{2}}$$

$$\sigma_{flowwater} = 2.453 \frac{liter}{min}$$

Percent Mass Accounted For

$$mass_{out} := mass_{producer} + m_{cy} + m_{filter} + mass_{water}$$

$$mass_{out} = 14.177 \frac{lb}{hr}$$

$$\eta_{mass} := \frac{mass_{out}}{mass_{in}}$$

$$\eta_{mass} = 102.65\,\%$$

Error in mass out

$$\sigma_{massout} := \sqrt{\left(\sigma_{mpro}^{2} + \sigma_{mf}^{2} + \sigma_{mcy}^{2} + \sigma_{massH2O}^{2}\right)}$$

$$\sigma_{massout} = 0.386 \frac{lb}{hr}$$

Error in mass balance

$$\sigma_{\eta mass} := \sqrt{\left[\left(\frac{1}{mass_{in}}\right)^{2} \cdot \sigma_{massout}^{2} + \left[-\left(\frac{mass_{out}}{mass_{in}^{2}}\right)\right]^{2} \cdot \sigma_{massin}^{2}\right]}$$

$$\sigma_{\eta mass} = 3.616\,\%$$

Percent Water

$$per_{water} := \frac{flow_{water}}{flow_{wet}}$$

$$per_{water} = 11.342\,\%$$

$$\sigma_{perh2o} := \sqrt{\left[\left(\frac{1}{flow_{wet}}\right)^{2} \cdot \sigma_{flowwater}^{2} + \left[-\left(\frac{flow_{water}}{flow_{wet}^{2}}\right)\right]^{2} \cdot \sigma_{flowwet}^{2}\right]}$$

$$\sigma_{perh2o} = 2.491\,\%$$

Thimble filter and collection Efficiencies

$\Delta thimb1 := t_{filt1\_fin} - t_{filt1\_start}$ $\Delta thimb1 = 9.8 \times 10^{-3}\,gm$ $\Delta V_{meter1} := vol_{meter1\_fin} - vol_{meter1\_start}$ $\Delta V_{meter1} = 20.08\,ft^3$

$\Delta thimb2 := t_{filt2\_fin} - t_{filt2\_start}$ $\Delta thimb2 = 8 \times 10^{-4}\,gm$ $\Delta V_{meter2} := vol_{meter2\_fin} - vol_{meter2\_start}$ $\Delta V_{meter2} = 5.6\,ft^3$

$\sigma_{\Delta thim} := \sqrt{2 \cdot \sigma_w^{\,2}}$ $\sigma_{\Delta Vmeter} := \sqrt{2 \cdot \sigma_V^{\,2}}$

$\sigma_{\Delta thim} = 7.071 \times 10^{-4}\,gm$ $\sigma_{\Delta Vmeter} = 0.014\,ft^3$

$thimb_{catch1} := \frac{\Delta thimb1}{t_1}$ $flow_{meter1} := \frac{\Delta V_{meter1}}{t_1}$

$thimb_{catch1} = 2.123 \times 10^{-3}\,\frac{gm}{hr}$ $flow_{meter1} = 2.053\,\frac{liter}{min}$

$\sigma_{thimcth1} := \sqrt{\left[\left(\frac{1}{t_1}\right)^2 \cdot \sigma_{\Delta thim}^{\,2} + \left[-\left(\frac{\Delta thimb1}{t_1^{\,2}}\right)\right]^2 \cdot \sigma_t^{\,2}\right]}$ $\sigma_{meter1} := \sqrt{\left[\left(\frac{1}{t_1}\right)^2 \cdot \sigma_{\Delta Vmeter}^{\,2} + \left[-\left(\frac{\Delta V_{meter1}}{t_1^{\,2}}\right)\right]^2 \cdot \sigma_t^{\,2}\right]}$

$\sigma_{thimcth1} = 1.579 \times 10^{-4}\,\frac{gm}{hr}$ $\sigma_{meter1} = 0.037\,\frac{liter}{min}$

$thimb_{catch2} := \frac{\Delta thimb2}{t_2}$ $flow_{meter2} := \frac{\Delta V_{meter2}}{t_2}$

$thimb_{catch2} = 6.154 \times 10^{-4}\,\frac{gm}{hr}$ $flow_{meter2} = 2.033\,\frac{liter}{min}$

$\sigma_{thimcth2} := \sqrt{\left[\left(\frac{1}{t_2}\right)^2 \cdot \sigma_{\Delta thim}^{\,2} + \left[-\left(\frac{\Delta thimb2}{t_2^{\,2}}\right)\right]^2 \cdot \sigma_t^{\,2}\right]}$ $\sigma_{meter2} := \sqrt{\left[\left(\frac{1}{t_2}\right)^2 \cdot \sigma_{\Delta Vmeter}^{\,2} + \left[-\left(\frac{\Delta V_{meter2}}{t_2^{\,2}}\right)\right]^2 \cdot \sigma_t^{\,2}\right]}$

$\sigma_{thimcth2} = 5.454 \times 10^{-4}\,\frac{gm}{hr}$ $\sigma_{meter2} = 0.13\,\frac{liter}{min}$

$part_{sample1} := \frac{thimb_{catch1}}{flow_{meter1}}$ $part_{sample2} := \frac{thimb_{catch2}}{flow_{meter2}}$

$part_{sample1} = 0.017\,\frac{gm}{m^3}$ $part_{sample2} = 5.045 \times 10^{-3}\,\frac{gm}{m^3}$

$\sigma_{psam1} := \sqrt{\left[\left(\frac{1}{flow_{meter1}}\right)^2 \cdot \sigma_{thimcth1}^{\,2} + \left[-\left(\frac{thimb_{catch1}}{flow_{meter1}^{\,2}}\right)\right]^2 \cdot \sigma_{meter1}^{\,2}\right]}$ $\sigma_{psam2} := \sqrt{\left[\left(\frac{1}{flow_{meter2}}\right)^2 \cdot \sigma_{thimcth2}^{\,2} + \left[-\left(\frac{thimb_{catch2}}{flow_{meter2}^{\,2}}\right)\right]^2 \cdot \sigma_{meter2}^{\,2}\right]}$

$\sigma_{psam1} = 1.319 \times 10^{-3}\,\frac{gm}{m^3}$ $\sigma_{psam2} = 4.483 \times 10^{-3}\,\frac{gm}{m^3}$

$part_{loading\_fabric1} := part_{sample1} \cdot flow_{dry}$ $part_{loading\_fabric2} := part_{sample2} \cdot flow_{dry}$

$part_{loading\_fabric1} = 0.092\,\frac{gm}{hr}$ $part_{loading\_fabric2} = 0.027\,\frac{gm}{hr}$

$\sigma_{ploadfab1} := \sqrt{flow_{dry}^{\,2} \cdot \sigma_{psam1}^{\,2} + part_{sample1}^{\,2} \cdot \sigma_{flow}^{\,2}}$ $\sigma_{ploadfab2} := \sqrt{flow_{dry}^{\,2} \cdot \sigma_{psam2}^{\,2} + part_{sample2}^{\,2} \cdot \sigma_{flow}^{\,2}}$

$\sigma_{ploadfab1} = 7.945 \times 10^{-3}\,\frac{gm}{hr}$ $\sigma_{ploadfab2} = 0.024\,\frac{gm}{hr}$

Char Loading

$$Pre_{CY} := \frac{(m_{cy} + m_{filter})}{flow_{wet}} + \frac{part_{sample1} + part_{sample2}}{2}$$

$$Pre_{CY} = 12.225 \frac{gm}{m^3}$$

$$Post_{CY} := \frac{m_{filter}}{flow_{wet}} + \frac{part_{sample1} + part_{sample2}}{2}$$

$$Post_{CY} = 3.392 \frac{gm}{m^3}$$

$$\sigma_{PreCy} := \sqrt{\left[\left(\frac{1}{flow_{wet}}\right)^2 \cdot \sigma_{mchar}^2 + \left(\frac{\sigma_{psam1} + \sigma_{psam2}}{2}\right)^2 + \left[-\left(\frac{m_{cy} + m_{filter}}{flow_{wet}^2}\right)\right]^2 \cdot \sigma_{flowwet}^2\right]}$$

$$\sigma_{PreCy} = 0.544 \frac{gm}{m^3}$$

$$\sigma_{PostCy} := \sqrt{\left[\left(\frac{1}{flow_{wet}}\right)^2 \cdot \sigma_{mf}^2 + \left(\frac{\sigma_{psam1} + \sigma_{psam2}}{2}\right)^2 + \left[-\left(\frac{m_{filter}}{flow_{wet}^2}\right)\right]^2 \cdot \sigma_{flowwet}^2\right]}$$

$$\sigma_{PostCy} = 0.18 \frac{gm}{m^3}$$

$$Load_{PreCy} := Pre_{CY} \cdot flow_{dry}$$

$$Load_{PreCy} = 65.29 \frac{gm}{hr}$$

$$\frac{m_{filter}}{m_{cy}} = 0.383$$

$$Load_{PostCy} := Post_{CY} \cdot flow_{dry}$$

$$Load_{PostCy} = 18.113 \frac{gm}{hr}$$

$$\sigma_{LoadPreCy} := \sqrt{\left(flow_{dry}^2 \cdot \sigma_{PreCy}^2 + Pre_{CY}^2 \cdot \sigma_{flow}^2\right)}$$

$$\sigma_{LoadPreCy} = 3.904 \frac{gm}{hr}$$

$$\sigma_{LoadPostCy} := \sqrt{\left(flow_{dry}^2 \cdot \sigma_{PostCy}^2 + Post_{CY}^2 \cdot \sigma_{flow}^2\right)}$$

$$\sigma_{LoadPostCy} = 1.203 \frac{gm}{hr}$$

Theoretical Ash

$$ash_{theo} := mdot_{fuel} \cdot t_{exp} \cdot x_{ash}$$

$$ash_{theo} = 271.679\,gm$$

Actual Ash

$$ash_{act} := Load_{PreCy} \cdot t_{exp}$$

$$ash_{act} = 538.644\,gm$$

$$Eff_{cy} := \frac{(Load_{PreCy} - Load_{PostCy})}{Load_{PreCy}}$$

$$Eff_{cy} = 72.257\,\%$$

$$\sigma_{EFFcy} := \sqrt{\left[\left(\frac{-1}{Load_{PreCy}}\right)^2 \cdot \sigma_{LoadPostCy}^2 + \left(\frac{Load_{PostCy}}{Load_{PreCy}^2}\right)^2 \cdot \sigma_{LoadPreCy}^2\right]}$$

$$\sigma_{EFFcy} = 2.479\,\%$$

$$Eff_{fabric1} := \frac{(Load_{PostCy} - part_{loading\_fabric1})}{Load_{PostCy}}$$

$$Eff_{fabric1} = 99.492\,\%$$

$$\sigma_{EFFfab1} := \sqrt{\left[\left(\frac{-1}{Load_{PostCy}}\right)^2 \cdot \sigma_{ploadfab1}^2 + \left(\frac{part_{loading\_fabric1}}{Load_{PostCy}^2}\right)^2 \cdot \sigma_{LoadPostCy}^2\right]}$$

$$\sigma_{EFFfab1} = 0.055\,\%$$

$$Eff_{fabric2} := \frac{(Load_{PostCy} - part_{loading\_fabric2})}{Load_{PostCy}}$$

$$Eff_{fabric2} = 99.851\,\%$$

$$\sigma_{EFFfab2} := \sqrt{\left[\left(\frac{-1}{Load_{PostCy}}\right)^2 \cdot \sigma_{ploadfab2}^2 + \left(\frac{part_{loading\_fabric2}}{Load_{PostCy}^2}\right)^2 \cdot \sigma_{LoadPostCy}^2\right]}$$

$$\sigma_{EFFfab2} = 0.133\,\%$$

$$Eff_{Col1} := \frac{(Load_{PreCy} - part_{loading\_fabric1})}{Load_{PreCy}}$$

$$Eff_{Col1} = 0.999$$

$$\sigma_{EFFcol1} := \sqrt{\left[\left(\frac{-1}{Load_{PreCy}}\right)^2 \cdot \sigma_{ploadfab1}^2 + \left(\frac{part_{loading\_fabric1}}{Load_{PreCy}^2}\right)^2 \cdot \sigma_{LoadPreCy}^2\right]}$$

$$\sigma_{EFFcol1} = 0.015\,\%$$

$$Eff_{Col2} := \frac{(Load_{PreCy} - part_{loading\_fabric2})}{Load_{PreCy}}$$

$$Eff_{Col2} = 1$$

$$\sigma_{EFFcol2} := \sqrt{\left[\left(\frac{-1}{Load_{PreCy}}\right)^2 \cdot \sigma_{ploadfab2}^2 + \left(\frac{part_{loading\_fabric2}}{Load_{PreCy}^2}\right)^2 \cdot \sigma_{LoadPreCy}^2\right]}$$

$$\sigma_{EFFcol2} = 0.037\,\%$$

Carbon Conversion

$Carbon_{in} := mdot_{fuel} \cdot x_{C\_fuel}$ $\sigma_{Cin} := \sqrt{\left(mdot_{fuel}^{2} \cdot \sigma_{C\_fuel}^{2} + x_{C\_fuel}^{2} \cdot \sigma_{fuel}^{2}\right)}$

$Carbon_{in} = 2.924 \frac{lb}{hr}$

$C_{conv} := \frac{Carbon_{in} - .4Load_{PreCy}}{Carbon_{in}}$

$C_{conv} = 98.031\,\%$

$\sigma_{conv} := \sqrt{\left[\left(\frac{-.4}{Carbon_{in}}\right)^{2} \cdot \sigma_{LoadPreCy}^{2} + \left(\frac{.4Load_{PreCy}}{Carbon_{in}^{2}}\right)^{2} \cdot \sigma_{Cin}^{2}\right]}$

$\sigma_{conv} = 0.167\,\%$

MOLE OF PRODUCTS

$mole_{N2} := \frac{mass_{N2}}{M_{N2}}$ $mol_{N2} = 97.046 \frac{mol}{hr}$

$mol_{H2} := \frac{mass_{H2}}{M_{H2}}$ $mol_{H2} = 18.858 \frac{mol}{hr}$

$mol_{O2} := \frac{mass_{O2}}{M_{O2}}$ $mol_{O2} = 0 \frac{mol}{hr}$

$mol_{CO} := \frac{mass_{CO}}{M_{CO}}$ $mol_{CO} = 45.016 \frac{mol}{hr}$

$mol_{CO2} := \frac{mass_{CO2}}{M_{CO2}}$ $mol_{CO2} = 32.935 \frac{mol}{hr}$

$mol_{CH4} := \frac{mass_{CH4}}{M_{CH4}}$ $mol_{CH4} = 12.523 \frac{mol}{hr}$

$mol_{C2H2} := \frac{mass_{C2H2}}{M_{C2H2}}$ $mol_{C2H2} = 0.21 \frac{mol}{hr}$

$mol_{C2H4} := \frac{mass_{C2H4}}{M_{C2H4}}$ $mol_{C2H4} = 5.554 \frac{mol}{hr}$

$mol_{C2H6} := \frac{mass_{C2H6}}{M_{C2H6}}$ $mol_{C2H6} = 0.914 \frac{mol}{hr}$

$mol_{H2O} := \frac{mass_{water}}{M_{H2O}}$ $mol_{H2O} = 27.979 \frac{mol}{hr}$

MOLE OF REACTANTS

$mole_{C} := x_{C\_fuel} \cdot \frac{dry_{fuel}}{M_{C}}$ $mole_{C} = 104.77 \frac{mol}{hr}$

$mole_{N} := x_{N\_fuel} \cdot \frac{dry_{fuel}}{M_{N}}$ $mole_{N} = 2.414 \frac{mol}{hr}$

$mole_{H} := x_{H\_fuel} \cdot \frac{dry_{fuel}}{M_{H}}$ $mole_{H} = 156.833 \frac{mol}{hr}$

$mole_{O} := x_{O\_fuel} \cdot \frac{dry_{fuel}}{M_{O}}$ $mole_{O} = 68.582 \frac{mol}{hr}$

$mole_{H2O} := .12 \cdot \frac{mass_{fuel}}{M_{H2O}}$ $mole_{H2O} = 18.144 \frac{mol}{hr}$

$M_{fuel} := 26.2 \frac{gm}{mol}$

$mole_{fuel} := \frac{dry_{fuel}}{M_{fuel}}$ $mole_{fuel} = 98.454 \frac{mol}{hr}$

Carbon Balance (Moles)

Carbon In

Carbon from dry fuel

$$mol_{C\_fueldry} := \frac{dry_{fuel} \cdot x_{C\_fuel}}{M_C} \qquad mole_{C\_IN} := mol_{C\_fueldry}$$

$$mol_{C\_fueldry} = 104.77 \frac{mol}{hr} \qquad mole_{C\_IN} = 104.77 \frac{mol}{hr}$$

$$\sigma_{C\_IN} := \sqrt{\left(\frac{x_{C\_fuel}}{M_C}\right)^2 \cdot \sigma_{dfuel}^{\ 2} + \left(\frac{dry_{fuel}}{M_C}\right)^2 \cdot \sigma_{C\_fuel}^{\ 2}}$$

$$\sigma_{C\_IN} = 6.673 \frac{mol}{hr}$$

Carbon Out

Carbon in CO

$$mol_{C\_CO} := \frac{mass_{CO}}{M_{CO}}$$

$$mol_{C\_CO} = 45.016 \frac{mol}{hr}$$

$$\sigma_{C\_CO} := \sqrt{\left(\frac{1}{M_{CO}}\right)^2 \cdot \sigma_{COmass}^{\ 2}}$$

$$\sigma_{C\_CO} = 1.896 \frac{mol}{hr}$$

Carbon in CO2

$$mol_{C\_CO2} := \frac{mass_{CO2}}{M_{CO2}}$$

$$mol_{C\_CO2} = 32.935 \frac{mol}{hr}$$

$$\sigma_{C\_CO2} := \sqrt{\left(\frac{1}{M_{CO2}}\right)^2 \cdot \sigma_{CO2mass}^{\ 2}}$$

$$\sigma_{C\_CO2} = 1.319 \frac{mol}{hr}$$

Carbon in CH4

$$mol_{C\_CH4} := \frac{mass_{CH4}}{M_{CH4}}$$

$$mol_{C\_CH4} = 12.523 \frac{mol}{hr}$$

$$\sigma_{C\_CH4} := \sqrt{\left(\frac{1}{M_{CH4}}\right)^2 \cdot \sigma_{CH4mass}^{\ 2}}$$

$$\sigma_{C\_CH4} = 0.557 \frac{mol}{hr}$$

Carbon in C2H6

$$mol_{C\_C2H6} := \frac{2mass_{C2H6}}{M_{C2H6}}$$

$$mol_{C\_C2H6} = 1.827 \frac{mol}{hr}$$

$$\sigma_{C\_C2H6} := \sqrt{\left(\frac{1}{M_{C2H6}}\right)^2 \cdot \sigma_{C2H6mass}^{\ 2}}$$

$$\sigma_{C\_C2H6} = 0.042 \frac{mol}{hr}$$

Carbon in C2H2

$$mol_{C\_C2H2} := \frac{2mass_{C2H2}}{M_{C2H2}}$$

$$mol_{C\_C2H2} = 0.419 \frac{mol}{hr}$$

$$\sigma_{C\_C2H2} := \sqrt{\left(\frac{1}{M_{C2H2}}\right)^2 \cdot \sigma_{C2H2mas}}$$

$$\sigma_{C\_C2H2} = 8.978 \times 10^{-3} \frac{mol}{hr}$$

Carbon in C2H4

$$mol_{C\_C2H4} := \frac{2mass_{C2H4}}{M_{C2H4}}$$

$$mol_{C\_C2H4} = 11.109 \frac{mol}{hr}$$

$$\sigma_{C\_C2H4} := \sqrt{\left(\frac{1}{M_{C2H4}}\right)^2 \cdot \sigma_{C2H4mas}}$$

$$\sigma_{C\_C2H4} = 0.234 \frac{mol}{hr}$$

Carbon from Char

$$mol_{C\_char} := \frac{.4mass_{char}}{M_C}$$

$$mol_{C\_char} = 2.453 \frac{mol}{hr}$$

$$\sigma_{C\_char} := \sqrt{\left(\frac{1}{M_C}\right)^2 \cdot \sigma_{mchar}^{\ 2}}$$

$$\sigma_{C\_char} = 0.073 \frac{mol}{hr}$$

$$mole_{C\_OUT} := mol_{C\_CO} + mol_{C\_CO2} + mol_{C\_CH4} + mol_{C\_C2H2} + mol_{C\_C2H4} + mol_{C\_char} + mol_{C\_C2H6}$$

$$mole_{C\_OUT} = 106.281 \frac{mol}{hr}$$

$$\sigma_{C\_OUT} := \sqrt{\sigma_{C\_CO}^{\ 2} + \sigma_{C\_CO2}^{\ 2} + \sigma_{C\_CH4}^{\ 2} + \sigma_{C\_C2H6}^{\ 2} + \sigma_{C\_C2H2}^{\ 2} + \sigma_{C\_C2H4}^{\ 2} + \sigma_{C\_char}^{\ 2}}$$

$$\sigma_{C\_OUT} = 2.389 \frac{mol}{hr}$$

$$mole_{C\_pro} := mol_{C\_CO} + mol_{C\_CO2} + mol_{C\_CH4} + mol_{C\_C2H2} + mol_{C\_C2H4} + mol_{C\_C2H6}$$

$$mole_{C\_pro} = 103.828 \frac{mol}{hr}$$

$$\sigma_{C\_pro} := \sqrt{\sigma_{C\_CO}^{\ 2} + \sigma_{C\_CO2}^{\ 2} + \sigma_{C\_CH4}^{\ 2} + \sigma_{C\_C2H6}^{\ 2} + \sigma_{C\_C2H2}^{\ 2} + \sigma_{C\_C2H4}^{\ 2}}$$

$$\sigma_{C\_pro} = 2.388 \frac{mol}{hr}$$

$$\frac{mole_{C\_OUT}}{mole_{C\_IN}} = 101.442\,\% \qquad \frac{mole_{C\_pro}}{mole_{C\_IN}} = 99.101\,\%$$

$$\sigma_{\%C} := \sqrt{\left(\frac{1}{mole_{C\_IN}}\right)^2 \cdot \sigma_{C\_OUT}^{\ 2} + \left(\frac{-mole_{C\_OUT}}{mole_{C\_IN}^{\ 2}}\right)^2 \cdot \sigma_{C\_IN}^{\ 2}}$$

$$\sigma_{\%C} = 6.851\,\%$$

$$\sigma_{\%Cpro} := \sqrt{\left(\frac{1}{mole_{C\_IN}}\right)^2 \cdot \sigma_{C\_pro}^{\ 2} + \left(\frac{-mole_{C\_pro}}{mole_{C\_IN}^{\ 2}}\right)^2 \cdot \sigma_{C\_IN}^{\ 2}}$$

$$\sigma_{\%Cpro} = 6.711\,\%$$

Nitrogen Balance (Moles)

Nitrogen In

Nitrogen from dry fuel

$$mol_{N2\_fueldry} := \frac{dry_{fuel} \cdot x_{N\_fuel}}{2M_N}$$

$$mol_{N2\_fueldry} = 1.207 \frac{mol}{hr}$$

Nitrogen from air

$$mol_{N2\_air} := .7808 \cdot mdot_{air} \cdot \frac{\rho_{air}}{M_{air}}$$

$$mol_{N2\_air} = 95.919 \frac{mol}{hr}$$

$$mole_{N2\_IN} := mol_{N2\_fueldry} + mol_{N2\_air}$$

$$mole_{N2\_IN} = 97.126 \frac{mol}{hr}$$

d

Nitrogen Out

Nitrogen

$$mol_{N2} := \frac{mass_{N2}}{M_{N2}}$$

$$mol_{N2} = 97.046 \frac{mol}{hr}$$

Nitrogen from char

$$mol_{N2\_char} := \frac{.0305 mass_{char}}{2M_N}$$

$$mol_{N2\_char} = 0.08 \frac{mol}{hr}$$

$$mole_{N2\_OUT} := mol_{N2} + mol_{N2\_char}$$

$$mole_{N2\_OUT} = 97.126 \frac{mol}{hr}$$

$$\frac{mole_{N2\_OUT}}{mole_{N2\_IN}} = 100\,\%$$

Oxygen Balance (Moles)

Oxygen In

Oxygen from dry fuel

$$mol_{O2\_fueldry} := \frac{dry_{fuel} \cdot x_{O\_fuel}}{2M_O}$$

$$mol_{O2\_fueldry} = 34.291 \frac{mol}{hr}$$

Oxygen from air

$$mol_{O2\_air} := .21 \cdot mdot_{air} \cdot \frac{\rho_{air}}{M_{air}}$$

$$mol_{O2\_air} = 25.798 \frac{mol}{hr}$$

Oxygen from water in fuel

$$mol_{O2\_fuelwater} := \frac{water_{fuel} \cdot \rho_{H2O}}{2M_{H2O}}$$

$$mol_{O2\_fuelwater} = 3.946 \frac{mol}{hr}$$

$$mole_{O2\_IN} := mol_{O2\_fueldry} + mol_{O2\_air} + mol_{O2\_fuelwater}$$

$$mole_{O2\_IN} = 64.035 \frac{mol}{hr}$$

Oxygen Out

Oxygen in CO

$$mol_{O2\_CO} := \frac{mass_{CO}}{2M_{CO}}$$

$$mol_{O2\_CO} = 22.508 \frac{mol}{hr}$$

Oxygen in CO2

$$mol_{O2\_CO2} := \frac{mass_{CO2}}{M_{CO2}}$$

$$mol_{O2\_CO2} = 32.935 \frac{mol}{hr}$$

Oxygen in water

$$mol_{O2\_H2O} := \frac{mass_{water}}{2M_{H2O}}$$

$$mol_{O2\_H2O} = 13.989 \frac{mol}{hr}$$

Oxygen from Char

$$mol_{O2\_char} := \frac{.1721 mass_{char}}{2M_O}$$

$$mol_{O2\_char} = 0.396 \frac{mol}{hr}$$

$$mole_{O2\_OUT} := mol_{O2\_CO} + mol_{O2\_CO2} + mol_{O2\_char} + mol_{O2\_H2O}$$

$$mole_{O2\_OUT} = 69.828 \frac{mol}{hr}$$

$$\frac{mole_{O2\_OUT}}{mole_{O2\_IN}} = 109.046\,\%$$

APPENDIX D.
RESULTS FROM EXPERIMENTS

TEST #1

Mass Balance				
Mass In			**Uncertainty**	
Air	3.543	kg/hr	0.142	kg/hr
Fuel	2.748	kg/hr	0.091	kg/hr
Total	6.291	kg/hr	0.168	kg/hr
Mass Out				
Pro Gas	6.234	kg/hr	0.194	kg/hr
Water	0.191	kg/hr	0.115	kg/hr
Cyclone	0.06	kg/hr	0.0008267	kg/hr
Fabric	0.025	kg/hr	0.0008314	kg/hr
Thimble	0.0000012	kg/hr	2.665E-08	kg/hr
Total	6.509	kg/hr	0.225	kg/hr
Efficiency	103.47	%	4.523	%

Oxygen Balance				
Oxygen In			**Uncertainty**	
Dry Fuel	34.623	mol/hr	2.199	mol/hr
Fuel H2O	3.984	mol/hr	1.532	mol/hr
Air	25.798	mol/hr	1.032	mol/hr
Total	64.405	mol/hr	2.872	mol/hr
Oxygen Out				
CO	23.718	mol/hr	1.428	mol/hr
CO2	37.767	mol/hr	2.175	mol/hr
H2O	5.295	mol/hr	3.182	mol/hr
Char	0.454	mol/hr	0.037	mol/hr
Total	67.234	mol/hr	4.111	mol/hr
Efficiency	104.392	%	7.9	%

Nitrogen Balance				
Nitrogen In			**Uncertainty**	
Dry Fuel	1.218	mol/hr	2.381	mol/hr
Air	95.919	mol/hr	3.837	mol/hr
Total	97.138	mol/hr	4.515	mol/hr
Nitrogen Out				
N2	97.046	mol/hr	5.257	mol/hr
Char	0.092	mol/hr	0.001277	mol/hr
Total	97.138	mol/hr	5.257	mol/hr
Efficiency	100	%	7.134	%

Flow Rates				
			Uncertainty	
System dry	92.693	liter/min	4.68	liter/min
Sample line	1.326	liter/min	0.017	liter/min

Carbon Conversion				
			Uncertainty	
Efficiency	97.587	%	0.234	%

Percent Water				
			Uncertainty	
water %	4.443	%	2.681	%

Carbon Balance				
Carbon In			**Uncertainty**	
Fuel	105.783	mol/hr	6.72	mol/hr
Total	105.783	mol/hr	6.72	mol/hr
Carbon Out				
CO	47.435	mol/hr	2.857	mol/hr
CO2	37.767	mol/hr	2.175	mol/hr
CH4	15.634	mol/hr	0.836	mol/hr
C2H2	0	mol/hr	0	mol/hr
C2H4	13.312	mol/hr	0.346	mol/hr
C2H6	2.261	mol/hr	0.06	mol/hr
C3H8	0	mol/hr	0	mol/hr
Char	2.815	mol/hr	0.098	mol/hr
Total	119.225	mol/hr	3.705	mol/hr
Pro Gas	116.409	mol/hr	3.703	mol/hr
Efficiency				
Carbon	112.707	%	7.97	%
Pro Gas	110.045	%	7.818	%

Hydrogen Balance				
Hydrogen In			**Uncertainty**	
Dry Fuel	79.174	mol/hr	5.029	mol/hr
Fuel H2O	7.969	mol/hr	3.064	mol/hr
Total	87.143	mol/hr	5.89	mol/hr
Hydrogen Out				
H2	28.159	mol/hr	1.583	mol/hr
CH4	31.268	mol/hr	1.673	mol/hr
C2H2	0	mol/hr	0	mol/hr
C2H4	13.312	mol/hr	0.692	mol/hr
C2H6	3.391	mol/hr	0.181	mol/hr
C3H8	0	mol/hr	0	mol/hr
H2O	10.59	mol/hr	6.364	mol/hr
Char	0.422	mol/hr	0.022	mol/hr
Total	87.143	mol/hr	6.806	mol/hr
Efficiency	100	%	10.328	%

Filtration Results				
Mass Loading			**Uncertainty**	
Out Gasifier	14.527	g/m^3	0.825	g/m^3
After Cyclone	4.244	g/m^3	0.273	g/m^3
After Fabric	0.015	g/m^3	0.000387	g/m^3
Efficiency				
Cyclone	70.783	%	3.264	%
Fabric	99.645	%	0.035	%
Collection	99.896	%	0.009843	%

TEST #2

Mass Balance				
Mass In			**Uncertainty**	
Air	3.543	kg/hr	0.142	kg/hr
Fuel	2.799	kg/hr	0.091	kg/hr
Total	6.342	kg/hr	0.168	kg/hr
Mass Out				
Pro Gas	6.453	kg/hr	0.203	kg/hr
Water	0.191	kg/hr	0.117	kg/hr
Cyclone	0.06	kg/hr	0.0008911	kg/hr
Fabric	0.026	kg/hr	0.0009064	kg/hr
Thimble	3.833E-07	kg/hr	2.416E-08	kg/hr
Total	6.73	kg/hr	0.234	kg/hr
Efficiency	106.125	%	4.648	%

Oxygen Balance				
Oxygen In			**Uncertainty**	
Dry Fuel	35.263	mol/hr	2.229	mol/hr
Fuel H2O	4.058	mol/hr	1.56	mol/hr
Air	25.798	mol/hr	1.032	mol/hr
Total	65.119	mol/hr	2.91	mol/hr
Oxygen Out				
CO	24.558	mol/hr	1.515	mol/hr
CO2	41.159	mol/hr	2.396	mol/hr
H2O	5.315	mol/hr	3.238	mol/hr
Char	0.458	mol/hr	0.04	mol/hr
Total	71.491	mol/hr	4.303	mol/hr
Efficiency	109.786	%	8.231	%

Nitrogen Balance				
Nitrogen In			**Uncertainty**	
Dry Fuel	1.241	mol/hr	2.425	mol/hr
Air	95.919	mol/hr	3.837	mol/hr
Total	97.16	mol/hr	4.539	mol/hr
Nitrogen Out				
N2	97.067	mol/hr	5.389	mol/hr
Char	0.093	mol/hr	0.001385	mol/hr
Total	97.16	mol/hr	5.389	mol/hr
Efficiency	100	%	7.252	%

Flow Rates				
			Uncertainty	
System dr	100.075	liter/min	5.137	liter/min
Sample lin	2.16	liter/min	0.03	liter/min

Carbon Conversion				
			Uncertainty	
Efficiency	97.606	%	0.233	%

Percent Water				
			Uncertainty	
water %	4.144	%	2.535	%

Carbon Balance				
Carbon In			**Uncertainty**	
Fuel	107.739	mol/hr	6.811	mol/hr
Total	107.739	mol/hr	6.811	mol/hr
Carbon Out				
CO	49.117	mol/hr	2.857	mol/hr
CO2	41.159	mol/hr	2.396	mol/hr
CH4	15.776	mol/hr	0.863	mol/hr
C2H2	0.408	mol/hr	0.01	mol/hr
C2H4	14.025	mol/hr	0.371	mol/hr
C2H6	2.433	mol/hr	0.066	mol/hr
C3H8	0	mol/hr	0.002953	mol/hr
Char	2.839	mol/hr	0.106	mol/hr
Total	125.873	mol/hr	3.977	mol/hr
Pro Gas	123.034	mol/hr	3.976	mol/hr
Efficiency				
Carbon	116.831	%	8.257	%
Pro Gas	114.196	%	8.107	%

Hydrogen Balance				
Hydrogen In			**Uncertainty**	
Dry Fuel	80.638	mol/hr	5.097	mol/hr
Fuel H2O	8.116	mol/hr	3.121	mol/hr
Total	88.754	mol/hr	5.977	mol/hr
Hydrogen Out				
H2	28.094	mol/hr	1.626	mol/hr
CH4	31.552	mol/hr	1.726	mol/hr
C2H2	0.204	mol/hr	0.01	mol/hr
C2H4	14.025	mol/hr	0.742	mol/hr
C2H6	3.65	mol/hr	0.198	mol/hr
C3H8	0.173	mol/hr	0.008859	mol/hr
H2O	10.631	mol/hr	6.476	mol/hr
Char	0.426	mol/hr	0.022	mol/hr
Total	88.754	mol/hr	6.939	mol/hr
Efficiency	100	%	10.318	%

Filtration Results				
Mass Loading			**Uncertainty**	
Out Gasifie	13.599	g/m^3	0.779	g/m^3
After Cyclo	4.1	g/m^3	0.269	g/m^3
After Fabri	0.002958	g/m^3	0.000191	g/m^3
Efficiency				
Cyclone	69.848	%	3.418	%
Fabric	99.928	%	0.008454	%
Collection	99.978	%	0.002453	%

TEST #3

Mass Balance				
Mass In			**Uncertainty**	
Air	3.543	kg/hr	0.142	kg/hr
Fuel	2.767	kg/hr	0.091	kg/hr
Total	6.31	kg/hr	0.168	kg/hr
Mass Out				
Pro Gas	6.169	kg/hr	0.196	kg/hr
Water	0.302	kg/hr	0.114	kg/hr
Cyclone	0.057	kg/hr	0.000859	kg/hr
Fabric	0.033	kg/hr	0.0009477	kg/hr
Thimble	0.000001283	kg/hr	2.955E-08	kg/hr
Total	6.561	kg/hr	0.227	kg/hr
Efficiency	103.975	%	4.537	%

Oxygen Balance				
Oxygen In			**Uncertainty**	
Dry Fuel	34.863	mol/hr	2.21	mol/hr
Fuel H2O	4.012	mol/hr	1.543	mol/hr
Air	25.798	mol/hr	1.032	mol/hr
Total	64.673	mol/hr	2.886	mol/hr
Oxygen Out				
CO	21.337	mol/hr	1.348	mol/hr
CO2	40.198	mol/hr	2.308	mol/hr
H2O	8.39	mol/hr	3.171	mol/hr
Char	0.481	mol/hr	0.04	mol/hr
Total	70.407	mol/hr	4.148	mol/hr
Efficiency	108.866	%	8.046	%

Nitrogen Balance				
Nitrogen In			**Uncertainty**	
Dry Fuel	1.227	mol/hr	2.425	mol/hr
Air	95.919	mol/hr	3.837	mol/hr
Total	97.146	mol/hr	4.524	mol/hr
Nitrogen Out				
N2	97.046	mol/hr	5.305	mol/hr
Char	0.097	mol/hr	0.001393	mol/hr
Total	97.146	mol/hr	5.035	mol/hr
Efficiency	100	%	7.177	%

Flow Rates			Uncertainty	
System dr	95.385	liter/min	4.845	liter/min
Sample lin	2.213	liter/min	0.031	liter/min

Carbon Conversion			Uncertainty	
Efficiency	97.521	%	0.006267	%

Percent Water			Uncertainty	
water %	6.682	%	2.551	%

Carbon Balance				
Carbon In			**Uncertainty**	
Fuel	106.516	mol/hr	6.754	mol/hr
Total	106.516	mol/hr	6.754	mol/hr
Carbon Out				
CO	42.674	mol/hr	2.696	mol/hr
CO2	40.198	mol/hr	2.308	mol/hr
CH4	14.019	mol/hr	0.767	mol/hr
C2H2	0.337	mol/hr	0.008559	mol/hr
C2H4	12.343	mol/hr	0.325	mol/hr
C2H6	2.061	mol/hr	0.056	mol/hr
C3H8	0	mol/hr	0.002667	mol/hr
Char	2.983	mol/hr	0.107	mol/hr
Total	114.721	mol/hr	3.647	mol/hr
Pro Gas	111.738	mol/hr	3.646	mol/hr
Efficiency				
Carbon	107.703	%	7.639	%
Pro Gas	104.902	%	7.48	%

Hydrogen Balance				
Hydrogen In			**Uncertainty**	
Dry Fuel	79.723	mol/hr	5.055	mol/hr
Fuel H2O	8.024	mol/hr	3.086	mol/hr
Total	87.747	mol/hr	5.922	mol/hr
Hydrogen Out				
H2	26.721	mol/hr	1.535	mol/hr
CH4	28.037	mol/hr	1.533	mol/hr
C2H2	0.169	mol/hr	0.008559	mol/hr
C2H4	12.343	mol/hr	0.65	mol/hr
C2H6	3.092	mol/hr	0.168	mol/hr
C3H8	0.157	mol/hr	0.008	mol/hr
H2O	16.78	mol/hr	6.343	mol/hr
Char	0.447	mol/hr	0.023	mol/hr
Total	87.747	mol/hr	6.737	mol/hr
Efficiency	100	%	10.233	%

Filtration Results				
Mass Loading			**Uncertainty**	
Out Gasifie	14.603	g/m^3	0.811	g/m^3
After Cyclo	5.309	g/m^3	0.324	g/m^3
After Fabri	0.009663	g/m^3	0.00026	g/m^3
Efficiency				
Cyclone	63.645	%	3.977	%
Fabric	99.818	%	0.018	%
Collection	99.934	%	0.006267	%

TEST #4

Mass Balance				
Mass In			**Uncertainty**	
Air	3.543	kg/hr	0.142	kg/hr
Fuel	3.111	kg/hr	0.091	kg/hr
Total	6.654	kg/hr	0.168	kg/hr
Mass Out				
Pro Gas	6.514	kg/hr	0.203	kg/hr
Water	0.119	kg/hr	0.128	kg/hr
Cyclone	0.044	kg/hr	0.000694	kg/hr
Fabric	0.03	kg/hr	0.000932	kg/hr
Thimble	0.0000057	kg/hr	8.26E-08	kg/hr
Total	6.707	kg/hr	0.24	kg/hr
Efficiency	100.798	%	4.413	%

Oxygen Balance				
Oxygen In			**Uncertainty**	
Dry Fuel	39.2	mol/hr	2.415	mol/hr
Fuel H2O	4.511	mol/hr	1.733	mol/hr
Air	25.798	mol/hr	1.032	mol/hr
Total	69.51	mol/hr	3.147	mol/hr
Oxygen Out				
CO	22.925	mol/hr	1.444	mol/hr
CO2	39.452	mol/hr	2.33	mol/hr
H2O	3.313	mol/hr	3.555	mol/hr
Char	0.397	mol/hr	0.036	mol/hr
Total	66.088	mol/hr	4.489	mol/hr
Efficiency	95.078	%	7.761	%

Nitrogen Balance				
Nitrogen In			**Uncertainty**	
Dry Fuel	1.38	mol/hr	2.696	mol/hr
Air	95.919	mol/hr	3.837	mol/hr
Total	97.299	mol/hr	4.689	mol/hr
Nitrogen Out				
N2	97.218	mol/hr	5.452	mol/hr
Char	0.08	mol/hr	0.001266	mol/hr
Total	97.299	mol/hr	5.452	mol/hr
Efficiency	100	%	7.391	%

Flow Rates				
			Uncertainty	
System dr	95.799	liter/min	5.011	liter/min
Sample lin	2.213	liter/min	0.031	liter/min

Carbon Conversion				
			Uncertainty	
Efficiency	98.099	%	0.188	%

Percent Water				
			Uncertainty	
water %	2.738	%	2.942	%

Carbon Balance				
Carbon In			**Uncertainty**	
Fuel	119.77	mol/hr	7.379	mol/hr
Total	119.77	mol/hr	7.379	mol/hr
Carbon Out				
CO	45.85	mol/hr	2.888	mol/hr
CO2	39.452	mol/hr	2.33	mol/hr
CH4	14.098	mol/hr	0.791	mol/hr
C2H2	0.384	mol/hr	0.01	mol/hr
C2H4	32.289	mol/hr	0.849	mol/hr
C2H6	2.146	mol/hr	0.06	mol/hr
C3H8	0	mol/hr	0.002696	mol/hr
Char	2.461	mol/hr	0.097	mol/hr
Total	136.783	mol/hr	3.889	mol/hr
Pro Gas	134.322	mol/hr	3.888	mol/hr
Efficiency				
Carbon	114.205	%	7.749	%
Pro Gas	112.15	%	7.634	%

Hydrogen Balance				
Hydrogen In			**Uncertainty**	
Dry Fuel	89.643	mol/hr	5.523	mol/hr
Fuel H2O	9.022	mol/hr	3.467	mol/hr
Total	98.666	mol/hr	6.251	mol/hr
Hydrogen Out				
H2	27.62	mol/hr	1.614	mol/hr
CH4	28.196	mol/hr	1.581	mol/hr
C2H2	0.192	mol/hr	0.01	mol/hr
C2H4	32.289	mol/hr	1.698	mol/hr
C2H6	3.218	mol/hr	0.179	mol/hr
C3H8	0.155	mol/hr	0.008088	mol/hr
H2O	6.627	mol/hr	7.109	mol/hr
Char	0.369	mol/hr	0.019	mol/hr
Total	98.666	mol/hr	7.652	mol/hr
Efficiency	100	%	10.19	%

Filtration Results				
Mass Loading			**Uncertainty**	
Out Gasifie	12.536	g/m^3	0.76	g/m^3
After Cyclo	5.119	g/m^3	0.337	g/m^3
After Fabri	0.043	g/m^3	0.000862	g/m^3
Efficiency				
Cyclone	59.165	%	4.742	%
Fabric	99.162	%	0.085	%
Collection	99.658	%	0.033	%

TEST #5

Mass Balance				
Mass In			**Uncertainty**	
Air	3.543	kg/hr	0.142	kg/hr
Fuel	2.581	kg/hr	0.091	kg/hr
Total	6.124	kg/hr	0.168	kg/hr
Mass Out				
Pro Gas	5.884	kg/hr	0.186	kg/hr
Water	0.324	kg/hr	0.107	kg/hr
Cyclone	0.042	kg/hr	0.0005246	kg/hr
Fabric	0.034	kg/hr	0.0007491	kg/hr
Thimble	0.00001826	kg/hr	1.993E-07	kg/hr
Total	6.284	kg/hr	0.214	kg/hr
Efficiency	102.613	%	4.496	%

Oxygen Balance				
Oxygen In			**Uncertainty**	
Dry Fuel	32.519	mol/hr	2.103	mol/hr
Fuel H2O	3.724	mol/hr	1.44	mol/hr
Air	25.798	mol/hr	1.032	mol/hr
Total	62.06	mol/hr	2.749	mol/hr
Oxygen Out				
CO	18.423	mol/hr	1.182	mol/hr
CO2	38.869	mol/hr	2.175	mol/hr
H2O	9.006	mol/hr	2.98	mol/hr
Char	0.408	mol/hr	0.029	mol/hr
Total	66.706	mol/hr	3.874	mol/hr
Efficiency	107.487	%	7.852	%

Nitrogen Balance				
Nitrogen In			**Uncertainty**	
Dry Fuel	1.144	mol/hr	2.236	mol/hr
Air	95.919	mol/hr	3.837	mol/hr
Total	97.064	mol/hr	4.441	mol/hr
Nitrogen Out				
N2	96.981	mol/hr	5.145	mol/hr
Char	0.083	mol/hr	0.0009962	mol/hr
Total	97.064	mol/hr	5.145	mol/hr
Efficiency	100	%	7.002	%

Flow Rates				
			Uncertainty	
System dr	89.445	liter/min	4.432	liter/min
Sample lin	1.916	liter/min	0.021	liter/min

Carbon Conversion				
			Uncertainty	
Efficiency	97.746	%	0.214	%

Percent Water				
			Uncertainty	
water %	7.576	%	2.538	%

Carbon Balance				
Carbon In			**Uncertainty**	
Fuel	99.357	mol/hr	6.424	mol/hr
Total	99.357	mol/hr	6.424	mol/hr
Carbon Out				
CO	36.846	mol/hr	2.364	mol/hr
CO2	38.869	mol/hr	2.175	mol/hr
CH4	12.158	mol/hr	0.659	mol/hr
C2H2	0.321	mol/hr	0.007949	mol/hr
C2H4	10.533	mol/hr	0.273	mol/hr
C2H6	1.807	mol/hr	0.049	mol/hr
C3H8	0	mol/hr	0.002221	mol/hr
Char	2.526	mol/hr	0.076	mol/hr
Total	103.149	mol/hr	3.292	mol/hr
Pro Gas	100.623	mol/hr	3.291	mol/hr
Efficiency				
Carbon	103.817	%	7.486	%
Pro Gas	101.274	%	7.338	%

Hydrogen Balance				
Hydrogen In			**Uncertainty**	
Dry Fuel	74.365	mol/hr	4.808	mol/hr
Fuel H2O	7.485	mol/hr	2.88	mol/hr
Total	81.85	mol/hr	5.605	mol/hr
Hydrogen Out				
H2	25.604	mol/hr	1.436	mol/hr
CH4	24.315	mol/hr	1.317	mol/hr
C2H2	0.16	mol/hr	0.007949	mol/hr
C2H4	10.533	mol/hr	0.546	mol/hr
C2H6	2.71	mol/hr	0.146	mol/hr
C3H8	0.134	mol/hr	0.006664	mol/hr
H2O	18.013	mol/hr	5.961	mol/hr
Char	0.379	mol/hr	0.019	mol/hr
Total	81.85	mol/hr	6.296	mol/hr
Efficiency	100	%	10.299	%

Filtration Results				
Mass Loading			**Uncertainty**	
Out Gasifie	13.21	g/m^3	0.699	g/m^3
After Cyclo	5.999	g/m^3	0.331	g/m^3
After Fabri	0.159	g/m^3	0.002448	g/m^3
Efficiency				
Cyclone	54.585	%	4.711	%
Fabric	97.353	%	0.24	%
Collection	98.798	%	0.107	%

TEST #6

Mass Balance				
Mass In			**Uncertainty**	
Air	3.543	kg/hr	0.142	kg/hr
Fuel	2.599	kg/hr	0.091	kg/hr
Total	6.142	kg/hr	0.168	kg/hr
Mass Out				
Pro Gas	6.049	kg/hr	0.19	kg/hr
Water	0.246	kg/hr	0.109	kg/hr
Cyclone	0.067	kg/hr	0.0006031	kg/hr
Fabric	0.029	kg/hr	0.0005602	kg/hr
Thimble	0.000008469	kg/hr	2.073E-07	kg/hr
Total	6.391	kg/hr	0.219	kg/hr
Efficiency	104.051	%	4.565	%

Oxygen Balance				
Oxygen In			**Uncertainty**	
Dry Fuel	32.748	mol/hr	2.113	mol/hr
Fuel H2O	3.769	mol/hr	1.45	mol/hr
Air	25.798	mol/hr	1.032	mol/hr
Total	62.315	mol/hr	2.763	mol/hr
Oxygen Out				
CO	20.523	mol/hr	1.286	mol/hr
CO2	39.259	mol/hr	2.22	mol/hr
H2O	6.831	mol/hr	3.022	mol/hr
Char	0.516	mol/hr	0.026	mol/hr
Total	67.129	mol/hr	3.964	mol/hr
Efficiency	107.726	%	7.955	%

Nitrogen Balance				
Nitrogen In			**Uncertainty**	
Dry Fuel	1.153	mol/hr	2.252	mol/hr
Air	95.919	mol/hr	3.837	mol/hr
Total	97.702	mol/hr	4.449	mol/hr
Nitrogen Out				
N2	96.967	mol/hr	5.199	mol/hr
Char	0.104	mol/hr	0.0008967	mol/hr
Total	97.072	mol/hr	5.199	mol/hr
Efficiency	100	%	7.049	%

Flow Rates				
			Uncertainty	
System	92.628	liter/min	4.622	liter/min
Sample 1	1.971	liter/min	0.031	liter/min
Sample 2	1.971	liter/min	0.048	liter/min

Carbon Conversion				
			Uncertainty	
Efficiency	97.13	%	0.274	%

Percent Water				
			Uncertainty	
water %	5.663	%	2.523	%

Carbon Balance				
Carbon In			**Uncertainty**	
Fuel	100.056	mol/hr	6.456	mol/hr
Total	100.056	mol/hr	6.456	mol/hr
Carbon Out				
CO	41.045	mol/hr	2.572	mol/hr
CO2	39.259	mol/hr	2.22	mol/hr
CH4	13.008	mol/hr	0.705	mol/hr
C2H2	0.338	mol/hr	0.008426	mol/hr
C2H4	11.278	mol/hr	0.293	mol/hr
C2H6	1.963	mol/hr	0.053	mol/hr
C3H8	0.086	mol/hr	0.002135	mol/hr
Char	3.197	mol/hr	0.069	mol/hr
Total	110.174	mol/hr	3.484	mol/hr
Pro Gas	106.977	mol/hr	3.483	mol/hr
Efficiency				
Carbon	110.113	%	7.912	%
Pro Gas	106.917	%	7.727	%

Hydrogen Balance				
Hydrogen In			**Uncertainty**	
Dry Fuel	74.888	mol/hr	4.832	mol/hr
Fuel H2O	7.537	mol/hr	2.9	mol/hr
Total	82.425	mol/hr	5.636	mol/hr
Hydrogen Out				
H2	27.748	mol/hr	1.549	mol/hr
CH4	26.015	mol/hr	1.41	mol/hr
C2H2	0.169	mol/hr	0.008426	mol/hr
C2H4	11.278	mol/hr	0.587	mol/hr
C2H6	2.945	mol/hr	0.158	mol/hr
C3H8	0.128	mol/hr	0.006404	mol/hr
H2O	13.662	mol/hr	6.043	mol/hr
Char	0.48	mol/hr	0.024	mol/hr
Total	82.425	mol/hr	6.425	mol/hr
Efficiency	100	%	10.368	%

Filtration Results				
Mass Loading			**Uncertainty**	
Out Gasifier	16.353	g/m^3	0.879	g/m^3
After Cyclone	4.915	g/m^3	0.275	g/m^3
After Fabric 1	0.096	g/m^3	0.0012	g/m^3
After Fabric 2	0.033	g/m^3	0.0012	g/m^3
Efficiency				
Cyclone	69.945	%	3.153	%
Fabric 1	98.044	%	0.181	%
Fabric 2	99.327	%	0.065	%
Collection 1	99.412	%	0.054	%
Collection 2	99.798	%	0.019	%

TEST #7

Mass Balance				
Mass In			**Uncertainty**	
Air	3.543	kg/hr	0.142	kg/hr
Fuel	2.545	kg/hr	0.091	kg/hr
Total	6.088	kg/hr	0.168	kg/hr
Mass Out				
Pro Gas	5.903	kg/hr	0.185	kg/hr
Water	0.289	kg/hr	0.106	kg/hr
Cyclone	0.062	kg/hr	0.0007244	kg/hr
Fabric	0.036	kg/hr	0.0007639	kg/hr
Thimble	0.000003822	kg/hr	2.015E-07	kg/hr
Total	6.29	kg/hr	0.214	kg/hr
Efficiency	103.325	%	4.526	%

Oxygen Balance				
Oxygen In			**Uncertainty**	
Dry Fuel	32.062	mol/hr	2.082	mol/hr
Fuel H2O	3.69	mol/hr	1.42	mol/hr
Air	25.798	mol/hr	1.032	mol/hr
Total	61.55	mol/hr	2.723	mol/hr
Oxygen Out				
CO	19.622	mol/hr	1.232	mol/hr
CO2	37.55	mol/hr	2.12	mol/hr
H2O	8.037	mol/hr	2.954	mol/hr
Char	0.524	mol/hr	0.033	mol/hr
Total	65.734	mol/hr	3.839	mol/hr
Efficiency	106.798	%	7.824	%

Nitrogen Balance				
Nitrogen In			**Uncertainty**	
Dry Fuel	1.128	mol/hr	2.205	mol/hr
Air	95.919	mol/hr	3.837	mol/hr
Total	97.048	mol/hr	4.425	mol/hr
Nitrogen Out				
N2	96.941	mol/hr	5.143	mol/hr
Char	0.106	mol/hr	0.001147	mol/hr
Total	97.048	mol/hr	5.143	mol/hr
Efficiency	100	%	6.992	%

Flow Rates			**Uncertainty**	
System	90.296	liter/min	4.469	liter/min
Sample 1	1.955	liter/min	0.035	liter/min
Sample 2	1.95	liter/min	0.08	liter/min

Carbon Conversion			**Uncertainty**	
Efficiency	97.065	%	0.28	%

Percent Water			**Uncertainty**	
water %	6.756	%	2.508	%

Carbon Balance				
Carbon In			**Uncertainty**	
Fuel	97.96	mol/hr	6.361	mol/hr
Total	97.96	mol/hr	6.361	mol/hr
Carbon Out				
CO	39.245	mol/hr	2.464	mol/hr
CO2	37.55	mol/hr	2.12	mol/hr
CH4	12.566	mol/hr	0.678	mol/hr
C2H2	0.32	mol/hr	0.007928	mol/hr
C2H4	10.889	mol/hr	0.281	mol/hr
C2H6	1.877	mol/hr	0.05	mol/hr
C3H8	0.088	mol/hr	0.002174	mol/hr
Char	3.247	mol/hr	0.088	mol/hr
Total	105.782	mol/hr	3.334	mol/hr
Pro Gas	102.535	mol/hr	3.333	mol/hr
Efficiency				
Carbon	107.985	%	7.794	%
Pro Gas	104.67	%	7.6	%

Hydrogen Balance				
Hydrogen In			**Uncertainty**	
Dry Fuel	73.319	mol/hr	4.761	mol/hr
Fuel H2O	7.379	mol/hr	2.84	mol/hr
Total	80.699	mol/hr	5.543	mol/hr
Hydrogen Out				
H2	25.01	mol/hr	1.411	mol/hr
CH4	25.132	mol/hr	1.355	mol/hr
C2H2	0.16	mol/hr	0.007928	mol/hr
C2H4	10.889	mol/hr	0.563	mol/hr
C2H6	2.815	mol/hr	0.151	mol/hr
C3H8	0.132	mol/hr	0.006522	mol/hr
H2O	16.074	mol/hr	5.907	mol/hr
Char	0.487	mol/hr	0.025	mol/hr
Total	80.699	mol/hr	6.25	mol/hr
Efficiency	100	%	10.352	%

Filtration Results				
Mass Loading			**Uncertainty**	
Out Gasifie	16.799	g/m^3	0.897	g/m^3
After Cyclo	6.179	g/m^3	0.348	g/m^3
After Fabri	0.031	g/m^3	0.002203	g/m^3
After Fabri	0.037	g/m^3	0.002203	g/m^3
Efficiency				
Cyclone	63.219	%	3.844	%
Fabric 1	99.5	%	0.047	%
Fabric 2	99.408	%	0.064	%
Collection	99.816	%	0.017	%
Collection	99.782	%	0.023	%

TEST #8

Mass Balance				
Mass In			**Uncertainty**	
Air	3.543	kg/hr	0.142	kg/hr
Fuel	2.726	kg/hr	0.091	kg/hr
Total	6.269	kg/hr	0.168	kg/hr
Mass Out				
Pro Gas	6.09	kg/hr	0.192	kg/hr
Water	0.331	kg/hr	0.112	kg/hr
Cyclone	0.052	kg/hr	0.0004912	kg/hr
Fabric	0.03	kg/hr	0.0005716	kg/hr
Thimble	0.000002332	kg/hr	8.292E-08	kg/hr
Total	6.503	kg/hr	0.222	kg/hr
Efficiency	103.739	%	4.509	%

Oxygen Balance				
Oxygen In			**Uncertainty**	
Dry Fuel	34.348	mol/hr	2.187	mol/hr
Fuel H2O	3.953	mol/hr	1.52	mol/hr
Air	25.798	mol/hr	1.032	mol/hr
Total	64.099	mol/hr	2.856	mol/hr
Oxygen Out				
CO	22.055	mol/hr	1.358	mol/hr
CO2	37.895	mol/hr	2.179	mol/hr
H2O	9.205	mol/hr	3.121	mol/hr
Char	0.444	mol/hr	0.024	mol/hr
Total	69.599	mol/hr	4.041	mol/hr
Efficiency	108.58	%	7.947	%

Nitrogen Balance				
Nitrogen In			**Uncertainty**	
Dry Fuel	1.209	mol/hr	2.362	mol/hr
Air	95.919	mol/hr	3.837	mol/hr
Total	97.128	mol/hr	4.506	mol/hr
Nitrogen Out				
N2	97.038	mol/hr	5.25	mol/hr
Char	0.09	mol/hr	0.0008209	mol/hr
Total	97.128	mol/hr	5.25	mol/hr
Efficiency	100	%	7.123	%

Flow Rates			Uncertainty	
System	92.83	liter/min	4.68	liter/min
Sample 1	2.027	liter/min	0.036	liter/min
Sample 2	1.999	liter/min	0.051	liter/min

Carbon Conversion			Uncertainty	
Efficiency	97.699	%	0.219	%

Percent Water			Uncertainty	
water %	7.469	%	2.563	%

Carbon Balance				
Carbon In			**Uncertainty**	
Fuel	104.945	mol/hr	6.681	mol/hr
Total	104.945	mol/hr	6.681	mol/hr
Carbon Out				
CO	44.111	mol/hr	2.716	mol/hr
CO2	37.895	mol/hr	2.179	mol/hr
CH4	13.604	mol/hr	0.739	mol/hr
C2H2	0.366	mol/hr	0.009222	mol/hr
C2H4	11.758	mol/hr	0.308	mol/hr
C2H6	2.021	mol/hr	0.055	mol/hr
C3H8	0.092	mol/hr	0.002311	mol/hr
Char	2.75	mol/hr	0.063	mol/hr
Total	112.595	mol/hr	3.574	mol/hr
Pro Gas	109.846	mol/hr	3.573	mol/hr
Efficiency				
Carbon	107.29	%	7.632	%
Pro Gas	104.67	%	7.483	%

Hydrogen Balance				
Hydrogen In			**Uncertainty**	
Dry Fuel	78.547	mol/hr	5	mol/hr
Fuel H2O	7.906	mol/hr	3.04	mol/hr
Total	86.453	mol/hr	5.852	mol/hr
Hydrogen Out				
H2	25.313	mol/hr	1.454	mol/hr
CH4	27.208	mol/hr	1.479	mol/hr
C2H2	0.183	mol/hr	0.009222	mol/hr
C2H4	11.758	mol/hr	0.616	mol/hr
C2H6	3.031	mol/hr	0.164	mol/hr
C3H8	0.138	mol/hr	0.006933	mol/hr
H2O	18.41	mol/hr	6.241	mol/hr
Char	0.412	mol/hr	0.021	mol/hr
Total	86.453	mol/hr	6.608	mol/hr
Efficiency	100	%	10.21	%

Filtration Results				
Mass Loading			**Uncertainty**	
Out Gasifie	13.723	g/m^3	0.738	g/m^3
After Cyclo	5.012	g/m^3	0.281	g/m^3
After Fabri	0.027	g/m^3	0.000477	g/m^3
After Fabri	0.008841	g/m^3	0.000477	g/m^3
Efficiency				
Cyclone	63.48	%	3.853	%
Fabric 1	99.469	%	0.05	%
Fabric 2	99.824	%	0.019	%
Collection	99.806	%	0.018	%
Collection	99.936	%	0.006722	%

TEST #9

Mass Balance				
Mass In			**Uncertainty**	
Air	3.543	kg/hr	0.142	kg/hr
Fuel	2.767	kg/hr	0.091	kg/hr
Total	6.31	kg/hr	0.168	kg/hr
Mass Out				
Pro Gas	6.085	kg/hr	0.192	kg/hr
Water	0.403	kg/hr	0.113	kg/hr
Cyclone	0.051	kg/hr	0.0004578	kg/hr
Fabric	0.031	kg/hr	0.0005466	kg/hr
Thimble	0.000003869	kg/hr	1.208E-07	kg/hr
Total	6.569	kg/hr	0.223	kg/hr
Efficiency	104.113	%	4.489	%

Oxygen Balance				
Oxygen In			**Uncertainty**	
Dry Fuel	34.863	mol/hr	2.21	mol/hr
Fuel H2O	4.012	mol/hr	1.543	mol/hr
Air	25.798	mol/hr	1.032	mol/hr
Total	64.673	mol/hr	2.886	mol/hr
Oxygen Out				
CO	24.933	mol/hr	1.483	mol/hr
CO2	34.024	mol/hr	2.015	mol/hr
H2O	11.197	mol/hr	3.141	mol/hr
Char	0.439	mol/hr	0.022	mol/hr
Total	70.593	mol/hr	4.016	mol/hr
Efficiency	109.154	%	7.893	%

Nitrogen Balance				
Nitrogen In			**Uncertainty**	
Dry Fuel	1.227	mol/hr	2.397	mol/hr
Air	95.919	mol/hr	3.837	mol/hr
Total	97.146	mol/hr	4.524	mol/hr
Nitrogen Out				
N2	97.057	mol/hr	5.267	mol/hr
Char	0.089	mol/hr	0.0007767	mol/hr
Total	97.146	mol/hr	5.267	mol/hr
Efficiency	100	%	7.147	%

Flow Rates				
			Uncertainty	
System	92.879	liter/min	4.698	liter/min
Sample 1	1.999	liter/min	0.037	liter/min
Sample 2	1.956	liter/min	0.045	liter/min

Carbon Conversion				
			Uncertainty	
Efficiency	97.79	%	0.209	%

Percent Water				
			Uncertainty	
water %	8.936	%	2.55	%

Carbon Balance				
Carbon In			**Uncertainty**	
Fuel	106.516	mol/hr	6.754	mol/hr
Total	106.516	mol/hr	6.754	mol/hr
Carbon Out				
CO	49.867	mol/hr	2.966	mol/hr
CO2	34.024	mol/hr	2.015	mol/hr
CH4	13.834	mol/hr	0.752	mol/hr
C2H2	0.44	mol/hr	0.011	mol/hr
C2H4	12.245	mol/hr	0.321	mol/hr
C2H6	1.981	mol/hr	0.054	mol/hr
C3H8	0.097	mol/hr	0.002459	mol/hr
Char	2.721	mol/hr	0.059	mol/hr
Total	115.208	mol/hr	3.679	mol/hr
Pro Gas	112.487	mol/hr	3.678	mol/hr
Efficiency				
Carbon	108.61	%	7.678	%
Pro Gas	105.605	%	7.534	%

Hydrogen Balance				
Hydrogen In			**Uncertainty**	
Dry Fuel	79.723	mol/hr	5.055	mol/hr
Fuel H2O	8.024	mol/hr	3.086	mol/hr
Total	87.747	mol/hr	5.922	mol/hr
Hydrogen Out				
H2	21.697	mol/hr	1.3	mol/hr
CH4	27.667	mol/hr	1.505	mol/hr
C2H2	0.22	mol/hr	0.011	mol/hr
C2H4	12.245	mol/hr	0.641	mol/hr
C2H6	2.971	mol/hr	0.161	mol/hr
C3H8	0.146	mol/hr	0.007376	mol/hr
H2O	22.393	mol/hr	6.282	mol/hr
Char	0.408	mol/hr	0.021	mol/hr
Total	87.747	mol/hr	6.623	mol/hr
Efficiency	100	%	10.125	%

Filtration Results				
Mass Loading			**Uncertainty**	
Out Gasifie	13.371	g/m^3	0.709	g/m^3
After Cyclo	5.03	g/m^3	0.277	g/m^3
After Fabri	0.036	g/m^3	0.000976	g/m^3
After Fabri	0.029	g/m^3	0.000976	g/m^3
Efficiency				
Cyclone	62.378	%	3.939	%
Fabric 1	99.289	%	0.067	%
Fabric 2	99.432	%	0.055	%
Collection	99.733	%	0.025	%
Collection	99.786	%	0.02	%

TEST #10

Mass Balance				
Mass In			**Uncertainty**	
Air	3.543	kg/hr	0.142	kg/hr
Fuel	2.767	kg/hr	0.091	kg/hr
Total	6.31	kg/hr	0.168	kg/hr
Mass Out				
Pro Gas	6.171	kg/hr	0.194	kg/hr
Water	0.355	kg/hr	0.114	kg/hr
Cyclone	0.053	kg/hr	0.0007846	kg/hr
Fabric	0.022	kg/hr	0.0008631	kg/hr
Thimble	0.000002465	kg/hr	4.044E-08	kg/hr
Total	6.601	kg/hr	0.225	kg/hr
Efficiency	104.607	%	4.525	%

Oxygen Balance				
Oxygen In			**Uncertainty**	
Dry Fuel	34.863	mol/hr	2.21	mol/hr
Fuel H2O	4.012	mol/hr	1.543	mol/hr
Air	25.798	mol/hr	1.032	mol/hr
Total	64.673	mol/hr	2.886	mol/hr
Oxygen Out				
CO	25.24	mol/hr	1.505	mol/hr
CO2	35.195	mol/hr	2.078	mol/hr
H2O	9.852	mol/hr	3.155	mol/hr
Char	0.402	mol/hr	0.036	mol/hr
Total	70.689	mol/hr	4.067	mol/hr
Efficiency	109.303	%	7.958	%

Nitrogen Balance				
Nitrogen In			**Uncertainty**	
Dry Fuel	1.227	mol/hr	2.397	mol/hr
Air	95.919	mol/hr	3.837	mol/hr
Total	97.146	mol/hr	4.524	mol/hr
Nitrogen Out				
N2	97.065	mol/hr	5.288	mol/hr
Char	0.081	mol/hr	0.001271	mol/hr
Total	97.146	mol/hr	5.288	mol/hr
Efficiency	100	%	7.164	%

Flow Rates				
			Uncertainty	
System dr	94.31	liter/min	4.781	liter/min
Sample lin	2.08	liter/min	0.028	liter/min

Carbon Conversion				
			Uncertainty	
Efficiency	97.953	%	0.196	%

Percent Water				
			Uncertainty	
water %	7.837	%	2.544	%

Carbon Balance				
Carbon In			**Uncertainty**	
Fuel	106.516	mol/hr	6.754	mol/hr
Total	106.516	mol/hr	6.754	mol/hr
Carbon Out				
CO	50.48	mol/hr	3.01	mol/hr
CO2	35.195	mol/hr	2.078	mol/hr
CH4	14.313	mol/hr	0.778	mol/hr
C2H2	0.446	mol/hr	0.011	mol/hr
C2H4	12.689	mol/hr	0.333	mol/hr
C2H6	2.064	mol/hr	0.056	mol/hr
C3H8	0.095	mol/hr	0.002397	mol/hr
Char	2.492	mol/hr	0.097	mol/hr
Total	117.774	mol/hr	3.756	mol/hr
Pro Gas	115.282	mol/hr	3.754	mol/hr
Efficiency				
Carbon	110.569	%	7.847	%
Pro Gas	108.229	%	7.715	%

Hydrogen Balance				
Hydrogen In			**Uncertainty**	
Dry Fuel	79.723	mol/hr	5.055	mol/hr
Fuel H2O	8.024	mol/hr	3.086	mol/hr
Total	87.747	mol/hr	5.922	mol/hr
Hydrogen Out				
H2	22.894	mol/hr	1.36	mol/hr
CH4	28.626	mol/hr	1.556	mol/hr
C2H2	0.223	mol/hr	0.011	mol/hr
C2H4	12.689	mol/hr	0.665	mol/hr
C2H6	3.095	mol/hr	0.168	mol/hr
C3H8	0.142	mol/hr	0.00719	mol/hr
H2O	19.703	mol/hr	6.31	mol/hr
Char	0.374	mol/hr	0.02	mol/hr
Total	87.747	mol/hr	6.675	mol/hr
Efficiency	100	%	10.17	%

Filtration Results				
Mass Loading			**Uncertainty**	
Out Gasifie	12.196	g/m^3	0.673	g/m^3
After Cyclo	3.585	g/m^3	0.236	g/m^3
After Fabri	0.02	g/m^3	0.00042	g/m^3
Efficiency				
Cyclone	70.601	%	3.288	%
Fabric	99.449	%	0.055	%
Collection	99.838	%	0.015	%

TEST #11

Mass Balance				
Mass In			**Uncertainty**	
Air	3.543	kg/hr	0.142	kg/hr
Fuel	2.545	kg/hr	0.091	kg/hr
Total	6.088	kg/hr	0.168	kg/hr
Mass Out				
Pro Gas	5.85	kg/hr	0.183	kg/hr
Water	0.401	kg/hr	0.105	kg/hr
Cyclone	0.053	kg/hr	0.0005896	kg/hr
Fabric	0.02	kg/hr	0.00064	kg/hr
Thimble	0.000001792	kg/hr	1.257E-07	kg/hr
Total	6.325	kg/hr	0.211	kg/hr
Efficiency	103.903	%	4.501	%

Oxygen Balance				
Oxygen In			**Uncertainty**	
Dry Fuel	32.062	mol/hr	2.082	mol/hr
Fuel H2O	3.69	mol/hr	1.42	mol/hr
Air	25.798	mol/hr	1.032	mol/hr
Total	61.55	mol/hr	2.723	mol/hr
Oxygen Out				
CO	22.49	mol/hr	1.338	mol/hr
CO2	32.908	mol/hr	1.91	mol/hr
H2O	11.142	mol/hr	2.924	mol/hr
Char	0.396	mol/hr	0.027	mol/hr
Total	66.936	mol/hr	3.74	mol/hr
Efficiency	108.751	%	7.75	%

Nitrogen Balance				
Nitrogen In			**Uncertainty**	
Dry Fuel	1.128	mol/hr	2.205	mol/hr
Air	95.919	mol/hr	3.837	mol/hr
Total	97.048	mol/hr	4.425	mol/hr
Nitrogen Out				
N2	96.967	mol/hr	5.124	mol/hr
Char	0.08	mol/hr	0.0009479	mol/hr
Total	97.048	mol/hr	5.124	mol/hr
Efficiency	100	%	6.976	%

Flow Rates				
			Uncertainty	
System	88.941	liter/min	4.391	liter/min
Sample 1	2.053	liter/min	0.037	liter/min
Sample 2	2.033	liter/min	0.13	liter/min

Carbon Conversion				
			Uncertainty	
Efficiency	97.844	%	0.204	%

Percent Water				
			Uncertainty	
water %	9.254	%	2.474	%

Carbon Balance				
Carbon In			**Uncertainty**	
Fuel	97.96	mol/hr	6.361	mol/hr
Total	97.96	mol/hr	6.391	mol/hr
Carbon Out				
CO	44.979	mol/hr	2.676	mol/hr
CO2	32.908	mol/hr	1.91	mol/hr
CH4	12.513	mol/hr	0.672	mol/hr
C2H2	0.419	mol/hr	0.01	mol/hr
C2H4	11.1	mol/hr	0.285	mol/hr
C2H6	1.826	mol/hr	0.049	mol/hr
C3H8	0.087	mol/hr	0.002147	mol/hr
Char	2.453	mol/hr	0.073	mol/hr
Total	106.284	mol/hr	3.369	mol/hr
Pro Gas	103.831	mol/hr	3.368	mol/hr
Efficiency				
Carbon	108.497	%	7.84	%
Pro Gas	105.993	%	7.694	%

Hydrogen Balance				
Hydrogen In			**Uncertainty**	
Dry Fuel	73.319	mol/hr	4.761	mol/hr
Fuel H2O	7.379	mol/hr	2.84	mol/hr
Total	80.699	mol/hr	5.543	mol/hr
Hydrogen Out				
H2	18.843	mol/hr	1.145	mol/hr
CH4	25.025	mol/hr	1.344	mol/hr
C2H2	0.209	mol/hr	0.01	mol/hr
C2H4	11.1	mol/hr	0.571	mol/hr
C2H6	2.738	mol/hr	0.146	mol/hr
C3H8	0.13	mol/hr	0.006441	mol/hr
H2O	22.285	mol/hr	5.848	mol/hr
Char	0.368	mol/hr	0.019	mol/hr
Total	80.699	mol/hr	6.137	mol/hr
Efficiency	100	%	10.248	%

Filtration Results				
Mass Loading			**Uncertainty**	
Out Gasifie	12.526	g/m^3	0.655	g/m^3
After Cyclo	3.477	g/m^3	0.207	g/m^3
After Fabri	0.017	g/m^3	0.001002	g/m^3
After Fabri	0.005045	g/m^3	0.001002	g/m^3
Efficiency				
Cyclone	72.239	%	2.933	%
Fabric 1	99.504	%	0.048	%
Fabric 2	99.855	%	0.032	%
Collection	99.862	%	0.013	%
Collection	99.96	%	0.008739	%

TEST #12

Mass Balance				
Mass In			**Uncertainty**	
Air	3.543	kg/hr	0.142	kg/hr
Fuel	2.953	kg/hr	0.091	kg/hr
Total	6.496	kg/hr	0.168	kg/hr
Mass Out				
Pro Gas	6.141	kg/hr	0.197	kg/hr
Water	0.492	kg/hr	0.119	kg/hr
Cyclone	0.048	kg/hr	0.0005454	kg/hr
Fabric	0.018	kg/hr	0.0006336	kg/hr
Thimble	0.0000076	kg/hr	2.163E-07	kg/hr
Total	6.699	kg/hr	0.23	kg/hr
Efficiency	103.134	%	4.436	%

Oxygen Balance				
Oxygen In			**Uncertainty**	
Dry Fuel	37.206	mol/hr	2.32	mol/hr
Fuel H2O	4.282	mol/hr	1.646	mol/hr
Air	25.798	mol/hr	1.032	mol/hr
Total	67.285	mol/hr	3.026	mol/hr
Oxygen Out				
CO	27.21	mol/hr	1.616	mol/hr
CO2	32.439	mol/hr	1.989	mol/hr
H2O	13.663	mol/hr	3.305	mol/hr
Char	0.359	mol/hr	0.026	mol/hr
Total	73.671	mol/hr	4.182	mol/hr
Efficiency	109.491	%	7.93	%

Nitrogen Balance				
Nitrogen In			**Uncertainty**	
Dry Fuel	1.309	mol/hr	2.559	mol/hr
Air	95.919	mol/hr	3.837	mol/hr
Total	97.229	mol/hr	4.612	mol/hr
Nitrogen Out				
N2	97.156	mol/hr	5.379	mol/hr
Char	0.073	mol/hr	0.0009107	mol/hr
Total	97.229	mol/hr	5.379	mol/hr
Efficiency	100	%	7.287	%

Flow Rates				
			Uncertainty	
System dr	95.38	liter/min	4.919	liter/min
Sample lin	2.193	liter/min	0.061	liter/min

Carbon Conversion				
			Uncertainty	
Efficiency	98.331	%	0.158	%

Percent Water				
			Uncertainty	
water %	10.443	%	2.585	%

Carbon Balance				
Carbon In			**Uncertainty**	
Fuel	113.676	mol/hr	7.089	mol/hr
Total	113.676	mol/hr	7.089	mol/hr
Carbon Out				
CO	54.421	mol/hr	3.231	mol/hr
CO2	32.439	mol/hr	1.989	mol/hr
CH4	13.619	mol/hr	0.758	mol/hr
C2H2	0.418	mol/hr	0.011	mol/hr
C2H4	11.841	mol/hr	0.317	mol/hr
C2H6	2.055	mol/hr	0.057	mol/hr
C3H8	0.116	mol/hr	0.002997	mol/hr
Char	2.222	mol/hr	0.07	mol/hr
Total	117.132	mol/hr	3.884	mol/hr
Pro Gas	114.909	mol/hr	3.883	mol/hr
Efficiency				
Carbon	103.04	%	7.278	%
Pro Gas	101.085	%	7.17	%

Hydrogen Balance				
Hydrogen In			**Uncertainty**	
Dry Fuel	85.082	mol/hr	5.306	mol/hr
Fuel H2O	8.563	mol/hr	3.292	mol/hr
Total	93.645	mol/hr	6.244	mol/hr
Hydrogen Out				
H2	23.442	mol/hr	1.405	mol/hr
CH4	27.237	mol/hr	1.515	mol/hr
C2H2	0.209	mol/hr	0.011	mol/hr
C2H4	11.841	mol/hr	0.634	mol/hr
C2H6	3.083	mol/hr	0.17	mol/hr
C3H8	0.174	mol/hr	0.008991	mol/hr
H2O	27.326	mol/hr	6.61	mol/hr
Char	0.333	mol/hr	0.017	mol/hr
Total	93.645	mol/hr	6.956	mol/hr
Efficiency	100	%	9.982	%

Filtration Results				
Mass Loading			**Uncertainty**	
Out Gasifie	10.491	g/m^3	0.565	g/m^3
After Cyclo	2.922	g/m^3	0.18	g/m^3
After Fabri	0.058	g/m^3	0.002298	g/m^3
Efficiency				
Cyclone	72.146	%	3.055	%
Fabric	98.023	%	0.205	%
Collection	99.449	%	0.054	%

APPENDIX E.
UNCERTAINTY ANALYSIS

The uncertainty, σ, of measurements and calculations depends on the accuracy of equipment used. Calculating the uncertainty is demonstrated in the following equations.

$$y = Ax_1^{\,m} + Bx_2^{\,n} \qquad \sigma_y = \sqrt{\left(\frac{\partial y}{\partial x_1}\right)^2 (\sigma_{x_1})^2 + \left(\frac{\partial y}{\partial x_2}\right)^2 (\sigma_{x_2})^2}$$

$$\sigma_y = \sqrt{\left(Amx_1^{\,m-1}\right)^2 (\sigma_{x_1})^2 + \left(Bnx_2^{\,n-1}\right)^2 (\sigma_{x_2})^2}$$

$$y = Ax_1^{\,m} x_2^{\,n} \qquad \sigma_y = \sqrt{\left(\frac{\partial y}{\partial x_1}\right)^2 (\sigma_{x_1})^2 + \left(\frac{\partial y}{\partial x_2}\right)^2 (\sigma_{x_2})^2}$$

$$\sigma_y = \sqrt{\left(Amx_1^{\,m-1} x_2^{\,n}\right)^2 (\sigma_{x_1})^2 + \left(Anx_1^{\,m} x_2^{\,n-1}\right)^2 (\sigma_{x_2})^2}$$

$$y = \frac{Ax_1^{\,m} x_2^{\,n}}{Cx_3^{\,p}} \qquad \sigma_y = \sqrt{\left(\frac{\partial y}{\partial x_1}\right)^2 (\sigma_{x_1})^2 + \left(\frac{\partial y}{\partial x_2}\right)^2 (\sigma_{x_2})^2 + \left(\frac{\partial y}{\partial x_2}\right)^2 (\sigma_{x_2})^2}$$

$$\sigma_y = \sqrt{\left(\frac{Amx_1^{\,m-1} x_2^{\,n}}{Cx_3^{\,p}}\right)^2 (\sigma_{x_1})^2 + \left(\frac{Anx_1^{\,m} x_2^{\,n-1}}{Cx_3^{\,p}}\right)^2 (\sigma_{x_2})^2 + \left(\frac{-pAx_1^{\,m} x_2^{\,n}}{Cx_3^{\,p+1}}\right)^2 (\sigma_{x_3})^2}$$

$$y = \frac{Ax_1^{\,m} + Bx_2^{\,n}}{Cx_3^{\,p}} \qquad \sigma_y = \sqrt{\left(\frac{\partial y}{\partial x_1}\right)^2 (\sigma_{x_1})^2 + \left(\frac{\partial y}{\partial x_2}\right)^2 (\sigma_{x_2})^2 + \left(\frac{\partial y}{\partial x_2}\right)^2 (\sigma_{x_2})^2}$$

$$\sigma_y = \sqrt{\left(\frac{Amx_1^{\,m-1}}{Cx_3^{\,p}}\right)^2 (\sigma_{x_1})^2 + \left(\frac{Bnx_2^{\,n-1}}{Cx_3^{\,p}}\right)^2 (\sigma_{x_2})^2 + \left(\frac{-p(Ax_1^{\,m} + Bx_2^{\,n})}{Cx_3^{\,p+1}}\right)^2 (\sigma_{x_3})^2}$$

For the above equations A, B, C, m, n, and p are constants; x_1, x_2, and x_3 are measured values; σ_{x_1}, σ_{x_2}, and σ_{x_3} are the uncertainties in the measured values. The uncertainty of a measured value is the accuracy in the measuring method. For instance the uncertainty of the mass caught by the fabric was determined by measuring the mass of char wiped from the walls of the filter housing with a paper towel. The mass from the sides was measured at roughly 4 gm. The mass was added to the accuracy of the scale, which was 1 gm, to get an uncertainty in the dust cake weight of +/- 5 gm. Additional values that affected the uncertainty in determining the filtration efficiency of the fabric are inputs into the system as well as outputs used to calculate values needed in the process of calculating the efficiency for the fabric filter.

Uncertainties from inputs consisted of the air and fuel feed rates, as well as the composition of the fuel. The uncertainty in the air flow rate was estimated at +/- 1.5 lpm from watching the digital read out on the mass flow controller, range from 88.5 to 91.5 lpm during the course of an experiment. The uncertainty in the fuel feed rate was computed from the

measured uncertainty of fuel in the hopper divided by the average time fuel was fed. Lab assistants were able to measure the weight of fuel in the hopper to within 2 lbs and fuel was fed for roughly 10 hours on average, so the uncertainty of the fuel feed was set to 0.2 lb/hr. The uncertainty in each element of the fuel was assumed to be 5% of the analyzed result done by Hazen Inc.

Measure outputs that attribute to uncertainty in the filtration efficiency include the volume fractions of gases in the producer gas measured by the Gas Chromatograph (GC), the volume of gas pulled through the sample line, and the mass of particulate caught by the quartz thimble filter. The standard deviation of gas fractions measured by the GC during the duration of sampling was used as the uncertainty in the volume fractions of gases in the producer gas. The uncertainty in the volume of gas sampled was the chosen to be half of the finest reading on the gas meter, which was 0.01 ft^3. The uncertainty in the mass collected by the quartz thimble filter was determined by using the standard deviation of 10 measurements performed with the AE ADAM AAA/L Series high precision scale used to weigh the thimble filter. The standard deviation of the 10 measurements was +/- 0.0005 gm.